Doctoral Dissertation

Spatio-temporal Analysis and Scenario-based Future Projection of Urban Sustainability Indicators in Coastal China

（中国沿岸部における都市の持続可能性指標の時空間分析とシナリオベース将来予測）

XIANGYUN SHI
(石 湘芸)

October 2021

Division of Sustainable Energy and Environmental Engineering
Graduate School of Engineering
Osaka University

Acknowledgement

First and foremost, I am extremely grateful to my supervisor and assistant professor, Machimura-sensei and Matsui-sensei, for their invaluable advice, support, and patience during my doctoral study. Their guidance helped me in all the time of research and writing of this thesis.

My gratitude extends to Saito-sensei and Hashimoto-sensei for their treasured help which was really influential in shaping my research method and critiquing the results. Additionally, I would like to express my gratitude to Haga Chihiro san for his technical support on my research.

I would also like to thank all the colleagues and members of the GE lab for a cherished time spent together. Everyone is very nice to me, I really enjoyed the time in our lab. They made my academic career more fun and wonderful. Thank you for letting me have many good memories.

Finally, but not least, I want to thank my family. They always encourage me to pursue my dream and have confidence in my ability to go after new things that inspired me. Thank you for your unfailing support and understanding through the ups and downs of my life abroad.

Again, my sincere thank you to all the people who have helped and supported me. This accomplishment would not have been possible without them.

Lists of Publication and Conferences

Original papers (peer reviewed)

1. Shi, X., Matsui, T., Machimura, T., Gan, X., & Hu, A. (2020). Toward sustainable development: Decoupling the high ecological footprint from human society development: A case study of Hong Kong. *Sustainability*, 12(10), 4177.

2. Shi, X., Matsui, T., Haga, C., Machimura, T., Hashimoto, S., & Saito, O. (2021). A Scenario- and Spatial-Downscaling-Based Land Use Modeling Framework to Improve the Projections of Plausible Futures: A Case Study of the Guangdong–Hong Kong–Macao Greater Bay Area, China. *Sustainability Science*, DOI: https://doi.org/10.1007/s11625-021-01011-z

3. Shi, X., Matsui, T., Machimura, T., Haga, C., Hu, A., & Gan, X. (2021). The Impact of Urbanization on the Food-Water-Land-Ecosystems Nexus: A Study of Shenzhen, China. *Science of the Total Environment*.

International Conference

1. Shi, X., Matsui, T., Haga, C., Machimura, T. Spatiotemporal assessment and future projection of land-use change and ecosystem services to explore the food-water-land ecosystems nexus towards the sustainable urban development. International Conference on Sustainable Technology and Development Conference, October 2021. Shenzhen, China.

Other Conference

1. Predicting and Assessing Natural Capitals and Ecosystem Services (PANCES) Modelling Training Seminar, March 2021. The University of Tokyo, Japan. (Online conference)

Abstract

Since sustainable development was put forward by the United Nations, it has had wide and far-reaching impact on the global communities. Many countries have actively responded to this call and been striving to achieve the goal of sustainable development (SDGs). Cities are deemed as the engines for achieving SDGs. Therefore, the study aims to assess the sustainability of urban areas in terms of the ecological dimension and explore the possible futures and consequences.

In Chapter 1, an introduction of sustainable development and research objectives were described. In order to achieve sustainability, the social, environmental, and economic dimensions of sustainable development need to be balanced, and this vision is interweaved with the 17 SDGs as well. Especially for the urban goal (SDG 11), that is, sustainable cities and communities, it is highlighted as a great potential for change to promote the implementation of the SDGs. In this sense, the urbanization of China, the country with the largest population and the fastest economic growth in the world, has attracted tremendous attention. An overview of background is given to demonstrate the significance and necessity of carrying out the study.

Chapter 2 evaluates the sustainable development level of Hong Kong considering the factors of ecological footprint, biocapacity, and the human development index (HDI) from 1995 to 2016. Moreover, a further comparative analysis and a SWOT analysis are made between Singapore and Hong Kong to explain how to decouple the large ecological footprint from the development of human society. The results indicate that Hong Kong is a “high HDI and high

footprint" development trend. Therefore, drawing lessons from Singapore's experience, on the basis of comparative analysis, this study puts forward some policy suggestions on transforming to a society with "high HDI and low footprint".

In Chapter 3, the research scope extends from Hong Kong to the Guangdong–Hong Kong–Macao Greater Bay Area (the Greater Bay Area), China. To explore possible land-use patterns that can help achieve sustainable development. A framework is proposed, which combines the scenario of global Shared Socioeconomic Pathways (SSPs) with local land planning policies to simulate land use change. Firstly, the Land Change Modeler was used to analyze the historical land-use changes and build transition potential sub-models. Then, the future projections of the Greater Bay Area were made for the "business-as- usual" (BaU) scenario and five localized SSP scenarios that were downscaled from global scenarios and modified based on the local land planning policy. And Hong Kong was taken as a typical case to demonstrate the application of the projected land-use maps.

Chapter 4 examines the influence of urbanization on food, water, land, and ecosystem (FWLE) by using the nexus thinking, an original framework of FWLE nexus is put forward. Shenzhen, which situated just across the border from Hong Kong, is selected as the study case. By continuing the land change modeling method used in Chapter 3, the land-use pattern in 2030 under BaU scenario is projected, and then the ecosystem services related to food, water, and habitat quality from 2000 to 2030 could be assessed based on the InVEST model and statistical materials. Thus, the spatiotemporal assessments and analyses of land-use changes and ecosystem services could be constituted for exploring the FWLE nexus, understanding its advantages and disadvantages and making tradeoffs.

Finally, Chapter 5 presents the summary and conclusion of the three sub-topics of the thesis. Besides, it also points out the limitations of the study, such as the deficiency of ecological footprint and SSPs, and puts forward the future prospects.

Table of Contents

List of Figures

List of Tables

CHAPTER 1: Introduction

1.1 Background

1.1.1 The global goals: sustainable development

For most of the last couple of hundred years in the western world, the relationship between human and environment was regarded as humanity's triumph over nature, the environment was largely deem as external to humanity [1]. People transformed and modified environment to obtain ecosystem services and goods, then along came the unintended consequences of global environmental changes that posed formidable challenges to human society [2]. Abundant evidence, such as the degradation of natural environment, the loss of biodiversity, the increase of greenhouse gas emissions and the deterioration of climate change, air pollution, and etc., had reflected that there were sharp contradictions between environment and human development. And various biophysical systems and geochemical processes at regional and global levels, have become highly stressed and even dysfunctional [3]. In turn, the environmental damage and ecosystem degradation have a significantly negative impact on human health, economic growth [4], and food security [5], [6]. For instance, in the Organization for Economic Co-operation and Development (OECD) member countries, the negative environmental changes are responsible for 2-6% of the total burden of disease [7]. Besides, the climate change, together with other global environmental degradation put pressure on the food system thus posing a threat to food security [8]. Thus, a vicious circle was formed and will continue in the future.

For helping save humanity and the Earth from imminent disaster, the "Our Common Future" report was proposed by the United Nations World Commission on Environment and Development in 1987, it marked a watershed in thinking on the relationship between

environment and human society [9], the global communities called for “sustainable development” to take fundamental changes in development patterns [10], and for the first time, the sustainable development was defined as “Development that meets the needs of the present without compromising the ability of future generations to meet their own needs” which is also the most widely used and cited definition [11].

Hereafter, sustainable development has been deem as a guiding principle and pathway for addressing the issues between environment and human development [12], such as the sustainable agriculture, sustainable urban transformation, sustainable consumption, and etc., its goal is to achieve sustainability [13]. There are three dimensions to sustainable development— society, environment, and economy [14] (as shown in ***Figure 1***), which are interconnected and indivisible. According to the description of Globalization and Livelihood Options of People living in Poverty (GLOPP) [15], they are described as:

- Environmental responsibility: reduce burden on the environment and use natural resources without damaging the equilibrium and integrity of ecosystems. When the productivity of life-supporting natural resources is conserved or enhanced for use by future generations, environmental sustainability is achieved.
- Social solidarity: sustainable human development, involving equality of opportunities for people, welfare, ending poverty and improving individuals' quality of life offering a secure life with full rights and liberties in the long term and social cohesion.
- Economic efficiency: efficiency of economic and technological activities, foster investment and productivity, economic growth, economic output potential.

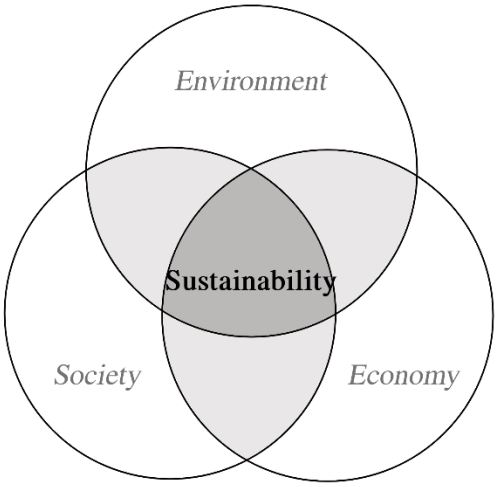

Figure 1. The three-ring dimension of sustainable development.
(This figure was referenced from the work by Ben Purvis, et al. [14])

Bringing the three together in a balanced way is crucial for achieving for achieving sustainability [16]. In 2015, the United Nations (UN) proposed 17 Sustainable Development Goals (SDGs) for transforming our world and pursuing a better and more sustainable future. All three dimensions were involved in the SDGs [17], as shown in ***Figure 2***, it is obvious that the environmental (biosphere) sustainability is the foundation of the development of society and economy, in turn, human can also shape the environment directly and indirectly, or consciously and unconsciously [18]. Since then, the environment issues were more closely linked to the socio-economic development, and these global goals have had a widespread and enormous impact on the global communities and governments. There are 193 countries officially adopted the SDGs [19], under this long term global priorities, the alignment and synergy between policy, business, civil society, and etc. will be much clearer and stronger [20].

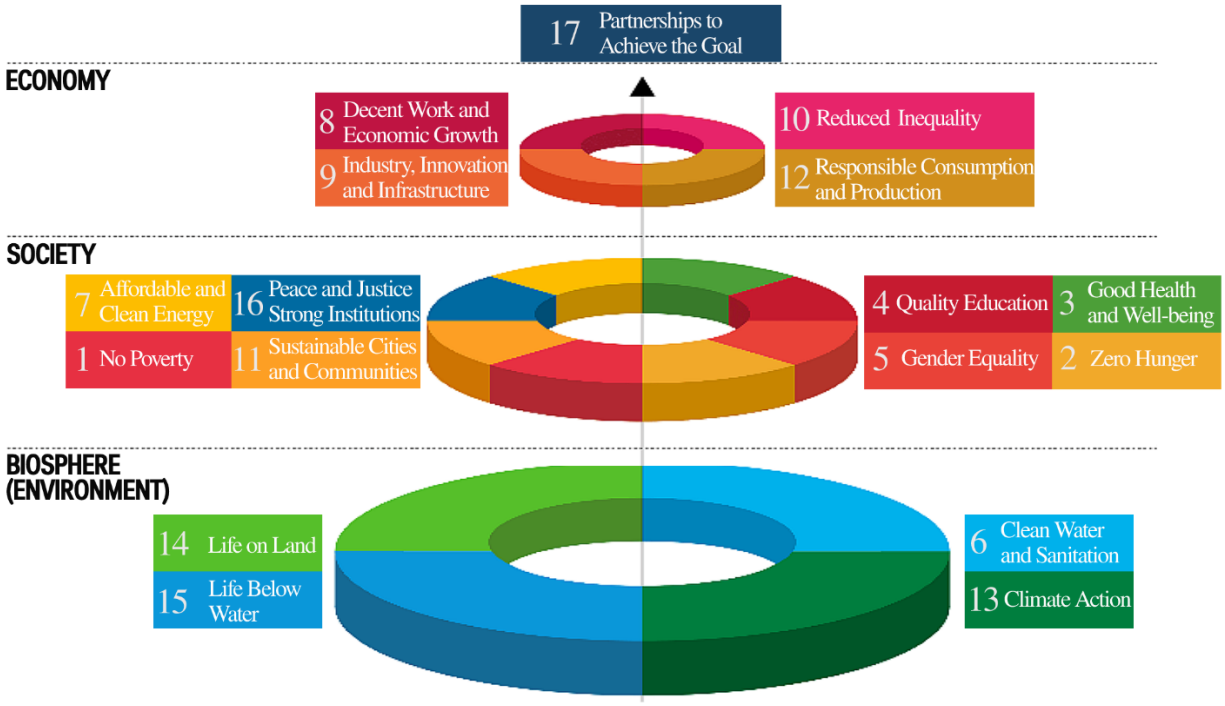

Figure 2. The SDGs intertwined together economically, societally and ecologically.
(This figure was referenced from the work by Carl Folke, et al. [18])

1.1.2 Urban transformations: sustainable urban development

Urban areas are the most densely populated places of human activity. At present, about half of the global population living in cities, by 2050, this figure is projected to rise to more than 60% [21]. Moreover, cities, which contribute about 60% of global GDP, are the important roles to boost economic growth, while they are also the major greenhouse gas emitting and resources consuming areas[22]. As can be seen, the linkages of three dimensions, environment, society, and economy are highly integrated and enhanced in urban areas, for this reason, urban areas have obtained great attentions of international and local communities, and at the forefront of addressing critical global development issues [23] and playing as engines for achieving SDGs [24].

The SDG 11 “Sustainable cities and communities”, a stand-alone goal on cities and urban development, aims to make cities and communities inclusive, safe, resilient and sustainable [25]. The environment-related targets are as follows [22]:

- By 2030, enhance inclusive and sustainable urbanization and capacity for participatory, integrated and sustainable human settlement planning and management in all countries
- By 2030, reduce the adverse per capita environmental impact of cities, including by paying special attention to air quality and municipal and other waste management
- Support positive economic, social and environmental links between urban, peri-urban and rural areas by strengthening national and regional development planning
- By 2020, substantially increase the number of cities and human settlements adopting and implementing integrated policies and plans towards inclusion, resource efficiency, mitigation and adaptation to climate change, resilience to disasters, and develop and implement, in line with the Sendai Framework for Disaster Risk Reduction 2015-2030, holistic disaster risk management at all levels

Under the current development forms of cities, which have been identified as unstainable in a large part [26], this urban goal (SDG 11) provided an opportunity for decision-makers, researchers, citizens, stakeholders, and etc. to rethink the transformation of sustainability with all three dimensions (social, environmental, and economic aspects). For realizing it, sustainable urban transformation is required, and urbanization was seen as a powerful transformative potential to achieve the goal. Especially for Asia where are urbanized rapidly and has about half of the world’s megacities (13 out of 22) [27]. By guiding the sound economic development and promoting the social cohesion, and without damaging the environment, urban planning and management were deem as the keys to help put cities on the sustainable development path [28].

Moreover, the New Urban Agenda [29] also proposed that urbanization can contribute to a better and more sustainable future for both developing and developed countries if cities could be well-planned and well-managed.

In addition, urban goal also could impact on other goals since its cross-cutting nature was recognized, such as the SDG 1—no poverty, SDG 7— affordable and clean energy, SDG 8—decent work and economic growth, SDG 12— responsible consumption and production, and etc. [30], in this view, a wide range of issues could be improved and tackled by finding the entry points from an urban perspective. In summary, urbanization has the ability to transform the three dimensions [31], and sustainable urban development will play as an essential role to contribute to the realization of sustainability.

1.1.3 Sustainable development and urbanization in China

With the sustainable development advocated by the global communities, China, the largest developing country with the most population in the world, also attached great importance to it. In 1992, after the United Nations Conference on Environment and Development which was held in Rio de Janeiro, Brazil, the sustainable development had been incorporated into Chinese basic national strategy. Next, the *China's Agenda 21 - White paper on China's Population, Environment and Development in the 21st Century* was proposed in 1994, and it is the world's first national development strategy that combined with sustainable development [32]. Since 1998, China has begun to invest massively in ecological protection projects and environmental protection infrastructure, such as the “Returning farmland to forest” and “Natural forest conservation” [33]. Since 2004, the circular economy, conservation of resources, and the development of renewable energy were put forward [34]. Then, in 2008, energy conservation and pollution reduction and the construction of ecological environment

were identified as the main focus for spurring the economic growth, which had greatly enhanced the capacity of environmental infrastructure in China [35]. In response to the UN's call for sustainable development, the *China's National Plan on Implementation of the 2030 Agenda for Sustainable Development* [36] was published in 2016. Furthermore, in 2018, "ecological civilization" was officially written into the Chinese Constitution, which became a core concept of national development.

Although these ambitious strategies, policies, and actions have been implementing, there are still many challenges on the way to the realization of sustainable development. Since the reform and opening up in 1978, China made socio-economy grew unprecedently as well as the rapid urbanization rate [37], its urbanization rate increased from 17.9% to 59.6% between 1978 and 2018 [38], especially in near-shore areas, such as the Guangdong–Hong Kong–Macao Greater Bay Area (Greater Bay Area), the urban development activities are intensive. Urban areas continuously playing as an engine to prompt the national economy [39], however, the characteristics of past urbanization form in China was described as "four highs": high consumption, high emissions, high investment, and high expansion [40], [41]. The process and structure of environment experienced dramatic changes under the pressure of urbanization [42], [43], the land-use types were changed from vegetation covered surfaces to the impervious surfaces thus causing negative impacts on water quality, groundwater recharge, and water circulation [44], [45]; besides, ecosystems were disturbed by other human activities, such as intensive industrialization, and agricultural activity, etc., resulting in the temperature change [46] and air pollution [47], habitat degradation, biodiversity loss [37], and etc. which are also harmful to human well-being in turn. In this way, urbanization was seen as both a challenge and an opportunity, what we need is to promote the sustainable urban transformation, and make the most of its positive impacts while mitigate the negative

impacts. As the economist and Nobel laureate Joseph Stiglitz said, China's urbanization was one of two transformative forces that would most impact global prosperity in the 21st century (the other: technological innovation in the USA) [48], thus the transformation for sustainable urbanization in China can make an profound and important contribution to the implementation of the SDGs.

1.1.4 Sustainability indicators

Ecosystem and the services provide underpin dimensions of societal and economic well-being [49], to achieve the SDGs, it is essential to monitor and manage ecosystems thus maintaining the sustainable supply of benefits and services [50]. Especially for the services involved provision of food and water, maintenance of habitat and biodiversity, which have drawn great attention from the academic communities and decision-makers [49].

Over the last two decades, there has been a prominent increase in the number of sustainability indicators and methods for tracking progress toward sustainability [51]. The ecological footprint approach has demonstrated good universality when considering different spatial scales—whether global, national, or regional [52], [53] . Moreover, combining it with biocapacity, both current ecological supply and demand and historical trends can be assessed to provide a basis for setting goals, identifying options for action, and tracking progress toward the stated goal. Furthermore, compared with other indicators, ecological footprint accounting allows for three unique approaches: (I) consumption (ecological footprint) can be compared to a biophysical budget limitation (biocapacity); (II) data can be aggregated to a single comparable unit of biocapacity (gha); and (III) time series of flows can be provided [54] . Moreover, the ecological footprint correlates with sustainable development and both take into account the following factors: (i) the increase in human consumption and its

consequences; (ii) the key resources for sustainable development, i.e., the biological production of land and oceans; (iii) the distribution of available resources; and (iv) the impact of trade on sustainable development and the redistribution of regional resources under environmental pressures [55] .

1.2 Objectives of the study

Sustainable cities are central to achieve all 17 Sustainable Development Goals [10]. Therefore, to improve the sustainability of urban development and help realize the SDGs, the study set out to:

1. Assess urban sustainability in terms of supply-demand aspect and explore the relations between the society development and high consumption mode, thus drawing implications for decision-making.
2. Combine with the multiple scenario simulation to project plausible land-use patterns in the future and analyze the possible impacts on ecosystem and human society.
3. Based on the business as usual scenario to project and assess the influence of urbanization on the correlations between land, water, food, and ecosystem.

The Greater Bay Area, China was chosen as the study case, it is the fourth largest bay area in the world, following San Francisco, New York, and Tokyo Bay Areas. Moreover, it is also the key to the strategic planning of the national development blueprint and will develop into a world-class city cluster [56]. Therefore, the Greater Bay Area is a typical and ideal region for studying the urban issues.

1.3 Structure of the dissertation

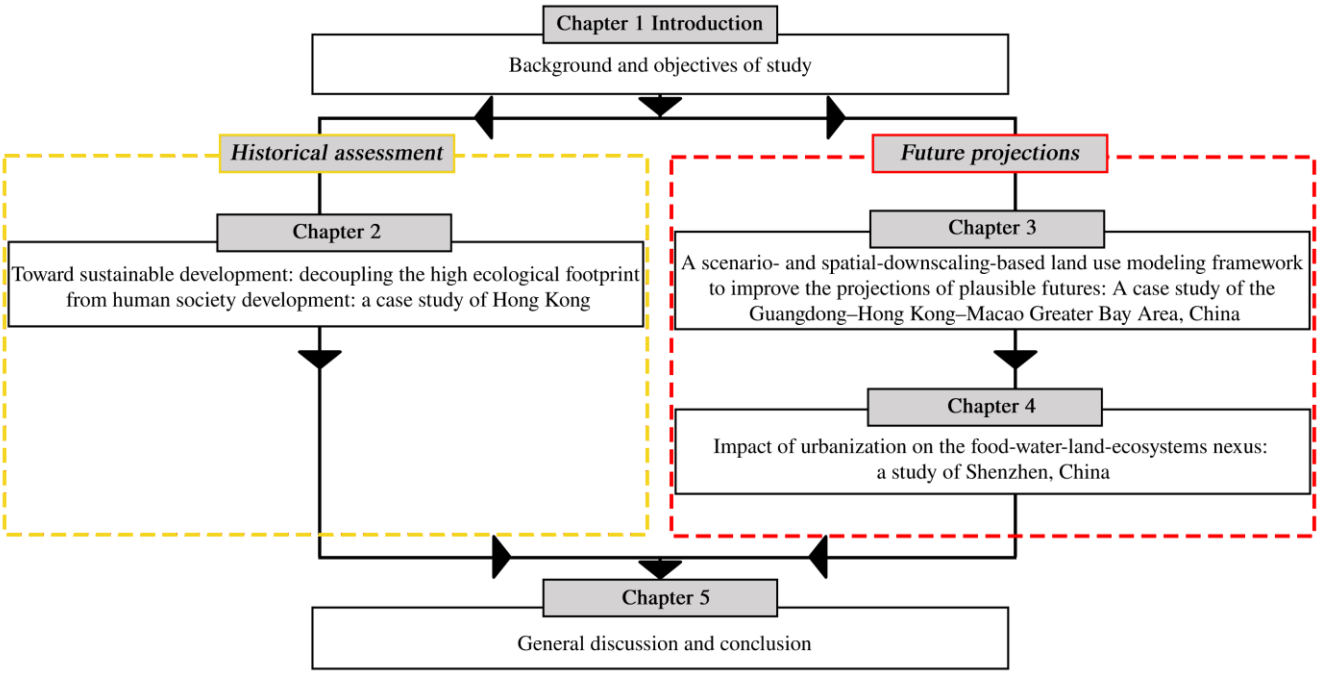

Figure 3. The schematic flow of the thesis.

The thesis can be divided into four parts. The first section is the introduction of general background, such as the description on sustainability, the role of urban transformation in the SDGs, the urbanization in China, and the sustainability indicators, then the three objectives were proposed. Next, the body of the study can be categorized into two components: (1) the historical trends of resource consumption (ecological footprint), supply (biocapacity), and human development index in a developed city were assessed, then the comparative analysis was made to draw implications for policies; (2) Based on the land-use change, which was deemed as a crucial driver to shape the interactions between society and environment, the future projection of urban area was conducted under multiple scenarios to explore the impacts on ecosystem, habitat, and provisioning services (food and water). Finally, the results of the thesis were summarized in chapter 5, the limitations and future work were also discussed.

CHAPTER 2: Toward Sustainable Development: Decoupling the High Ecological Footprint from Human Society Development: A Case Study of Hong Kong

2. 1. Introduction

2.1.1. Current challenge of an Asian megacity—Hong Kong

As sustainable development has been promoted and implemented by the international community and domestic government, it has also been presented in the future strategy of Hong Kong. As an important guideline for planning, the Hong Kong 2030+ [57] pioneers a vision wherein Hong Kong will become an international metropolis of Asia, which advocates sustainable development to meet the current and future requirements of society, the environment, and economic growth.

Nevertheless, there is an obvious gap between the current situation and attainment of the SDGs. Environmental protection and resource conservation in Hong Kong is lacking [58] . For instance, per capita, seafood consumption in Hong Kong was ranked second in Asia, and Hong Kong handled about 50% of the global shark fin trade [59] , which increased the burden on the global scale. Hong Kong also lacks incentives to improve energy efficiency and develop renewable energy. For the past decade, renewable energy accounted for only 0.1% of the primary energy used to generate electricity [60] . Moreover, the rapid growth of the population and economy of Hong Kong also put a heavy burden on land supply. For instance, about 1,200 ha extra land area is required to meet the needs of housing (200 ha), economic uses (300 ha) and public spaces (700 ha, including government, institution, community and transport facilities) [57] , aggravating the tension in the supply and demand relationship between human

development and the environment. On the road to sustainable development, climate change, an aging population, and air pollution also present further challenges [61] .

2.1.2. Researches on ecological footprint and human development in China

Ecological footprint research in China can be classified into two categories [62] : (I) adopting the ecological footprint method to synthetically measure the demand of natural resources on national and provincial scales, and (II) describing the ecological footprint of a particular production/consumption, such as tourism, transportation, water resources, etc. Although considerable ecological footprint-related research has been conducted in China, some deficiencies still exist: (i) research tends to focus on national and provincial areas and tends to neglect small scales, such as urban and rural areas [63] ; (ii) dynamic research on temporal series is limited and is mainly focused on Midwest regions [64] ; and (iii) ecological footprint research in China tends to neglect the Chinese special administrative regions, such as Hong Kong and Macau, due to the limitation of data sources, [65]–[68] , which indicates a research gap in these regions.

Besides, in order to measure human dimensions [69] that are necessary for indicating how societies should develop, the Human Development Index (HDI) was created as an overarching and composite index to evaluate the well-being of human societies. That is, human development is about expanding the richness of human life, rather than focusing on the richness of the economy only. As a summary measure, HDI evaluates long-term progress in three basic dimensions: a long and healthy life, access to knowledge, and a decent standard of living [70] . These three dimensions correspond to three of the SDGs: Goal 3 (good health and well-being), Goal 4 (quality education), and Goal 8 (decent work and economic growth).

The HDI has become widely accepted as a useful metric in the sustainability field [71] . With respect to the application of HDI in China, before 2000, economic development was China's major target, so social policies were poorly adopted. Education and health received minor attention in the human development of China. However, since the start of the millennium, social policies have received more attention [72] , although the gap between education, health, and economic growth is still significant and gradually increasing.

2.1.3. Purpose of this chapter

In the context described above, we take Hong Kong as the research object, studying sustainable development issues from the urban perspective, corresponding to Sustainable Development Goal 11, "sustainable cities and communities." The cross-cutting nature of urban issues also impacts other SDGs, such as SDGs 3, 4, 8, 12, 14, and 15 [30] . Therefore, HDI, the ecological footprint, and biocapacity are combined in this study. HDI evaluates the human well-being that relates to a healthy life (Goal 3), education (Goal 4), and a decent standard of living (Goal 8); the ecological footprint measures the natural resources consumed by the urban population (Goal 12, 14, and 15). All above assessments are analyzed in the long-term, namely from 1995 to 2016. Thereby, the characteristics and dynamic changes of Hong Kong development can be observed deeply. Subsequently, a SWOT analysis is performed and Hong Kong is compared with Singapore, a more sustainable city in Asia, in order to elaborate how human society development can be decoupled from a large ecological footprint, and to share recommendations for a sustainable transformation.

2.2. Materials and methods

2.2.1. Study area

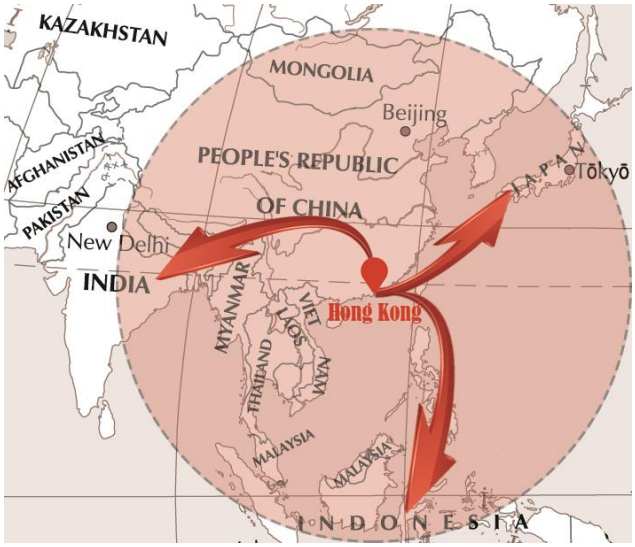

Figure 4. Five hours' flying time circle of Hong Kong.

(Our own elaboration from Hong Kong 2030+ [57] and Standard Map services [73])

Hong Kong is located in the southeast of China and consists of Hong Kong Island, Lantau Island, Kowloon and the New Territories (including 262 outlying islands). Due to its geographical location, half of the world's population can be reached within 5 hours flying time (***Figure 4***). The total population in 2016 was 7.34 million, the average population growth rate from 1995 to 2016 was 1.08% per annum, and by 2043, the population will increase to 8.22 million [57]. The total land area is approximately 1,110 square kilometers and the sea area is about 1,649 square kilometers. At present, less than 25% of Hong Kong's land has been developed, and parks and nature reserves account for approximately 40%. Hong Kong's economy is dominated by the service industry. Trading and logistics, financial services, producer and professional services, and tourism are the four pillar industries of Hong Kong. It also enjoys a worldwide reputation for its financial center.

2.2.2. Data sources

To ensure the accuracy and reliability of the research, the data in this chapter were mainly derived from the Hong Kong Annual Digest of Statistics (2001–2018) [74] , the Hong Kong Energy Statistics [75] , the Agriculture, the Fisheries and Conservation Department Report of Hong Kong [76] , the Food and Agriculture Organization of the United Nations (FAO) [77] , the Yearbook of Statistics Singapore [78] , and the United Nations Development Programme [70] .

2.2.3. Ecological Footprint

The ecological footprint calculates the combined demand for ecological resources and energy, focusing on six main categories of biologically productive land that are required by human activities: arable land, grazing land, forest land, water area, fossil land, and built-up land [79] . However, the ecological footprint calculated in a case can vary depending on the accuracy of statistical data, the scope of analysis, and the use of different equivalence factors and yield factors [80] . In this study, the calculation of ecological footprint consists of two parts: the biological accounts and the energy accounts, as shown in ***Table 1***.

The biological accounts are mainly related to agricultural products, forest products, livestock products, and aquatic products. As for the energy accounts, according to the *General Principles for Calculation of Comprehensive Energy Consumption* (GB / T2589-2008) in China, the low calorific value generated by 1 kg of fossil fuel is taken as a standard to convert the energy consumption into fossil energy land and construction land, as shown in ***Table 2***.

In addition, due to the vast territory of China, the land productivity of each province is different. Liu and Li [81] and Liu, Li, and Xie [82] used a net primary productivity approach to calculate the equivalence factors and yield factors for each province. We adopted those factors that correspond to Hong Kong to make the results more reliable (***Table 1***).

Table 1. Ecological footprint accounts and subjects of Hong Kong.

Accounts	Subjects	Land types	Equivalence factors	Yield factors
Biological accounts	rice, wheat, cereals, vegetables, tea, sugar and honey, pigs, other poultry, chickens, meat and meat preparations	arable land	1.96	1.65
	fruit, timber, coffee, cocoa	forest land	0.98	1.03
	cattle, sheep, dairy products	grazing land	0.82	2.71
	fish and fishery products, crustacean, mollusks.	water area	0.64	2.71
	residential, commercial, industrial, open area, transportation	built-up land	1.96	1.65
Energy accounts	Coke oven gas, kerosene, gasoline, diesel oil, fuel oil, LPG, natural gas, coal, electricity	fossil land	0.98	0.00

Note: Equivalence and yield factors for Hong Kong were derived from Liu and Li [81] ; Liu, Li, and Xie [82] .

Table 2. The average low heat value of energy and global average specific energy footprint.

Types	Average low heat value GJ/t	Specific energy footprint global average in GJ/ha per year	Land types
Kerosene	43.070	71	fossil energy land
Gasoline	43.070	93	fossil energy land
Diesel oil	42.652	93	fossil energy land
Coal	20.908	55	fossil energy land
Fuel oil	41.816	71	fossil energy land
LPG	50.200	71	fossil energy land
Coke oven gas	17.981	93	fossil energy land
Natural gas	35544①	93	fossil energy land
Electricity	3600②	71	fossil energy land

Note: ①The unit is kJ / m^3 ②The unit is kJ / kW·h

The basic equation (equation 1) of the ecological footprint EF (gha) *[83]* is:

$$EF = \sum_i \frac{P_i}{Y_{w,i}} . EQF_i \quad (1)$$

The per capita ecological footprint ef (gha/cap) calculated by equation 2:

$$ef = \frac{EF}{N} = \sum_i \frac{P_i}{N.Y_{w,i}} . EQF_i \quad (2)$$

where P (kg) is the amount of each primary product i that is harvested; N is the population; $Y_{W,i}$ (kg ha^{-1}) is the average world yield for commodity i; and EQF_i is the equivalence factor for the land use type producing products i. The detailed calculation methods of $Y_{W,i}$ and EQF_i are explained in reference [81], [82].

This study uses a consumer-based approach, which measures the biocapacity demanded by the final consumption of the region in question. The consumer-based method has become the

most widely used calculation [84] , especially for regions that rely heavily on imported products due to poverty in natural resources, such as Hong Kong.

For each land use type, the ecological footprint of consumption (EF_C) [85] is thus calculated by equation 3:

$$EF_C = EF_P + EF_I - EF_E \quad (3)$$

where EF_C (gha) is the ecological footprint of consumption, which indicates the consumption of biocapacity by inhabitants. EF_P (gha) is the ecological footprint of production, which indicates the consumption of biocapacity resulting from production processes within a given geographic area. EF_I (gha) and EF_E (gha) are the ecological footprint of imports and exports, respectively, and indicate the use of biocapacity within international trade.

According to the subjects in ***Table 1***, after transferring the corresponding values into equation (2), and calculating the EF_P, EF_I, and EF_E of the six land types, equation (3) can be used to calculate the EF_C.

2.2.4. Biocapacity

Biocapacity (BC) is a measure of the amount of biologically productive land and sea area available to provide the ecosystem services that humanity consumes—as our ecological budget or nature's regenerative capacity, it represents the total area of biologically productive land that the region can provide to humans [83] . BC calculated by equation 4:

$$bc = \sum_i \frac{A_i}{N} . YF_i . EQF_i \quad (4)$$

where bc (gha/cap) is the per capita biocapacity; Ai (ha) is the available area of a given land use type; N is the population; and YF_i and EQF_i are the yield factors and equivalence factors, respectively, for the land use type.

2.2.5. Ecological reserve/deficit

Ecological reserve and ecological deficit are based on the calculation of the regional ecological footprint and biocapacity to ascertain whether the demands of society exceed the regional biocapacity. Thereby a determination can be made about whether development in the region is sustainable [86], it calculated by equation 5:

$$\begin{cases} ed = ef - bc & (ef > bc) \\ er = bc - ef & (ef < bc) \end{cases} \quad (5)$$

where ed (gha) is the total ecological deficit; er (gha) is the total ecological reserve; bc (gha) is the total biocapacity; and ef (gha) is the total ecological footprint. If bc-ef >0, then there is an ecological reserve (er), indicating that the demands of humans in the region are within its biocapacity; if bc-ef <0, then there is an ecological deficit (ed), indicating that the demands exceed the biocapacity.

2.2.6. Human Development Index

As an overarching index, HDI was created for assessing three key dimensions of human development: a long and healthy life, acquisition of knowledge, and a decent standard of living. An overview of the calculation of HDI is shown in ***Figure 5***.

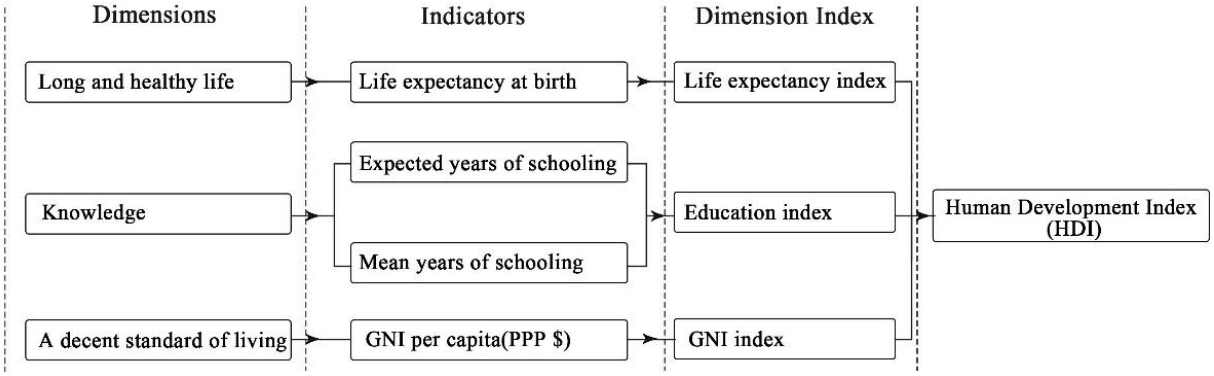

Figure 5. The calculation of HDI.

(Our own elaboration from United Nations Development Programme [70])

The calculation process consists of (1) identifying the minimum and maximum values of life expectancy at birth, expected years of schooling, mean years of schooling, and GNI, respectively. And then transforming these different unit indicators into indices between 0 and 1 by applying equation 6:

$$\text{Dimensionindex} = \frac{\text{actual value} - \text{minimum value}}{\text{maximum value} - \text{minimum value}} \quad (6)$$

(2) Finally, all indices are aggregated by equation 7:

$$\text{HDI} = (\text{I}_{\text{health}} \cdot \text{I}_{\text{education}} \cdot \text{I}_{\text{income}})^{1/3} \quad (7)$$

Where I_{health}, $\text{I}_{\text{education}}$, and I_{income} are the results calculated by equation (6).

2.3. Results and analysis

2.3.1. Results of ecological footprint

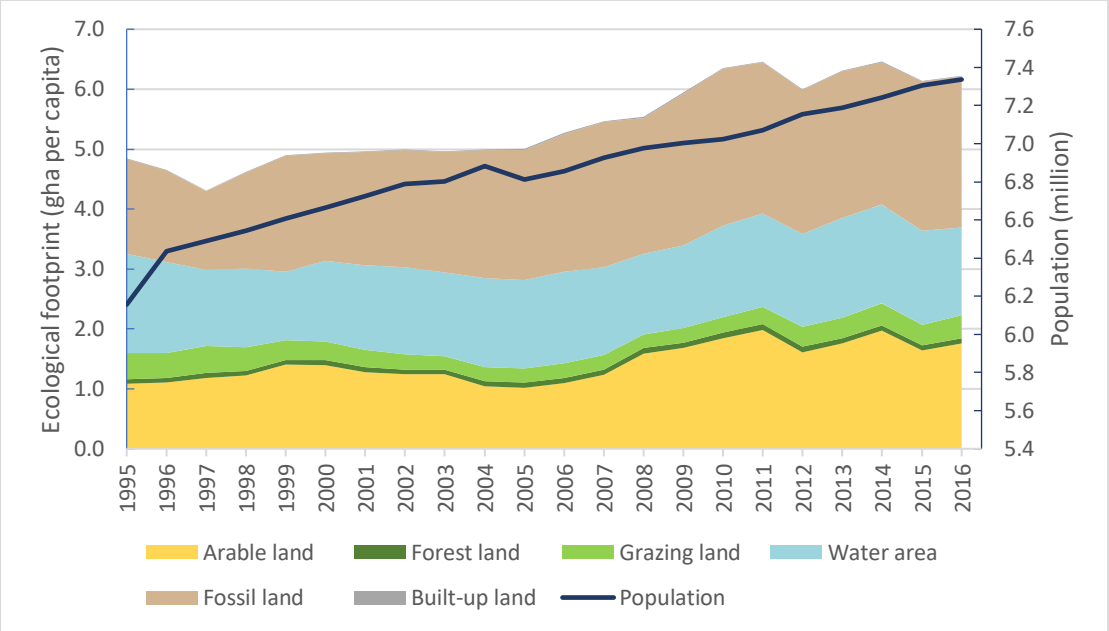

Figure 6. Hong Kong's population and per capita ecological footprint by land category during 1995-2016.

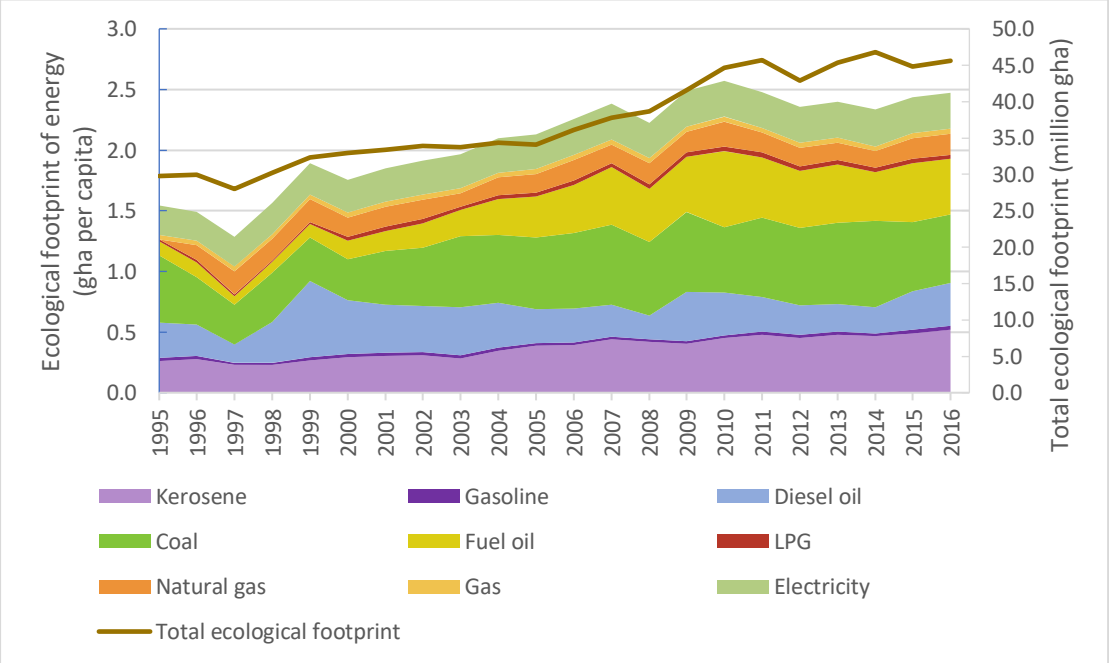

Figure 7. Hong Kong's total ecological footprint and per capita ecological footprint of energy. Each area shows the major components of energy consumption each year during 1995-2016.

Each area shows the major components of energy consumption each year. There are two main sources of electricity supply in Hong Kong: the imports of electricity from the mainland of China and the electricity generated at local plants. Coal is the main source of energy of local electric plants.

Using equations (1)–(3), the six categories of biologically productive lands of Hong Kong were calculated from 1995 to 2016, respectively. ***Figure 6*** (for details please see ***Table S 1***) illustrates that the per capita ecological footprint of Hong Kong increased from 4.842 gha/cap (1995) to 6.223 gha/cap (2016), with an average annual growth rate of 1.3%. The ecological footprint of arable land, fossil land, and water area made up the main consumptions of Hong Kong.

With regard to the biological accounts, according to statistical data from Agriculture, Fisheries and Conservation Department, Food and Health Bureau [87] , in 2016, the most common types of fresh food consumed each day (ranked from most to least consumed) were vegetables, fruits, pigs, salt-water fish, and eggs. More than 90% of this food was supplied by mainland China. In order to maintain stable supply chains, frozen food was also imported from Brazil, Norway, Philippines, and Thailand. It can be seen that the ecological footprint of Hong Kong does not just cover a regional scale, but extends to a global scale.

As for the energy accounts, fossil energy consumption accounted for the largest proportion of growth (***Figure 6***). It rose from 1.578 gha/cap to 2.518 gha/cap between 1995 and 2016, with an average proportion of 39%. ***Figure 7*** (for details: ***Table S 2***) shows the components of Hong Kong's energy ecological footprint. Fuel oil, coal, electricity, and kerosene were the major

types of energy consumption. Although the proportion of coal consumption declined slightly over time, it was still the largest type of consumed energy. Coal was the primary source of energy for generating electricity [75].

2.3.2. Results of biocapacity

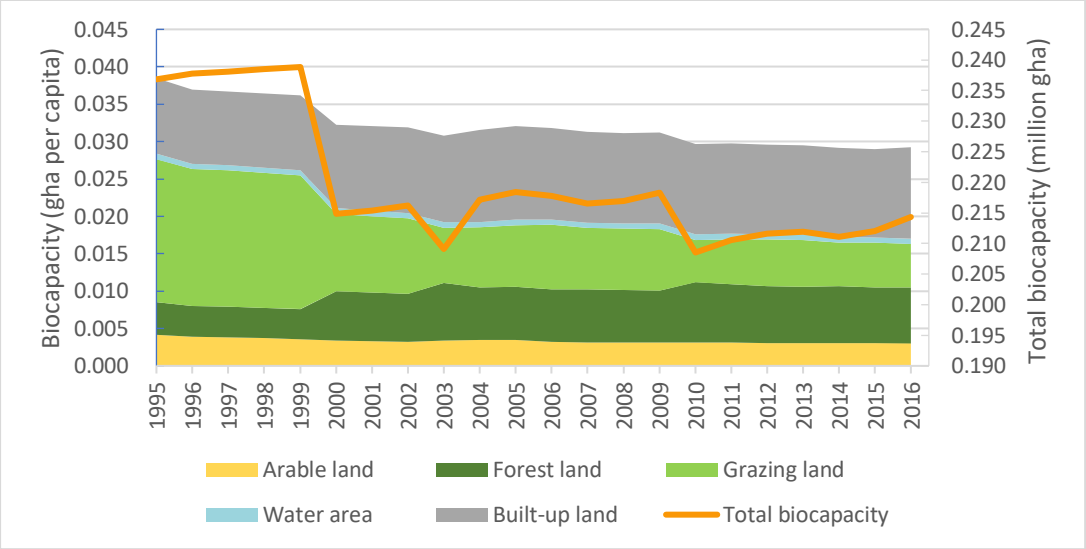

Figure 8. Hong Kong's total biocapacity and per capita biocapacity by land category during 1995-2016.

Arable land represents the agriculture area in Hong Kong, grazing land represents the grassland, forest land includes woodland, shrubland, and mangrove, and built-up land includes residential area, commercial area, industrial area, open space, the land for transportation, etc. The water area mainly represents reservoirs, streams and nullahs.

As shown in ***Figure 8***, from 1995 to 2016, biocapacity declined over time (for details: ***Table S 3***). The biocapacity of grazing land decreased significantly, from 0.0192 gha/cap to 0.0058 gha/cap, followed by arable land, which declined from 0.0042 gha/cap to 0.0030 gha/cap, while the biocapacities of forest land and built-up land increased. The biocapacity of water land remained constant.

In 1995, the agriculture area and built-up land area were 9100 ha and 17200 ha respectively. The vegetation area, including forest, shrub, grassland, and wetland, was 78300 ha. However, as the land became more urbanized, by 2016, the agriculture area, vegetation area and built-up land were 6800 ha, 73600 ha, and 27000 ha, respectively. In order to meet the needs of urban expansion, the agriculture and vegetation areas were shrinking, and the abandoned farmland and grassland contributed to the built-up land.

2.3.3. Results of ecological deficit

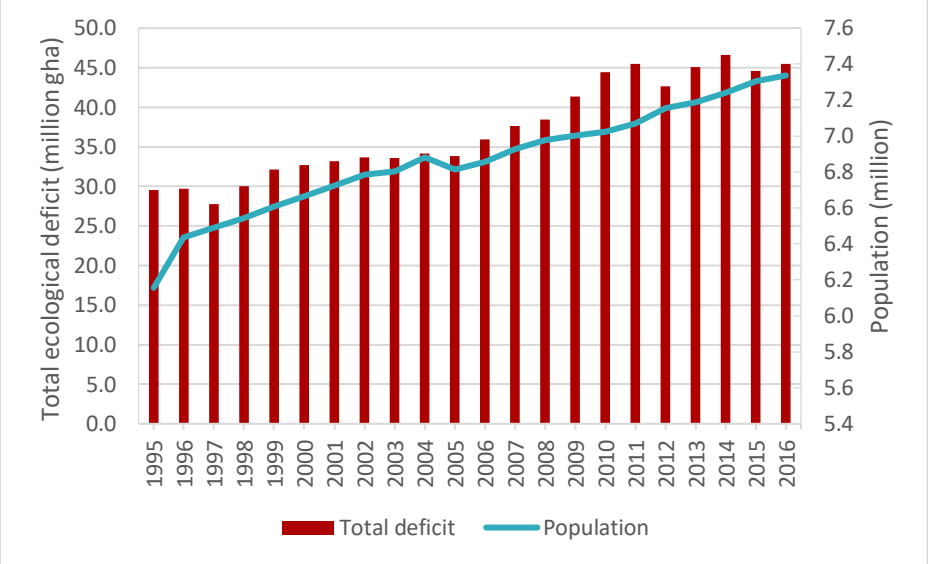

Figure 9. Hong Kong's population and total ecological deficit during 1995-2016.

According to the equation (5), the ecological deficit results can be calculated based on ecological footprint and biocapacity, as shown in ***Figure 9***. Obviously, consumption by Hong Kong's population exceeded the local biocapacity, and the trend continued each year. Compared with 1995, the ecological deficit increased by approximately 1.3 times by 2016.

As a natural resource poverty city, Hong Kong relies heavily on the ecosystem outside its own boundaries [80]. Further, Hong Kong's fisheries, which were historically unrestricted and very exploitative have already deteriorated the marine ecosystem around Hong Kong [88]. In addition to overfishing, the negative effects resulting from reclamation and waste discharge are also considerable. With the increasing consumption of the growing population, these human activities are eroding the ecosystem, resulting in a weaker biocapacity and a more aggravated ecological deficit.

2.3.4. Human Development Index of Hong Kong

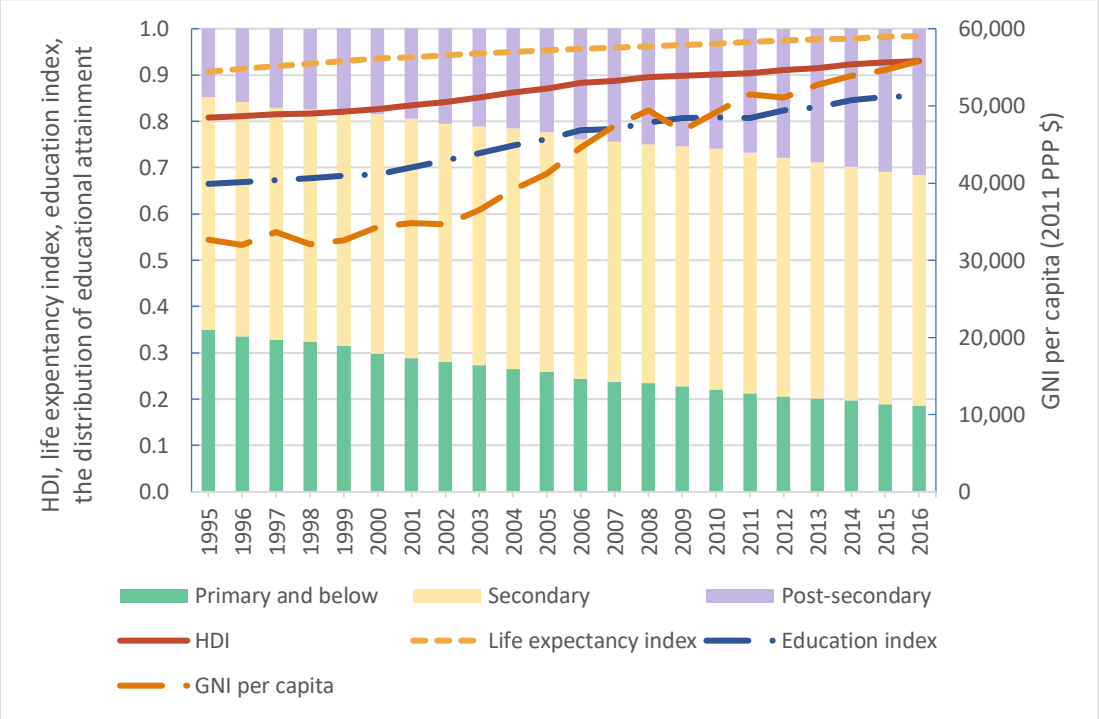

Figure 10. Life expectancy index, education index, GNI per capita, HDI of Hong Kong, and the distribution of educational attainment of people aged 15 and over.

The primary and below group includes people with no schooling, or kindergarten or a primary level of education. The secondary group includes people with lower secondary and upper secondary education. The post-secondary includes people with technical schooling, or non-degree or degree coursework. (This figure was drawn by our own elaboration. Data sources: Life expectancy index, education index, GNI per capita, and HDI data are sourced from the UNDP- Human development data [89] . The distribution of educational attainment of population data is sourced from the Census and Statistics Department of Hong Kong [90])

The HDI and its component indicators, namely life expectancy index, education index, and GNI per capita of Hong Kong are shown in ***Figure 10***. In 1995, the HDI of Hong Kong was 0.808 and followed a trend of increasing over time, so that by 2010, Hong Kong's HDI exceeded 0.9, which indicates that Hong Kong had achieved a high level of human well-being. Moreover, all three of these component indicators showed an upward trend over 22 years. According to the World Bank classification, high-income economies are those with a GNI per capita more than $12,746 [91]. In 1995, Hong Kong's GNI ($32,678, ***Figure 10***) was already higher than this value, and by 2016, the GNI of Hong Kong was $55,809, with an average annual growth rate of 2.71% from 1995 to 2016, which implies that for the people of Hong Kong, both incomes and quality of life improved over time. The life expectancy index was consistently at the highest level among these indicators. The life expectancy at birth rose from 79.0 years (1995) to 84.0 years (2016), an above-average value for most countries in East Asia and the Pacific, such as China (76.3 years, 2016), Singapore (83.0 years, 2016), and Japan (83.8 years, 2016) [89], reflecting the relatively good health of the people of Hong Kong.

The education index was lower than 0.7 between 1995 and 2000. However, from 2001 to 2008, it increased meaningfully to exceed 0.8, which reflected a higher knowledge level in Hong Kong. To illustrate this change further, as shown in ***Figure 10***, the distribution of educational attainment of population, it was not just that the expected years of schooling increased each year (from 13.4 (1995) to 16.3 (2016)), but also the structure of educational attainment that was optimized. Moreover, since 2010, the category of those whose education ended at the secondary level (including technical, non-degree and degree courses) also began

to shrink, indicating a trend of people obtaining higher levels of education, creating a more healthy and sustainable society in Hong Kong. Above all, when sustainability is viewed through the lens of human development, the HDI of Hong Kong indicates a high level of sustainability, and in 2017, it ranked seventh in the world.

2.4. Discussion and implications

2.4.1. The state of sustainable development in Hong Kong

Sustainable development of human society relates not only to the improvements of humanity, but also the sustainability of the environment. Therefore, the ecological footprint and biocapacity were adopted to measure human consumptions and natural supplies. ***Figure 10*** shows that the economic growth and human improvements of Hong Kong progressed significantly from 1995 to 2016. But this also caused an obvious increase in the size of the ecological footprint and a decline in biocapacity, which resulted in a serious ecological deficit (***Figure 9***). This reveals that although both economy and human well-being improved in Hong Kong, in terms of environmental considerations, development in Hong Kong is still following an unsustainable development trajectory.

Naveh [92] asserted that the human urban ecosystem was primarily driven by fossil fuels, as is the case in Hong Kong (***Figure 6***), and environmental pollution and greenhouse gas emission will be aggravated by the heavy dependence on fossil fuel energy. In turn, the effects of climate change, such as a rising temperature could also impact energy consumption [93] .

Second, it is notable that the ecological footprint of the water area was also very large (***Figure 6***), even larger than the fossil fuel footprint before 1998. As the productivity of local waters is

very limited, Hong Kong's seafood consumption mainly relies on imports from other parts of the world. The overconsumption has had a significant negative impact not only on the local marine ecosystem but also on the Indo-Pacific [94]. Unfortunately, such problems have not been mitigated in recent years but have tended to escalate. By 2016, the local fishery resources dropped by 27% [95]. At present, only 1.5% of all marine areas are designated as being protected by Hong Kong, and there are other threats to the biocapacity of the water area: (I) the lack of an explicit coverage area, goals, or a time schedule for the establishment of a future marine protection zone; (II) the lack of specific and effective management for existing protection zones; and further, (III) the failure of the government and experts to effectively organize positive discussion for the protection site selection, and failure of fishermen to timely participate [96].

In brief, although sustainability viewed through the lens of human development was maintained at a high level in Hong Kong, the large ecological footprint and environmental issues prevent Hong Kong from approaching Goal 12 (sustainable consumption), 14 (sustainably use the marine resources) and 15 (sustainable use of terrestrial ecosystems). To prevent the negative impacts mentioned above and move toward a more sustainable development future, the large ecological footprint should be decoupled from human society development.

2.4.2. Comparison of Hong Kong with the best sustainable practice city-states—Singapore

As Asian city-states, Singapore and Hong Kong have many similarities. Both were colonized by the British in the nineteenth century and created by immigrant populations from China, and

both have economies that grew out of their status as entrepots [97]. Both face the problems of limited land, high urban density, and poverty of natural resources.

In the 1960s, Singapore started its journey toward sustainability. Thereafter, a series of policies and movements were implemented, such as the Keep Singapore Clean Campaign in 1968 and the Clean Air Act in 1971, which transformed Singapore into a more sustainable city [98]. However, the development of Hong Kong shows an obviously different trend. For instance, although the HDI of Hong Kong and Singapore both reached 0.93 in 2016 (***Figure 11***), the size of their ecological footprints has diverged in recent years. In order to explore how a human society can advance without an increased ecological footprint, we compare Hong Kong with Singapore.

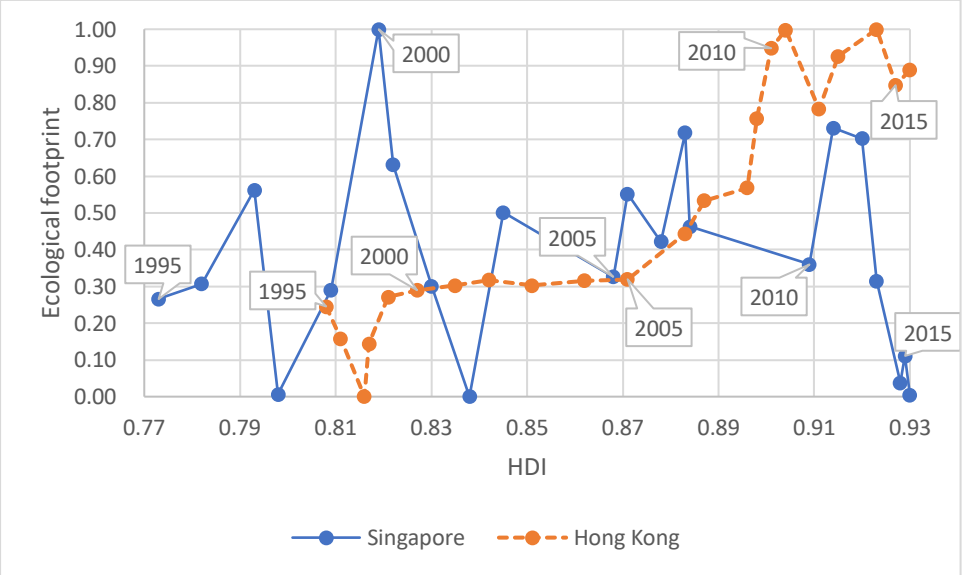

Figure 11. The normalization of HDI and the ecological footprints of Hong Kong and Singapore. Because the ecological footprint results of Singapore and Hong Kong are from different data sources, they cannot be compared directly. Therefore, to focus on the comparison of trends instead of the specific numerical value, the rescaling (min-max normalization) method was used to present the vertical axis. This method does not change the distribution characteristics of data. The general equation for a min-max of [0, 1] is given as: $X_{norm}=$

$\frac{X-X_{min}}{X_{max}-X_{min}}$ where X is an original value, X_{norm} is the normalized value, X_{max} and X_{min} are the maximum and minimum of the original dataset. (The HDI values of Hong Kong and Singapore are our own elaboration from UNDP- Human development data [89])

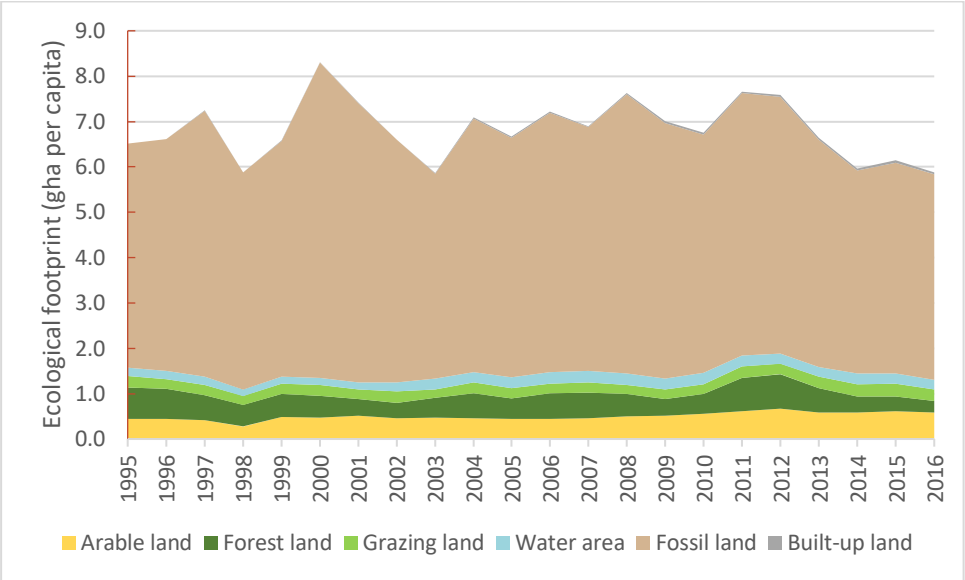

Figure 12. Singapore's per capita ecological footprint by land category during 1995-2016.
(Our own elaboration from Global Footprint Network [99])

Singapore is an island city-state in Southeast Asia with only 719.2 km^2 land area and a population of about 5.6 million (2016). Although it is about half the size of Hong Kong, its natural resource consumption rate is quite high. Singapore had one of Asia-Pacific's largest ecological footprints per capita [100]. Similar to Hong Kong, the consumption of the water area resource was also very large, as an average of more than 100,000 tons of seafood is consumed each year in Singapore, making it one of the biggest seafood consumers in the Asia-Pacific region [101]. In addition, the fossil fuel footprint historically took up the largest proportion of the total ecological footprint (***Figure 12***, ***Table S 4***)--its average value over the past 22 years is 5.36 gha/cap.

However, it is notable that the size of Singapore's ecological footprint has decreased continuously since 2011, while the HDI has continued to rise (***Figure 11***). By contrast, in this time, the size of Hong Kong's ecological footprint has continued to increase.

To decouple an increased ecological footprint from improvements in human society, Singapore decreased its fossil fuel footprint and followed by reducing the forest land footprint. Market liberalization of Singapore has led to rapid replacement of oil-fired steam plants with gas-fired combined-cycle gas turbines, which has lowered the carbon intensity [102]. Besides, compared with the pipeline natural gas that imported from Indonesia and Malaysia, the liquefied natural gas, a form of natural gas that can be more easily transported on a global scale, has started to be imported in 2013, to diversity and secure energy source for Singapore [103]. Furthermore, solar photovoltaic (PV) systems have been actively deployed since 2010 [104]. And beyond 2020, the adoption of solar power will be further raised to 1 GigaWatt peak (GWp). Undoubtedly, this will help Singapore to achieve its climate change pledge of reducing the emissions intensity by 36% from 2005 levels by 2030 [105].

On the other hand, because Singapore has no wind, hydro, or geothermal resources, and the land for deploying solar power is also limited, the government must rely on more innovative, resilient and sustainable energy strategies:

(I). Transportation. One of the key elements in managing environmental footprint [106] and urban sustainable development is sustainable transport [107]. In Singapore, it has been achieved by enhancing public transport, improving resource efficiency, and reducing carbon emissions [106] , such as the use of electric vehicles was assessed on a national scale, and it was determined that their efficiency was higher than that of gas vehicles [108].

(II). Electricity. The government is optimizing smart metering technology to reduce the cost of electricity. These automation devices could help people cut wasteful or unintentional usage, and potentially shift usage patterns to off-peak periods when the electricity price is lower. Moreover, this technology has been introduced as a part of the Intelligent Energy System project, which uses a smart grid to better manage electricity [108].

(III). Raising the awareness of energy conservation. For instance, a new mobile app was created to help households compare their electricity, water, and gas consumption with neighbors, to enable consumers to use energy efficiently, and to potentially lower their utility bills and carbon footprint [109].

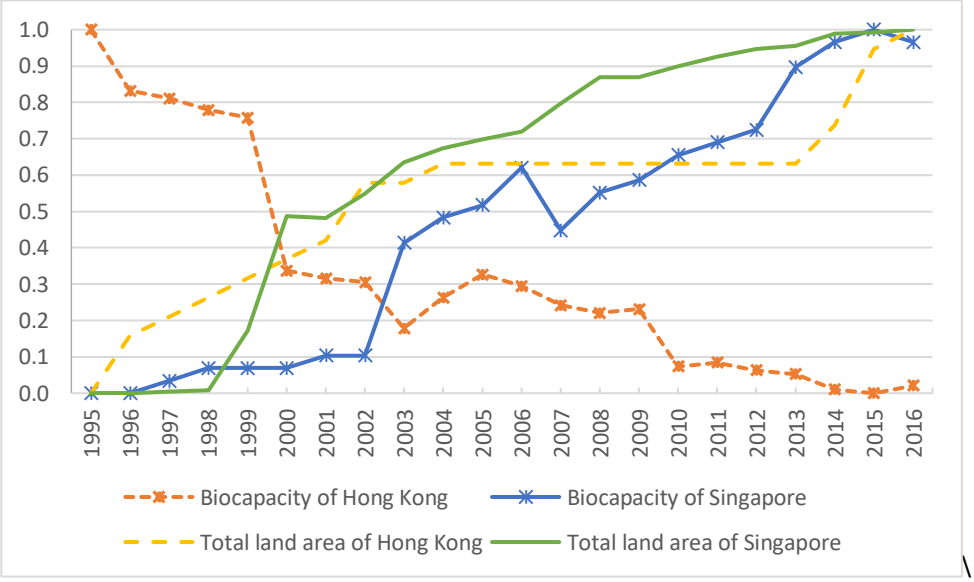

Figure 13. The normalization of biocapacity and total land area of Hong Kong and Singapore.

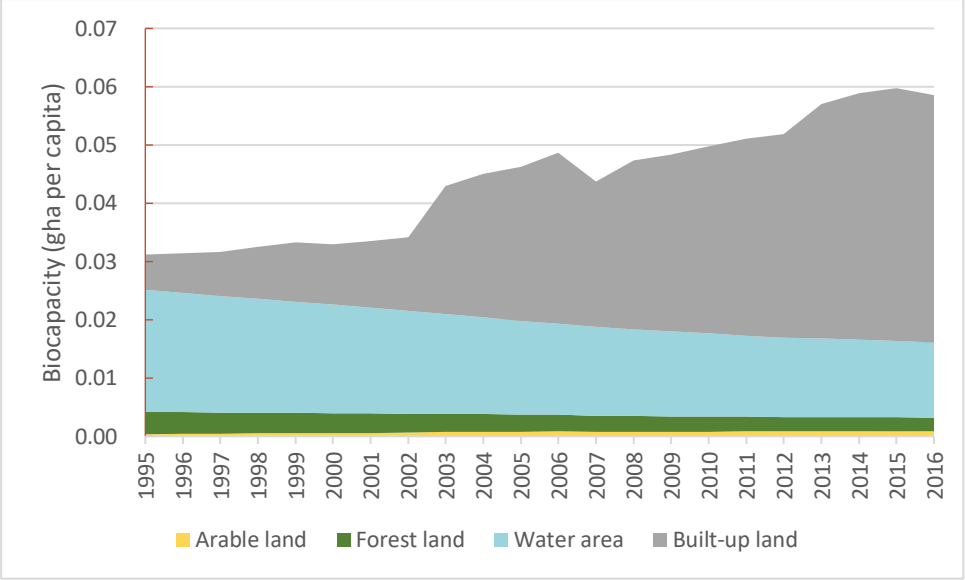

Figure 14. 1995–2016 Singapore's per capita biocapacity by land category.
(Our own elaboration from Global Footprint Network [99])

From 1995 to 2016, the biocapacity trends of Hong Kong and Singapore were obviously opposite although both total land areas increased (***Figure 13***). With regard to the biocapacity of Singapore, the biocapacity of water area and forest land decreased gradually, whereas, the striking growth of built-up land caused the total biocapacity to rise significantly (***Figure 14***, ***Table S 5***). This mainly resulted from long-term sea reclamation. The land area of Singapore increased from 581.5 km^2 to 719.2 km^2 between 1965 and 2016, namely, land area increased by 23.6%. Before 2000, the reclamation area grew slowly, increasing by 5.98 km^2 from 1990 to 2000. However, the reclamation rate rose dramatically to 1185% between 2000 and 2010 [110]. This is why the biocapacity of Singapore has increased rapidly since 2000.

Although reclamation projects were also implemented in Hong Kong, the reclamation rate was far less than in Singapore. The total land area increased from 1092 km^2 (1995) to 1111 km^2 (2016) with an average annual growth rate of 0.08%. In addition, the brownfield and

deserted agricultural land in rural areas will also be developed into urban space [57]. Therefore, it can be expected that the biocapacity of arable land and grazing land will shrink further, whereas the biocapacity of built-up land will increase.

The high rate of reclamation in Singapore had come at a significant cost to the marine ecosystem. About 65% of the original reefs had been lost to reclamation since the 1960s [111]. With the increased public awareness of the need for environmental protection, the government realized that the reclamation paradigm needed to change, which led to more positive recent actions. This transformation provides an optimized way to balance the socio-ecological system and make the coastal ecosystem more sustainable where the development is intensive.

2.4.3. SWOT analysis and policy implications for decoupling ecological footprint from the development of human society

In order to provide scientific evidence and tailor-made suggestions for policy based on the comparative analysis above, a SWOT analysis was adopted to summarize the current strengthens, weaknesses, future opportunities, and threats to Hong Kong and Singapore. SWOT analysis is a tool used for formulating strategic planning and management, helping planners leverage strengths and opportunities to reduce weaknesses and threats [112] , as shown in ***Table 3***.

Table 3. SWOT analysis of sustainable development of Hong Kong and Singapore.

SWOT	Hong Kong	Singapore
Strengths	·Strategic geographical location. ·Global financial hub. ·Well-protected terrestrial nature reserves, such as country parks [57]. ·High level of HDI. ·Sustainable transport system [113].	·Advantageous geographic position. ·The central trade hub in Asia. ·Effective government. ·High level of HDI. ·Relatively strong in innovation and technology [114]. ·High vegetation coverage rate. ·Sustainable transport system.
Weaknesses	·Limited developable land. ·Relatively weak in innovation and technology [61]. ·Air pollution and municipal solid waste generation and disposal [61]. ·High ecological footprint. ·Government deficiencies in efficiency of environmental protection [115], [116].	·Lack of land resource. ·High ecological footprint, especially for the water area. ·No indigenous energy resources. ·Habitat fragmentation and biodiversity loss [117].
Opportunities	·Optimizing use of developed land and creating new land [57]. ·Current policies for promoting urban sustainable development, such as creating environmental capacity.	·Integrating sustainability directly in policy process. ·Clean energy companies are building capabilities, such as wind plants, smart grid [114]. ·Optimizing space by transforming existing areas into new growth districts [117].
Threats	·Limited indigenous resources, especially energy resources and the deterioration of water resources [61], [118]. ·Climate change [61], [117] . ·Waste Management [61], [98] .	

Note: This table mainly describes the SWOT of the environment and resources-related sustainable development. The "Threats" shows the issues that both Hong Kong and Singapore face.

Sustainable development includes environmental, economic and social sustainability [119]. However, based on the ecological footprint and HDI assessment (see ***Figure 10*** and ***Figure 11***), while the economy and society developed well in Hong Kong, the level of environmental sustainability lagged behind, as shown in the "Weakness" and "Threats" in SWOT analysis (see ***Table 3***). In 1995, Brown [120] claimed that to ensure a sustainable future, people need to carry out an environmental sustainability revolution. To this end, close engagement and support from government are indispensable, and this is where the Hong Kong government falls short (see ***Table 3***). Hereby, in this part, we put forward some policy suggestions for energy consumption, marine environment protection, and changes in the behavior of citizens and government—to decouple a large ecological footprint from the development of human society.

2.4.3.1. Energy consumption

Because fossil energy consumption took up the largest part of the ecological footprint, there is a great potential to decrease the entire ecological footprint significantly by replacing fossil energy with renewable energy. Singapore is not the only one running on this trajectory—Beijing also presented a positive trend. The energy structure had been adjusted effectively in Beijing, and with an increasing proportion of power generation from renewable sources and the decline of fossil fuel consumption, the ecological footprint decreased by approximately 25.8% from 1997 to 2014 [121] . Hopefully, the ecological footprint can also be significantly reduced in Hong Kong by using renewable energy. We propose these policy suggestions for Hong Kong:

1. Accelerate the development of the smart metering infrastructure and the smart grid. The electricity accounted for about 50% of energy end-uses between 2004 and 2014 in Hong Kong [122]. Thus, efficiently managing and allocating electricity could significantly contribute to the decline of energy consumption. Although the smart grids have been introduced in Hong Kong already, the related research and application are limited and small in scale [123]. Technical aspects of smart grids, the formulation of a specific policy framework, plans, and implementation of the program should be accelerated.

2. Deploy/import more renewable energy, such as from mainland China. The government could also simplify market rules and regulations for electricity consumers to make it easier for small consumers to receive payment for injecting renewable energy into the power grid and streamlining the metering requirements for renewable energy owners [104].

3. Spur research into promising energy technologies and systems-level innovation. The government could formulate a suit of incentive mechanisms to support applied research in smart grid, energy conservation, and storage, etc. For instance, Singapore has awarded more than $100 million in funding to date to support a Research and Development project which aims at addressing Singapore's energy challenges, such as the smart grids, solar forecasting, and power utilities.

4. Facilitate the commercialization of energy innovation. For instance, the government can build a bridge to engage company members, industry players, researchers, academia, and youth to better communicate needs and opportunities [104].

2.4.3.2. The protection of the coastal and marine environment

According to the results of Hong Kong's ecological footprint, it is noteworthy that the water area footprint was also relatively large (see 2.3.1, and ***Figure 6***). However, the marine

ecosystem, which provides numerous services to human society, has deteriorated due to the negative impacts of human activities. Therefore, policies and regulations that protect the marine environment need to be formulated and monitored further.

1. Expand the area of the marine environment protection zone. Although the Hong Kong government has established marine protection zones since 1966, the area covered by protection zones is still quite small to date. WWF has suggested that the area of protection zones should account for at least 10% of Hong Kong's offshore and marine waters before 2020. In addition, Russ et al. [124] noted that the establishment of marine protected areas can also benefit the development of local fishery resources.

2. Strictly forbid marine litter. Marine litter is a long-standing and prominent problem (see ***Table 3***: "Threats"). Each year, the Hong Kong government cleans about 15,000 tons of marine litter. However, vast quantities of garbage remain [125]. Actually, the source of about 95% of marine litter is local garbage [126], meaning that a significant improvement can be achieved by the efforts of local communities and government.

3. Do not allow commercial fishing and sea reclamation in marine ecological hotspots (see 2.4.2: point (II) and (III)). Hotspots are the areas featuring exceptional concentrations of endemic species and species facing the threat of human activities [127]. Protecting these hotspots not only supports the holistic management of marine resources but it can also strengthen the resilience of the marine ecosystem to natural disasters and climate change [128].

4. Apply green infrastructure (GI) to the coastal and reclamation projects. Drawing lessons from the coastal development experience of Singapore (see 4.2), protection of the natural environment should be considered while addressing the land requirements for urban expansion. Recently, the GI has received attention and has been widely implemented in many

places, such as the US, Canada, and Europe [129]. GI is not only contributing to the enhancement of ecosystem services but it can also support an increasing population's demands for resources [130], [131]. It is an environmentally-friendly and economical method for achieving urban sustainable development, resilient communities, and climate change mitigation [129].

2.4.3.3. The improvement of citizens' awareness and government's executive action

To progress toward a sustainable future, the joint efforts of citizens and government are indispensable. Nevertheless, the Hong Kong government lacks efficiency in management and protection of the environment (see 4.1: point (I) to (III) and ***Table 3***), in addition, Hong Kong is also characterized by high per capita resource consumption. Hereby, we offer the following suggestions:

1. To citizens: Reduce overconsumption. In light of the International Fashion Consumption Survey report [132], about 68% of Hong Kong people admitted that they consumed far more clothes than they actually need and use. Further, food consumption through waste could be reduced, especially during festivals. For instance, during the Mid-Autumn festival in 2010, about 1.87 million mooncakes were discarded in Hong Kong, which is equivalent to 1,200 tons of carbon dioxide emissions [133]. By educating the younger generation through public campaigns and commercial advertisement to reduce overconsumption and the related ecological footprint can be declined.

2. To government: Separate duties for each government department clearly and strengthen supervision. For instance, as shown in the weaknesses part of SWOT analysis(***Table 3***),the vague separation of duties of departments and the simple management mode of garbage disposal in Hong Kong makes environmental action less effective [115],

[116]. Therefore, the adjustment of relevant government departments is needed so that duties are allocated explicitly and supervision is enhanced. If necessary, enforcement regulations can be formulated according to the situation, to control the behavior of citizens and provide supervisors with support.

2.5. Conclusion

This chapter provides an analysis that combines ecological footprint, biocapacity, and HDI to assess the sustainable development state of Hong Kong from 1995 to 2016. The results show that the ecological footprint had exceeded the local biocapacity significantly and fossil energy consumption was the biggest contribution. Although Hong Kong's economy, educational level, and standard of living have been rising over the past 22 years, the growth behind this was based on the imbalance of environment development, with an increasing ecological deficit year by year. This indicates that there is a significant gap between the current development model and Hong Kong's goal of becoming Asia's most sustainable city [134]. Furthermore, through the comparison of Hong Kong and Singapore, we conclude that there is a great potential to decouple the high ecological footprint from the development of human society, and reach a high HDI and low footprint society by replacing fossil energy with renewable energy. Moreover, an optimum balance value, which is the lowest footprint for maintaining a sustainable human society development, could be explored further to quantify the boundary relation of ecological footprint and human society. Finally, based on the SWOT analysis and implications from the experience of Singapore, we put forward some policy suggestions (energy consumption, marine environment protection, and changes in the behavior of citizens and government) for Hong Kong's sustainable transformation. As a world-class metropolis, Hong Kong plays an important role not only in China but also around

the world, and we hope this research achievement could assist Hong Kong in achieving Goal 11 of SDGs and make a positive impact on the world.

CHAPTER 3: A Scenario- and Spatial-Downscaling-Based Land Use Modeling Framework to Improve the Projections of Plausible Futures: A Case Study of the Guangdong–Hong Kong–Macao Greater Bay Area, China

3.1. Introduction

Scenario analysis is widely recognized as a powerful tool for assessing and investigating the changes in social, climatic, and environmental systems [135], [136] to support governments in developing strategies to achieve the 17 Sustainable Development Goals (SDGs) and development planning [137]. For this purpose, multiple scenarios have been created to explore alternative futures. For instance, the shared socioeconomic pathways (SSPs), which were catalyzed by the International Panel on Climate Change (IPCC) [138] in 2010, are comprehensive global frameworks that can make significant advances from the previous scenarios [139] and provide a wide range of information on possible future socioeconomic developments [140], [141]. The SSPs have been developed by climate change research community and describe five different plausible pathways, with varying degrees of mitigation and adaptation potentials [142], [143]. The pathways are as follows: SSP1–sustainability (taking the green road); SSP2–middle of the road; SSP3–regional rivalry (a rocky road); SSP4–inequality (a divided road); and SSP5–fossil-fueled development (taking the highway) [142]. SSP1 and SSP5 are relatively optimistic trends with high levels of human development and economic growth, as well as efficient environmental management, whereas SSP3 and SSP4 are relatively pessimistic trends with poor social development and environmental protection [144] (see O'Neill, et al. [142] for more details on SSPs).

Land use and land cover (LULC), being an important and direct driver of global environmental changes, is crucial for achieving sustainable development [145]–[149] . Thus, the spatio-temporal dynamic analysis and projection of LULC were considered as effective ways to understand the changes in LULC [150], [151] . Moreover, the SSPs provided LULC scenarios based on several assumptions, such as land productivity, food consumption, and land regulations [152] , thus enabling the exploration of different land-use changes and their consequences in the context of fundamental future uncertainties [143] . Furthermore, there are growing attentions in the SSPs applications to regional and local scales for serving to assist policy makers in developing robust climate change adaptation strategies and national or subnational planning, while also providing researchers working at regional, national, and subnational levels with multiple pathways [153]–[155] . For instance, based on the SSPs, Chen, et al. [156] used the Global Change Analysis Model and a land use spatial downscaling model to generate a new global gridded land-use data set. Gomes, et al. [157] used an interdisciplinary approach to develop spatially explicit projections of LULC under various SSPs in the Zona da Mata, Brazil, to help in the regional development and forest conservation planning. Hewitt, et al. [158] used SSP1 and SSP5, which were downscaled from Europe, at a regional level to study the impacts and trade-offs of future land-use changes in Scotland, UK.

In China, the LULC changes of the past two decades have been arguably the most widespread in the history of the country [159] . Unprecedented urban development poses a huge challenge to sustainable development. Therefore, numerous studies were conducted to project future land-use changes and provide references and suggestions to identify sustainable pathways and make policy decisions [160]–[163]. For instance, Liu, et al. [164] proposed a future land use simulation (FLUS) model to simulate multiple land use scenarios in China. Liao, et al. [165] performed land use simulations using the FLUS model under plant functional type

classification in the context of various SSPs in China. Chen, et al. [166] combined an urban growth simulation model with a multiregion input–output model to explore the teleconnections between the future urban growth of China and its impacts on the ecosystem services under different SSPs. However, the previous land-use projections related to China were performed on a national/provincial scale, with medium to coarse resolution (e.g., 1×1 km^2) [163], [167]. As these land-use projections made with a coarse resolution can lead to an underestimation of the influence of urbanization [165], a downscaled simulation at a higher resolution was required.

Thus, this chapter aimed to project the future land-use patterns at a higher resolution to explore the SSPs implications and the possible land-use changes caused by urban development on SDG 11: Sustainable cities and communities. For this purpose, we proposed a spatial downscaling framework that couples the global SSPs narratives and local land planning policy using a land change modeling method to simulate the future land-use scenarios.

3.2. Study area

The Guangdong–Hong Kong–Macao Greater Bay Area (Greater Bay Area) was used as the research object for the simulations of future land-use scenarios, it represents one of the most prominent and fastest growing regions of China [168]. However, for a long period, the urban development activities in the region have been concentrated in near-shore areas, and the ecosystem of the region has undergone degradation [169], such as an ecological deficit, due to an increased ecological footprint [170]. Therefore, the Greater Bay Area was chosen for a case study. The Greater Bay Area comprises the two special administrative regions, namely, Hong Kong and Macao, and nine municipalities, namely, Guangzhou, Shenzhen, Zhuhai, Zhongshan,

Jiangmen, Zhaoqing, Foshan, Huizhou, and Dongguan in the Guangdong Province, covering an area of approximately 56,000 km^2. Its total population was estimated to be over 71 million by the end of 2018 [171]. The Greater Bay Area is surrounded by mountains on three of its sides and is bordered by the sea on its southern side. Moreover, it has the Pearl River Delta plain at its center (***Figure 15***). Most of its area is at an elevation that is less than 200 m above sea level. The Greater Bay Area is the fourth largest bay area in the world, following San Francisco, New York, and Tokyo Bay Areas. Being one of the most open and economically vibrant regions of China, the Greater Bay Area is the key to the strategic planning of the development blueprint of the country and will develop into an international first-class bay area and a world-class city cluster [56].

In addition, Hong Kong was used as an example to demonstrate the application of the projected land-use maps owing to the fact that it is among the top cities in the world in terms of per capita consumption of goods and resources [172]. The rapid growth of its population and economy places a heavy burden on land supply, which is being overcome by the reclamation of land from the sea [173]. In 2018, its total population was 7.48 million [174], and its total land area was approximately 1,110 km^2. Hong Kong occupies only 1.98% of the Greater Bay Area (***Figure 16***), although its population is approximately 10.54% of the total population of the Greater Bay Area. Being a developed and typically high-consumption city of the Greater Bay Area, Hong Kong could be used to demonstrate the sustainable development of cities. Therefore, we have confined our observations to Hong Kong.

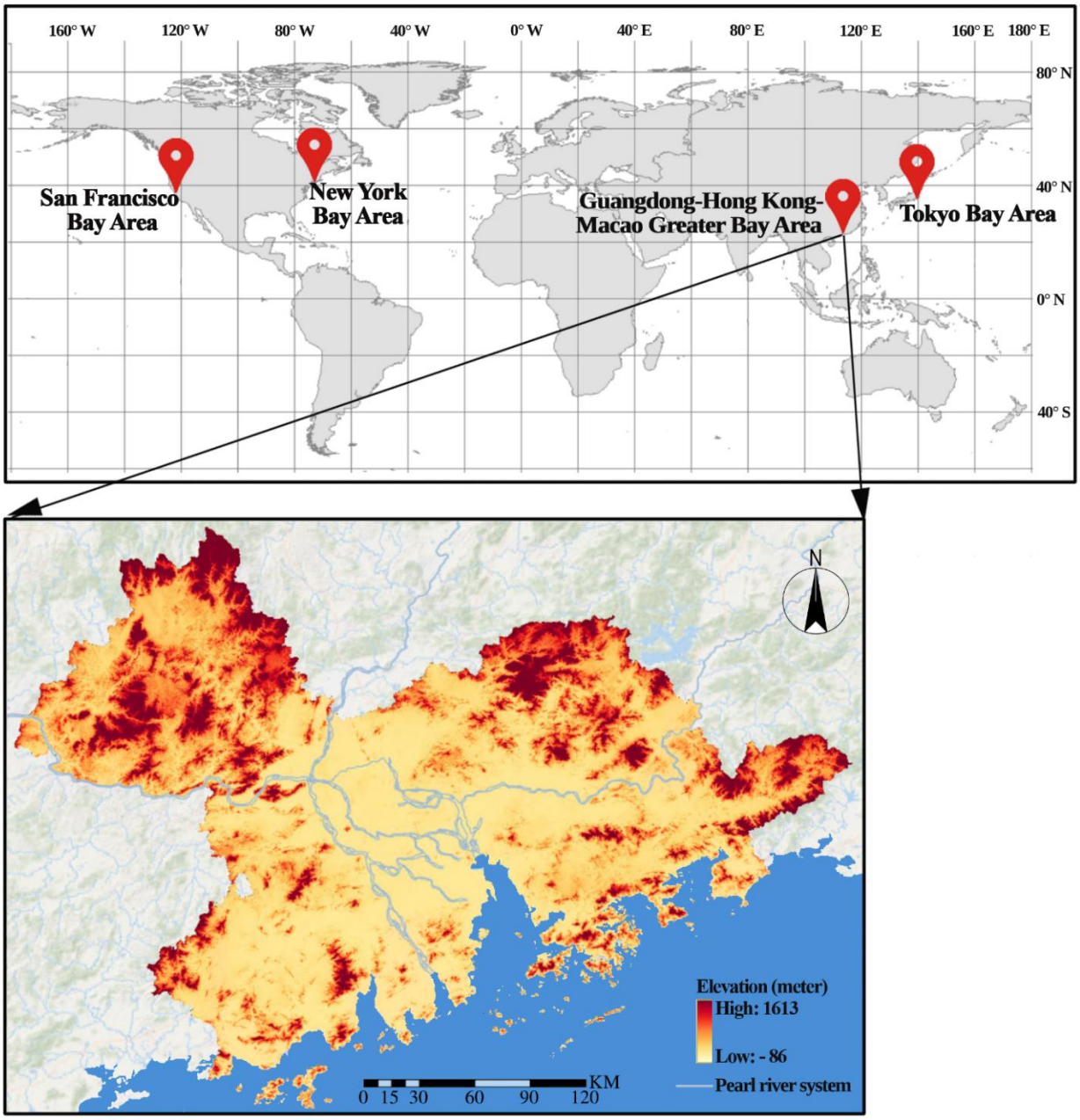

Figure 15. Location of the Greater Bay Area, China.

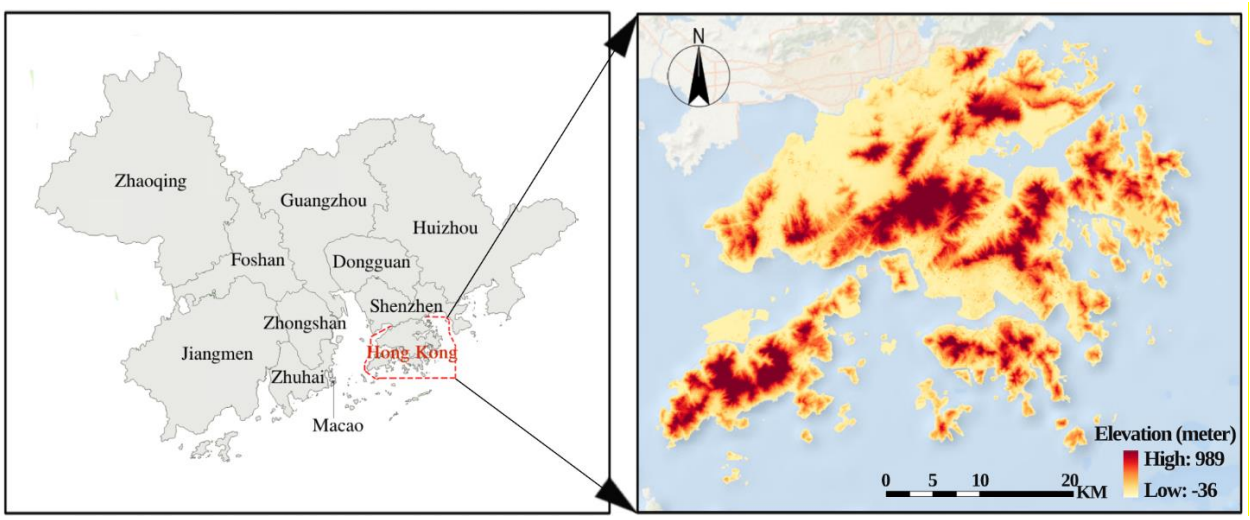

Figure 16. Location of the Hong Kong Special Administrative Region, China.

3.3. Materials and methods

Figure 17 presents the framework used in the study. The core feature of the framework is the spatial downscaling simulation that can be used in the projections of future land-use scenarios. It combines the global SSPs narratives with the local land planning policy using a land change modeling method. Two types of outcomes were projected by using the Land Change Modeler (LCM) software, which is an integrated module of TerrSet 18.31 [175]. One outcome consists of the business-as-usual (BaU) land-use map, which represents the continuation of the past trends in the Greater Bay Area and could be directly generated using its default transition probability matrix without any interventions (*Figure 17*). The other outcome represents land-use maps under various global SSPs combined with the local land planning policy and used the 1-km resolution future land-use gridded maps. These maps were projected by Liao, et al. [165] and Li, et al. [176] as initial reference data to adjust the transition probability matrix in order to generate outcomes at a 300-m resolution, thereby achieving spatial downscaling. Considering the implementation period of the current local land planning policy and roughly the same pattern of population distribution from 2020 to 2030 [177], 2030 was selected as the time

horizon in the scenario simulations. Furthermore, the nature reserves and future population distribution maps were used as the planning constraints and incentives to further shape the spatially explicit future land-use patterns. Finally, Hong Kong was used as an example to demonstrate the application of the projected land-use maps. The following section describes the reasons for choosing the LCM and its specific operations.

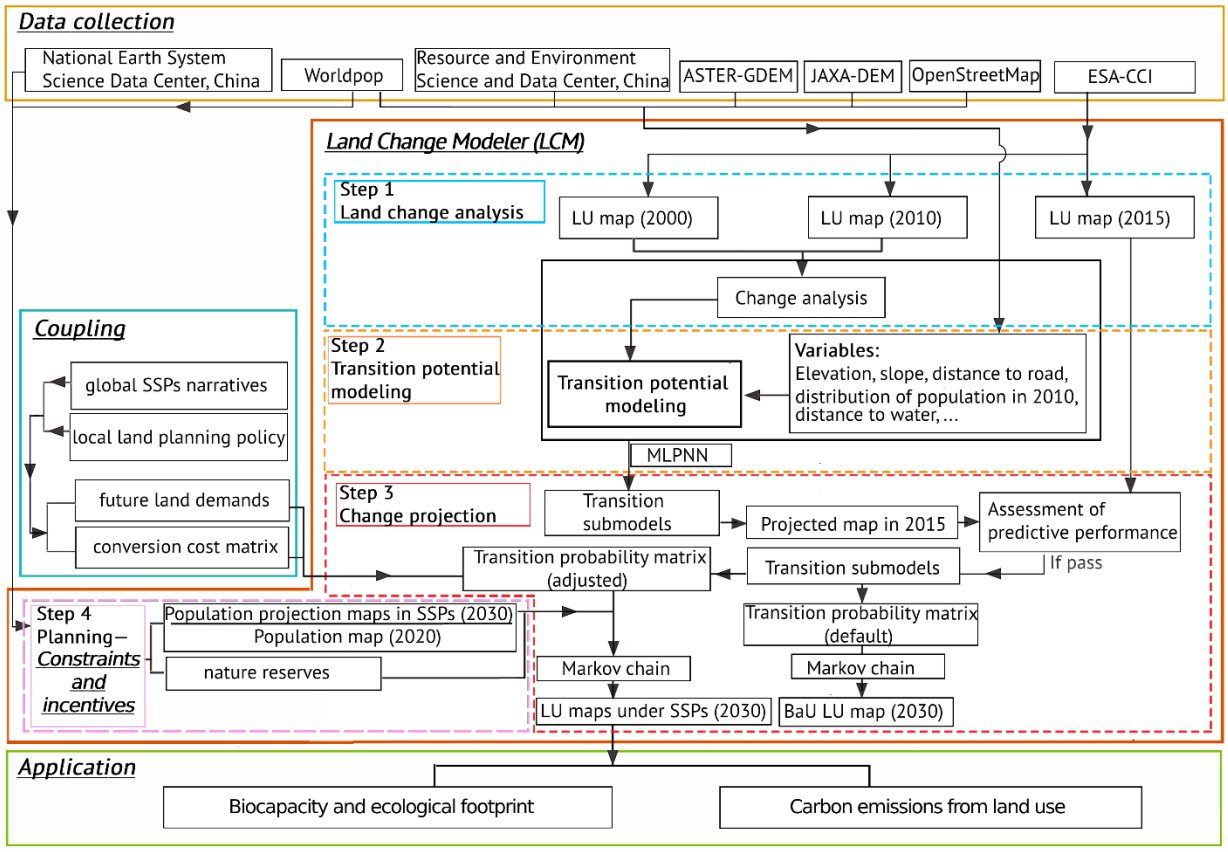

Figure 17. Research framework.

LU stands for land use and MLPNN for multilayer perceptron neural network. The yellow, red, cyan, and green solid lines indicate data collection, LCM simulation, coupling of global SSPs narratives with the local planning policy, and application that is based on projected land-use maps, respectively; the blue, yellow, red, and pink dashed lines denote the four subcomponents of LCM.

3.3.1. LCM

Out of the various methods used for scenario building, the Markov chain modeling is the most common approach used to quantify future changes, particularly in pattern-based models [178]–[180]. The Markov chain modeling calculates the transition areas/probability matrix *via* cross-tabulation between the land-use categories of two maps [181]. The LCM is being applied in many disciplines [182] and is being widely used to project land-use changes under different future scenarios/land-use policy interventions [183], [184]. The LCM is an effective and powerful model owing to its Markov chain-based neural network [168], [185]. Therefore, we selected the LCM (version 18.31) to project the land-use patterns of the Greater Bay Area for 2030. Four major subcomponents of the LCM ***(Figure 17***) were used: (1) land change analysis, (2) transition potential modeling, (3) change projection, and (4) planning.

3.3.1.1. Step 1: Land change analysis

Two land-use maps of 2000 and 2010 (***Figure 17***, ***Table 4***) were utilized in the land change analysis. Six land-use classes were identified, namely, cropland, forest, bush and grassland, urban area, barren land, and water. The land transitions were identified based on the calculated gains and losses of the land-use classes. Land transitions in areas less than 10 km^2 in extent were disregarded; only the dominant transitions that included 99% of the transitions were used for the modeling.

Table 4. Data sources.

Name	Time	Resolution	Organization	Source
Land-use and land cover map	2000, 2010, 2015	300 m	ESA-CCI	https://www.esa-landcover-cci.org/?q=node/158
Road map	2013	Shape file	OpenStreetMap	https://download.geofabrik.de/
River map	——	Shape file	Resource and Environment Science and Data Center, China	http://www.resdc.cn/data.aspx?DATAID=221
DEM	2019	30 m	ASTER-GDEM; JAXA-DEM	https://ssl.jspacesystems.or.jp/ersdac/GDEM/E/ https://www.eorc.jaxa.jp/ALOS/en/aw3d30/
Nature reserves	2015	Shape file	National Earth System Science Data Center, China	http://www.geodata.cn/data/datadetails.html?dataguid=120209853934500&docId=9768
Population map	2010, 2020	100 m	Worldpop	https://www.worldpop.org/geodata/listing?id=69
Population projection maps in SSPs	2030	100 m	Chen, et al. [186]	

Note: Due to the fact that the population projection maps of the SSPs that were created by Chen et al. (2020b) do not involve Hong Kong and Macao and based on the data obtained from IIASA [187], the population projection maps of these two areas were computed using the spatial distribution pattern of the population in 2020. Please refer to supplementary material for more details.

3.3.1.2. Step 2: Transition potential modeling

Two setups of the transition submodels, namely, the submodel structure and simulation approach, were employed to compute the transition potentials. Initially, 14 potential independent drivers (***Figure 18***) related to land-use changes were selected. Then, using

Cramer's V approach that can measure the association between each driver and each land class, 12 strongly associated variables exceeding 0.2 in value were identified [188] to build the submodel structure.

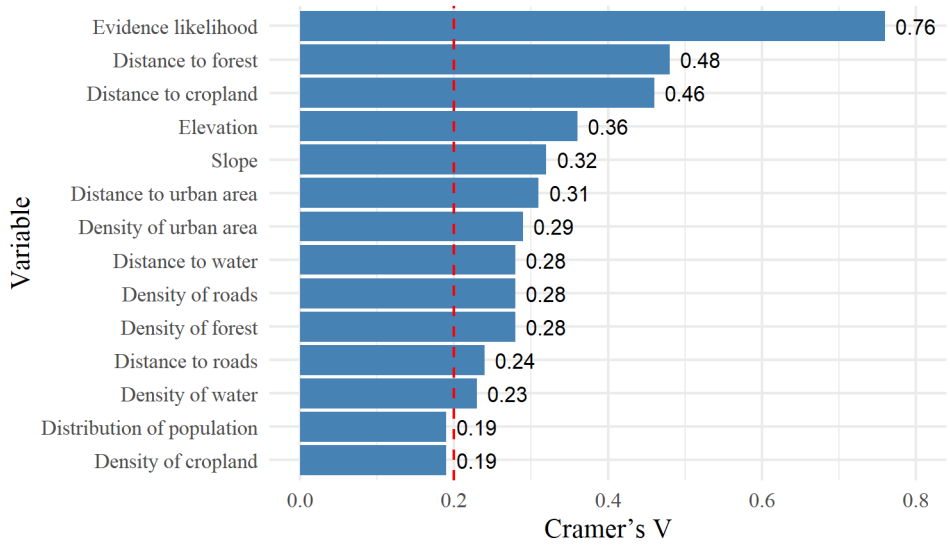

Figure 18. Variables used for building the submodels of the LCM.

Evidence likelihood is effective for incorporating categorical variables into an analysis [189] and can be generated in the *variable transformation utility* panel of the LCM.

The submodel has three options for the simulation approach, namely, multilayer perceptron neural network (MLPNN), similarity-weighted instance-based machine learning (SimWeight), and logistic regression. However, both the SimWeight and logistic regression approaches can perform only one transition per submodel, whereas the MLPNN can run multiple transitions (up to nine) per submodel [189] and robustly simulate nonlinear relationships [183]. Therefore, the MLPNN simulation was adopted to model the land-use transitions from 2000 to 2010.

3.3.1.3. Step 3: Change projection

The changing quantity of each transition can be modeled to generate a plausible future land-use map through a Markov chain or specification of the transition probability matrix [189]. The BaU case in the present study was generated using the default transition probability matrix without any modifications (***Figure 17***). The LCM can produce two modes of change projection, namely, hard and soft projections. A hard projection is a commitment to a specific scenario. Contrarily, soft projection is a continuous mapping of the degree of vulnerability to change in the 0 to 1 range, with high values indicating high susceptibilities to change. The soft projection indicates the extent to which an area has the conditions adequate to undergo changes, without showing what exactly will change [189]. Therefore, hard projection was adopted to assess the predictive performance under the BaU scenario.

3.3.1.4. Step 4: Planning constraints and incentives

The constraints and incentives, which are embedded in the planning subsection of the LCM, can be specified for each of the transitions to enable the integration of change allocation into the projection process thus making the model more robust [189] and can shape the future land-use pattern further. Zero values on the map relate to absolute constraints, values between zero and one to disincentives, values equal to one as no-constraints, and values greater than one to incentives. In the study, two types of maps were considered as the constraints and incentives: (1) the population distribution maps under SSPs were used to create constraint and incentive layer by dividing the future population projection map for 2030 (100 m resolution) [186] by the population distribution map for 2020 (100m resolution) [190]. The total population of the Greater Bay Area for 2030 was estimated to be 99,575,075 by SSP1; 101,190,772 by SSP2;

102,183,566 by SSP3; 98,826,910 by SSP4; and 99,993,406 by SSP5 (***Table 6***). In 2020, the population of the area was 63,050,321; (2) the nature reserves in the Greater Bay Area (***Table 4***) were specified as constraints by assigning a value of zero to indicate that development was not allowed in the areas.

3.3.2. Correlating land use modeling with local land planning policy-coupled SSPs

The land transition probability matrix in the LCM could be edited to facilitate future projections and was determined by two key factors (***Figure 17***) : (1) future land demands and (2) the conversion cost matrix describing the difficulty of converting from the current land-use class to the target class [163], [164]. Therefore, land-use modeling and scenarios could be correlated by adjusting the two factors according to the local land planning policy and SSPs narratives.

First, with regard to the future land demands in the Greater Bay Area under the different SSPs, the studies by Liao, et al. [165], Li, et al. [176], and Li and Chen [191] were used as the main reference points. Liao, et al. [165] projected the future land use maps of China at a resolution of 1 km under the plant functional type classification of the SSPs. Therefore, the future areas of forest, urban area, barren land, and water could be calculated directly using the ArcGIS pro (version 2.2) software to extract the Greater Bay Area from China. Furthermore, the policy document named *Letter of support for the Guangdong–Hong Kong–Macao Greater Bay Area and Shenzhen to explore the reform of natural resources* [192] was introduced by the Ministry of Natural Resources in 2020. It urges the local government to adopt the cultivated land requisition–compensation balance policy to develop built-up land. Accordingly, if the local cultivated land is converted into built-up land, a piece of land of the same size and quality has to be reclaimed in another region for farming, thus guaranteeing the balance of cultivated land

throughout the country [193]. Thus, the demand for cropland was adjusted considering this important policy and according to Li and Chen [191], who projected the future impacts of the cropland balance policy of China under different SSPs. The bush and grassland area was determined based on the demands for the five land-use classes and the 1-km global land use data set [176]. In this way, the future land demands for the six land-use classes of the Greater Bay Area could be determined for 2030 (***Table 5***).

Table 5. Land demands (km^2) in the Greater Bay Area in 2030 under each SSPs, categorized according to land-use class.

	Cropland	Forest	Bush and grassland	Urban area	Barren land	Water
SSP1	20,567	19,746	2,373	9,561	50	3,461
SSP2	18,387	21,080	3,354	9,327	149	3,461
SSP3	17,158	21,463	4,872	8,703	101	3,461
SSP4	20,335	19,960	2,386	9,471	145	3,461
SSP5	20,539	20,112	2,006	9,471	169	3,461

Note: The BaU case was generated using the default transition probability matrix in the LCM (***Figure 17*** and Step 3), therefore, no extra adjustment of land demand or conversion cost matrix was required for BaU.

Second, the conversion cost matrix had to be determined in two steps: (1) combining SSPs narratives with local land planning policy to qualitatively determine the difficulty levels of land-use conversion and (2) quantifying those difficulty levels. In the first step, the policy documents named *Land Planning of Guangdong Province* [194], [195] and *Letter of support for the Guangdong–Hong Kong–Macao Greater Bay Area and Shenzhen to explore the reform of natural resources* [192] were used as the references. The future land-use policies relevant to the period around 2030 were then extracted and taken as a reference for SSP1 as the sustainable

development of the Guangdong province was integrated into a strategic goal [196]. The difficulty of combining land-use narratives [152] (***Table 6***) with the local land planning policy under each SSP can be at one of three levels: difficult, moderate, and easy (***Table 7***). In the second step, SSP2 was considered to be the basic reference, and the conversion cost matrix derived from Liu, et al. [164] was assumed to be the SSP2 conversion cost matrix (***Table 8***) as it was estimated based on the opinions of local experts and the analysis of historical land use. Next, 1.5, 1.0, and 0.5 were identified as the difficult, moderate, and easy levels, respectively, using test methods. Considering the qualitative difficulty level of land-use conversion in each SSP (***Table 7***) and the values of the three difficulty levels used to adjust the SSP2 conversion cost matrix, the conversion cost matrices for SSP1, SSP3, SSP4, and SSP5 were obtained (***Table S 6***-***Table S 9***).

Finally, after defining the future land demands and conversion cost matrix for each SSP, the linear programming (LP) method was used to determine the land transition probability matrices for each SSP (***Table S 10***-***Table S 14***) using the solver function of Microsoft Excel (Plus 2019 version). The LP approach for determining the land transition probability is a relatively new method employed in scenario analysis [197]. The derivation of the land transition probability matrix M (=[m_{ij}]), where the m_{ij} values denote the land transition probability from land-use class i to j for a given period, was proposed by Hashimoto, et al. [188].

Based on all the processes described above, the land-use maps of the Greater Bay Area under the different SSPs could be projected for 2030 using the LCM.

Table 6. Overview of land-use narratives and demographic factors of the five SSPs.

	SSP1	SSP2	SSP3	SSP4	SSP5
	Sustainability	Middle of the road	Regional rivalry	Inequality	Fossil-fueled development
Land-use					
Land-use change regulation	Strong regulation to avoid environmental disruption	Medium regulation	Limited regulation; continued deforestation	Highly regulated in MICs and HICs; lack of regulation in LICs	Medium regulation
Land productivity growth	High improvements in agricultural productivity	Medium pace of technological change	Low technology development	High improvements for large-scale industrial farming; low for small-scale farming	Highly managed, rapid increase in productivity
Environmental impact of food consumption	Low growth in food consumption, low-meat	Material-intensive consumption, medium meat consumption	Resource-intensive consumption	Elites: high consumption; Rest: low consumption	Material-intensive consumption, meat-rich diets
Population growth					
High fertility	Low	Medium	High	High	Low
Other low fertility	Low	Medium	High	Medium low	Low
Rich low fertility	Medium	Medium	Low	Medium low	High

Population projections of the Greater Bay Area in 2030	99,575,075	101,190,772	102,183,566	98,826,910	99,993,406
Urbanization level					
HICs	Fast	Central	Slow	Central	Fast
MICs	Fast	Central	Slow	Fast	Fast
LICs	Fast	Central	Slow	Fast	Fast

HICs, MICs, and LICs stand for high-, middle-, and low-income countries, respectively. The land-use narrative was derived from the work by Popp, et al. [152] . The narratives of population growth and urbanization level were derived from the work by Jones and O'Neill [141] . The demographic factors driving population change in countries were categorized into the following groups as a function of the fertility and income levels: high fertility, low fertility with high income (i.e., as in the member countries of the Organization for Economic Cooperation and Development), and low fertility. The population projections of the Greater Bay Area in 2030 under SSPs were derived from the work by Chen, et al. [186] , and their spatial distribution maps were used to shape the future land-use patterns in LCM, please see the section "Step 4: planning constraints and incentives" for details.

Table 7. Land-use conversion difficulty levels in the Greater Bay Area under each SSP.

Land-use conversion	SSP1	SSP2	SSP3	SSP4	SSP5	Reference policy
Transition from cropland to urban area	moderate	moderate	easy	easy	easy	The cultivated land requisition–compensation balance policy [a, b, c]
Transition from cropland to others	difficult	moderate	easy	moderate	moderate	Implement the strictest cropland protection system [b, c]

The increase in well-facilitated farmland	easy	moderate	difficult	difficult	easy	Promote the development of well-facilitated farmland [b, c]
Transition from forest to cropland	easy	moderate	easy	easy	easy	The cultivated land requisition–compensation balance policy [a, b, c]
Transition from forest to others	difficult	moderate	easy	moderate	moderate	Restore forest ecosystem [b, c]
The increase in forest	easy	moderate	difficult	difficult	moderate	Expand forest cover [b, c]
The increase in urban built-up land	moderate	moderate	easy	moderate	moderate	Improve the urbanization rate while strictly controlling the approval of new built-up land [b, c]
The increase in rural built-up land	difficult	moderate	easy	difficult	difficult	Revitalize the existing rural built-up land; the abandoned houses and hollow villages in rural areas will be demolished and reclaimed into new built-up land for urban development [b, c]
Transition from barren land to built-up land	easy	moderate	difficult	easy	easy	
Transition from water to others	difficult	moderate	easy	moderate	moderate	Strictly protect the water ecological space along the shoreline of the water area and prohibit the reclamation of lakes or encroachment on river courses [b, c]

The superscripts [a], [b], and [c] indicate that the policy was derived from *Letter of support for the Guangdong–Hong Kong–Macao Greater Bay Area and Shenzhen to explore the reform of natural resources*, *Land Planning of Guangdong Province (2016–2030)*, and *Land Planning of Guangdong Province (2016–2035)*, respectively.

Table 8. Conversion cost matrix of SSP2.

Land-use classes	Cropland	Bush and grassland	Forest	Water	Urban area	Barren land
Cropland	0.000	0.100	0.900	0.800	0.100	0.400
Bush and grassland	0.500	0.000	0.800	0.400	0.300	0.100
Forest	0.700	0.300	0.000	0.990	0.990	0.800
Water	0.900	0.900	0.900	0.000	0.990	0.500
Urban area	1.000	1.000	1.000	1.000	0.000	1.000
Barren land	0.900	0.500	0.990	0.800	0.300	0.000

The table was derived from Table 1 provided by Liu, et al. [164] .

3.3.3. Biocapacity calculations under various SSPs

Biocapacity (BC) expresses the supply of resources and ecological services, whereas the ecological footprint (EF) is a measure of the human demand for resources and ecological services [55]. BC and EF could be used as indicators for the examination of the possibility of achieving sustainable development [198]. In this study, the BC values for the six land-use classes were calculated based on the land-use maps projected for 2030 under each SSP. The values were compared with the BC and EF values of 2015 to estimate the extent of the sustainable trend. The BC value was calculated using the following equation (see Borucke, et al. [199] for the methodological details):

$$BC = \sum_i \frac{A_i}{N} \cdot YF_i \cdot EQF_i \quad (8)$$

where BC (gha/cap) is the per capita biocapacity; A_i (ha), the area available for the land-use class i; N, the population; and YF_i (wha/ha) and EQF_i (gha/wha), the yield factors and equivalence factors of the land-use class i, respectively (***Table 9***). The units "gha" and "wha" stand for global hectare and world average hectare, respectively [see Global footprint network [200] and the Working Guidebook to the National Footprint and Biocapacity Accounts (NFAs) [201] for more details.]

The yield factors were derived from the study by Liu, et al. [82] and the other equivalence factors from the NFA [201]. The original equivalence factors of grassland and bush were 0.46 and 1.29, respectively, and the corresponding yield factors were 2.71 and 1.03, respectively. As grassland and bush were grouped into one land-use class in this study, they were represented by average values.

Table 9. Equivalence and yield factors of different land-use classes.

Land-use classes	Cropland	Forest	Bush and grassland	Water	Urban area	Barren land
Equivalence factors	2.52	1.29	0.88	0.37	2.52	2.52
Yield factors	1.65	1.03	1.87	2.71	1.74	1.74

3.3.4. Carbon emissions coming from land use

Being a typical human activity, land use has influenced the global carbon balance by changing the natural carbon sources and sinks, such as forest, grassland, and cropland [202], [203]. However, with the increased industrialization and urbanization, changes in the land-use patterns are causing increased carbon emissions [204]. Therefore, the carbon emission trend associated with land use under each SSP was estimated [205], [206] using the following equation:

$$E_s = \sum_i A_{si} \cdot \delta_i \tag{9}$$

where E_s (tC.y^{-1}) denotes carbon emissions occurring under Scenario *s*; A_{si} (ha), the area of land-use class *i* under Scenario *s*; and δ_i, the carbon emission (absorption) coefficient (tC/(ha y^{-1})) of a given land-use class *i*. The carbon emission (absorption) coefficients are shown in ***Table 10***.

Table 10. Carbon emission coefficient [in tC/(ha y^{-1})] of each land-use class.

Land-use class	Cropland	Forest	Bush and grassland	Urban area	Barren land	Water
Value	0.422	−0.644	−0.021	40.73	−0.005	−0.253
Reference	[207]	[207]	[208]	[208]	[208]	[208]

3.4. Results

3.4.1. Historical land-use changes and transition modeling

Table 11. Past land-use changes (km^2) and their percentages (given within parenthesis) in the Greater Bay Area from 2000 to 2010.

Land-use class	2000		2010		Gain	Loss	Net
Cropland	22,603	(40.54)	20,839	(37.37)	336	−2,100	−1,764
Forest	23,283	(41.76)	23,096	(41.42)	508	−696	−188
Bush and grassland	3,191	(5.72)	2,261	(4.06)	408	−1,337	−929
Urban area	2,886	(5.18)	5,904	(10.59)	3,018	0	3,018
Barren land	6	(0.01)	3	(0.01)	0	−3	−3
Water	3,789	(6.80)	3,655	(6.56)	25	−158	−133
Total	55,758		55,758				

From ***Table 11***, it can be seen that all land-use classes except urban area experienced both a gain and a loss; urban area recorded only an increase in the land area (3,018 km^2). The contributors to the net increase in the urban area, in the descending order of their contributions, are cropland (2000 km^2), bush and grassland (847 km^2), forest (95 km^2), water (73 km^2), and barren land (3 km^2).

In the study, 26 transitions (covering 99% of the total transitions) and persistence were grouped into five submodels (***Table S 15***). The MLPNN method demonstrated good performance. All of the accuracy rates of the submodels were higher than 0.800. Moreover, all the transitions showed a high skill measure with the lowest at 0.631 (transition from water to bush and grassland) and the highest at 1.000 (transition from forest to cropland and cropland to forest).

Using historical changes and transition potential sub-models, the LCM could determine how the 12 variables (***Figure 18***) influenced future changes and the magnitude of those changes. The

extent of land use transitions in 2030 was then calculated for the BaU scenario. Based on BaU scenario model, land-use projections for different SSPs were generated by adjusting the land transition probability matrix as shown in ***Figure 17*** and as described in the section "Correlating land-use modeling with the local land planning policy-coupled SSPs".

3.4.2. Assessment of predictive performance of the model

The projected land-use map of 2015 and the actual land-use map of 2015 were used to calculate the confusion matrix (***Table 12***). The overall accuracy and Kappa coefficient [209] were 0.96 and 0.93, respectively. Precision and recall are two important model evaluation metrics [210]. Precision is the fraction of the images that project a particular land-use class that turns out to actually have that land-use class; recall is the fraction of images with a particular land-use class that have been projected to have that land-use class [211]. Furthermore, the F-score enables the combination of the precision and recall metrics into a single measure that captures both properties [212], it is calculated as (2 * Precision * Recall) / (Precision + Recall). The F-scores of cropland (0.96), forest (0.98), urban area (0.88), and water (0.96), which constitute the largest proportion of the land area in the Greater Bay Area, were very high. By contrast, the F-score of bush and grassland (0.78) and barren land (0.70) were relatively low. However, these two land-use classes do not significantly affect the predictive accuracy as their contributions to it are small. Therefore, the validation demonstrated that the proposed model has a high predictive ability.

Table 12. Validation of predictive performance of the model.

		Projected land-use map in 2015							
	Land-use classes	Cropland	Bush and grassland	Forest	Water	Urban area	Barren land	Area (km^2)	Recall
Actual land-use map in 2015	Cropland	19,526	8	93	2	876	0	20,506	0.95
	Bush and grassland	36	1,627	283	6	312	0	2,264	0.72
	Forest	147	243	22,563	10	16	0	22,979	0.98
	Water	15	28	7	3,520	30	0	3,600	0.98
	Urban area	285	20	15	48	6,037	1	6,406	0.94
	Barren land	0	0	0	0	0	1	1	1.00
	Area (km^2)	20,008	1,927	22,962	3,586	7,271	3	55,758	
Precision		0.98	0.84	0.98	0.98	0.83	0.53		Overall accuracy: 0.96
F-score		0.96	0.78	0.98	0.98	0.88	0.70		Kappa: 0.93

Decimal figures of area were converted to the nearest integers.

3.4.3. Future land-use changes under different scenarios

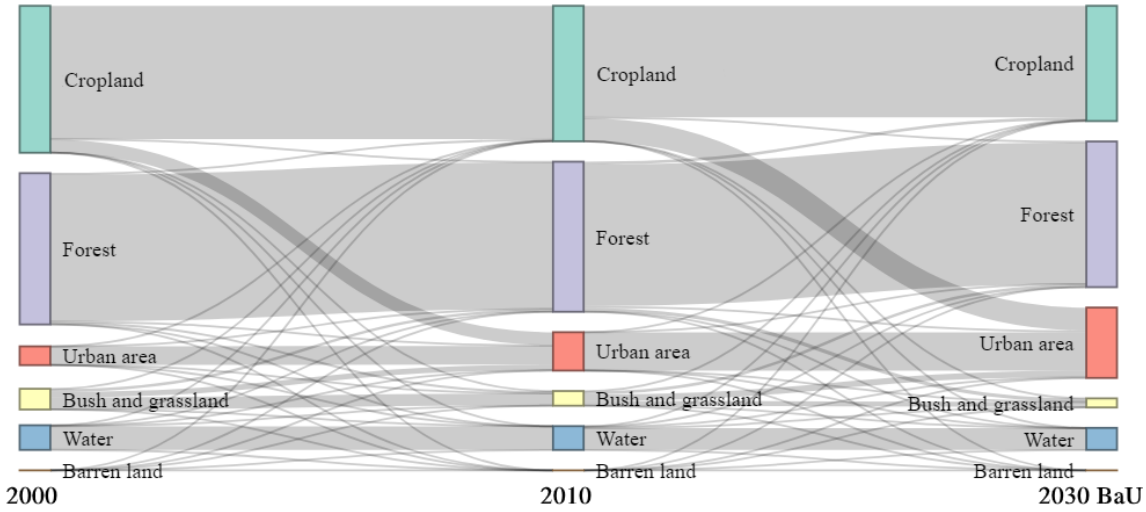

Figure 19. Land-use change flow in the Greater Bay Area for three time slices: 2000, 2010, and 2030 BaU map.

The historical trends of land use changes in the Greater Bay Area (***Figure 19***) from 2000 to 2030 demonstrate that, in general, the dominant land-use classes were cropland, forest, and urban area. Moreover, the proportion of land classified as urban area continuously and significantly increased; cropland, bush, and grassland experienced a significant decline, and forest exhibited a relatively small decrease. The conversion of cropland into urban area was a major contributor to urban development; approximately 22% of cropland had been converted into urban area between 2000 and 2030.

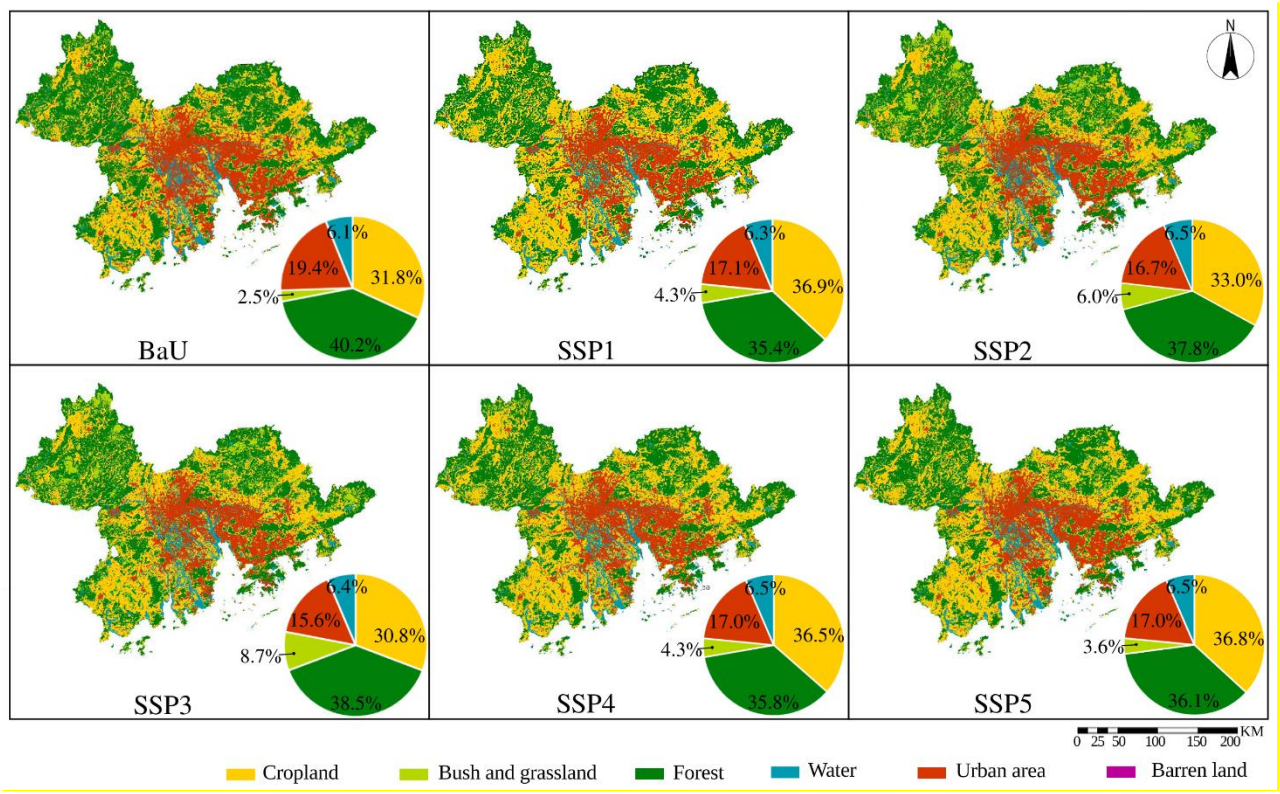

Figure 20. Projected land-use maps of the Greater Bay Area in 2030 under various SSPs at a 300-m resolution.

Table 13. Land-use areas of the Greater Bay Area in 2030 under different SSPs and BaU (in km^2).

The figure given within the brackets denotes the proportion with respect to that observed under the BaU assumption.

Scenarios	Cropland		Forest		Bush and grassland		Urban area		Barren land		Water	
BaU	17,728		22,414		1,396		10,829		3		3,388	
SSP1	20,568	(1.16)	19,747	(0.88)	2,372	(1.70)	9,557	(0.88)	3	(1.00)	3,511	(1.04)
SSP2	18,386	(1.04)	21,080	(0.95)	3,354	(2.40)	9,325	(0.86)	3	(1.00)	3,610	(1.07)
SSP3	17,159	(0.97)	21,463	(0.96)	4,871	(3.49)	8,703	(0.80)	3	(1.00)	3,559	(1.05)
SSP4	20,336	(1.15)	19,959	(0.89)	2,386	(1.71)	9,468	(0.87)	3	(1.00)	3,606	(1.06)
SSP5	20,538	(1.16)	20,112	(0.90)	2,006	(1.44)	9,468	(0.87)	3	(1.00)	3,631	(1.07)

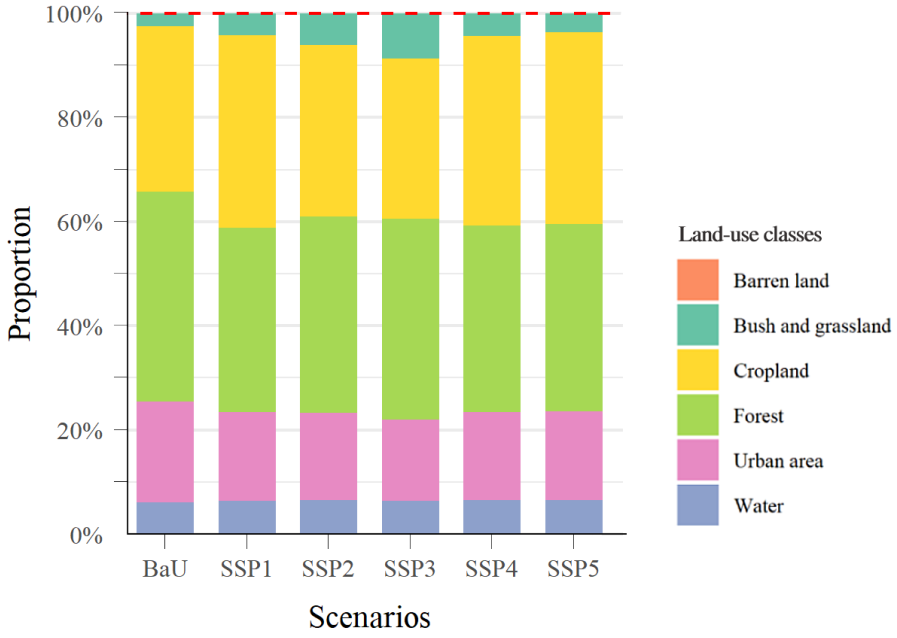

Figure 21. Proportion of each land-use class of the Greater Bay Area in 2030 under various SSPs and BaU assumption.

The spatial land-use distribution pattern of each scenario has not significantly changed (***Figure 20***); thus, urban development still revolves around Pearl River Delta, which is surrounded by cropland, with forest predominantly located on its north side. The proportions of cropland, forest, and urban area are the highest. In the BaU scenario, which assumes the continuation of past trends without any constraints or incentives, the proportions of urban area (19.4%) and forest (40.2%) are larger than those under the SSP scenarios (***Table 13*** and ***Figure 21***), whereas the proportion of bush and grassland (2.5%) is relatively low. In the SSPs, cropland and urban area were the largest in SSP1, being 1.16 and 0.88 times the size of BaU, respectively, followed by their respective areas in SSP5 and SSP4. Contrarily, the forest area in SSP1 (19,747 km^2) was relatively low. In SSP3, the urban area (8,703 km^2; 0.80 times the size of BaU) and cropland (17,159 km^2; 0.97 times the size of BaU) were the lowest. Significantly, only in SSP3, cropland was smaller than that in BaU.

3.4.4. Assessment of Hong Kong under various SSPs

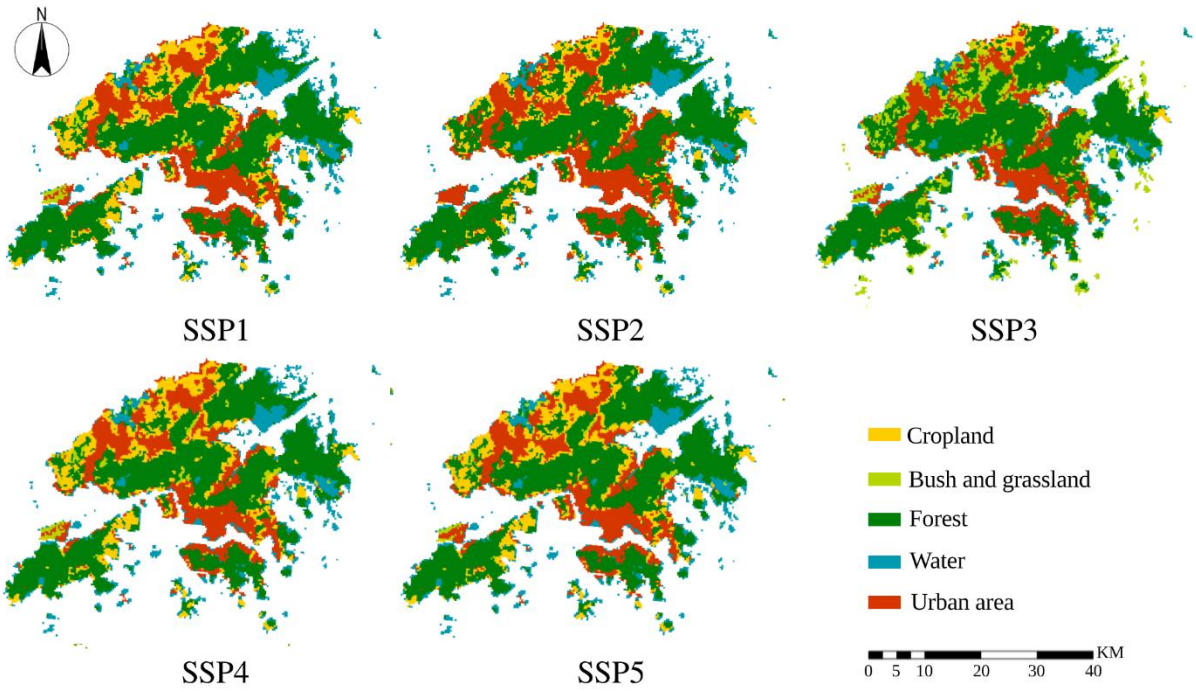

Figure 22. Projected land-use maps of Hong Kong in 2030 under various SSPs.

The projected land-use maps of Hong Kong were extracted from those of Greater Bay Area by using ArcGIS pro (the projected land-use maps can be obtained for other metropolitan regions, such as Shenzhen, Guangzhou, and Macao). As shown in ***Figure 22***, Hong Kong has five land-use classes. Although the areas of the different land-use classes depend on the scenario considered, the land-use spatial distributions under different SSPs are similar. The forest, and bush and grassland areas under SSP1, SSP2, SSP4, and SSP5 are less than the respective areas under SSP3. The urban area under SSP3 has become small and the cropland area has shrunk significantly. These results agree with SSPs narratives; because of limited land use regulation the lowest urbanization level occurs under SSP3 (***Table 6***), and the transition from cropland to other land-use classes is easy, whereas increasing well-facilitated farmland is difficult under SSP3 (***Table 7***). Under the other SSPs, the urbanization level is

central or fast, land-use regulation is medium or strong, and the growth of land productivity is high (*Table 6*).

3.4.5. Future biocapacity of Hong Kong under each SSP scenario

Table 14. Per capita biocapacity of Hong Kong in 2015 and 2030 under each SSP (gha/cap).

	Cropland	Forest	Bush and grassland	Urban area	Water	Total
SSP1	0.00903	0.00895	0.00054	0.01313	0.00171	0.0334
SSP2	0.00650	0.00989	0.00003	0.01350	0.00171	0.0316
SSP3	0.00140	0.01039	0.00351	0.01176	0.00154	0.0286
SSP4	0.00898	0.00903	0.00054	0.01265	0.00188	0.0331
SSP5	0.00871	0.00849	0.00039	0.01192	0.00177	0.0313
2015	0.00749	0.01117	0.00059	0.01313	0.00208	0.0345

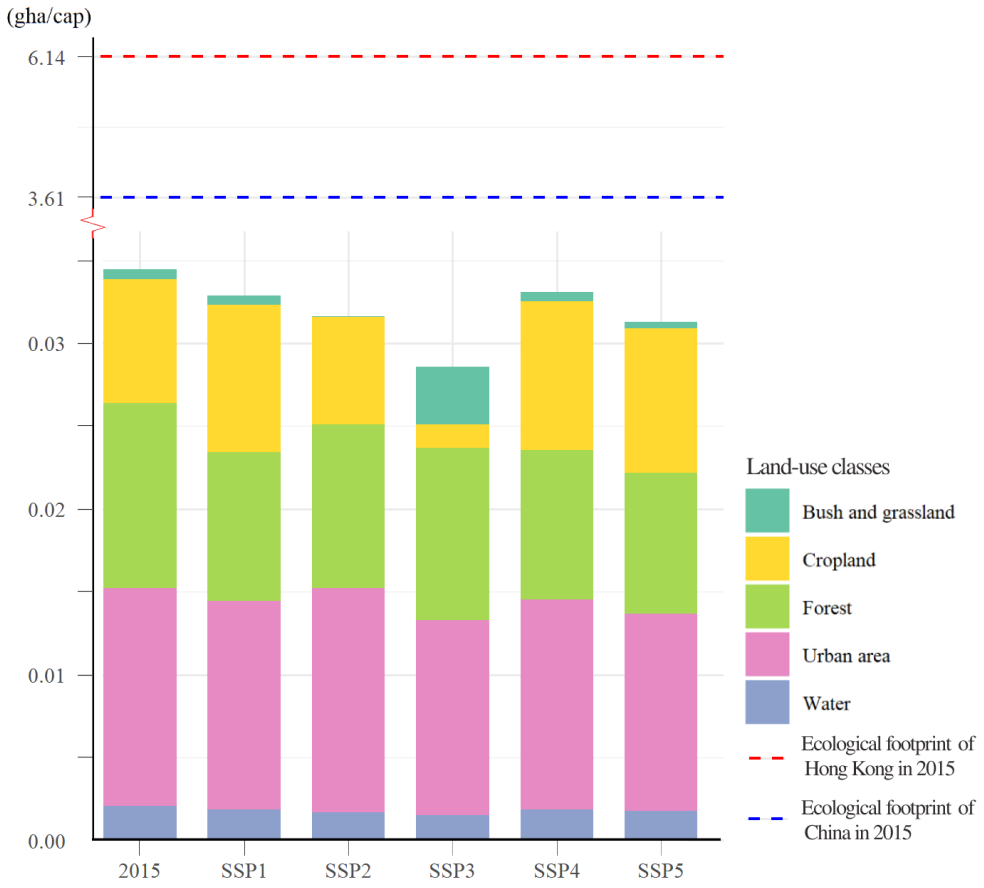

Figure 23. A comparison of the per capita ecological footprint (EF) of China and Hong Kong in 2015 and 2030 and a comparison of the per capita biocapacities of China and Hong Kong in 2015 and 2030 under each SSP.

(The bar chart and dashed lines denote the biocapacity and EF in gha/cap, respectively. The data pertaining to the biocapacity and EF of Hong Kong in 2015 were obtained from the study by Shi, et al. [213] . The data pertaining to the EF of China in 2015 were derived from the Global footprint network [214])

As can be seen from ***Figure 23***, the biocapacities of urban area, forest, and cropland are the dominating categories. As ***Table 14*** shows, the per capita biocapacity in 2030 under each of the SSPs has declined from its value in 2015 (0.0345 gha/cap). In 2015, it has the highest value under SSP1 (0.0334 gha/cap) and the lowest value under SSP3 (0.0286 gha/cap). During the period from 2015 to 2030, the per capita biocapacities of cropland under SSP1, SSP4, and SSP5 have improved but decreased under SSP2 and SSP3. However, the per capita biocapacity of urban area has increased (0.01350 gha/cap) only under SSP2, whereas under each of the other

SSPs, its value is less than or equal to its value in 2015 (0.01313 gha/cap). The per capita biocapacities of forests have reduced in 2030 in all SSPs.

Between the per capita EF of Hong Kong in 2015 (6.14 gha/cap) and that in 2030 under SSP1, which is the highest among all the SSPs, a significant gap exists (***Figure 23***). The per capita ecological footprint of Hong Kong is around 184 times the per capita biocapacity; this indicates that the demands made by the population far exceed the supplies of the local ecosystem. In addition, being a developed city, the per capita consumption in Hong Kong is approximately 1.7 times the per capita consumption of China (3.61 gha/cap).

3.4.6. Future carbon emissions from land-use in Hong Kong

Table 15. Carbon emissions/absorptions (10^2 $tC.y^{-1}$) from different land-use classes in Hong Kong in 2030 under each SSP. The figure in brackets denotes the value converted to CO_2 (10^2 $tCO_2.y^{-1}$).

	Total		Cropland		Forest		Bush and grassland		Urban area		Water	
SSP1	9,666	(35,474)	75	(275)	−355	(−1,303)	−0.56	(−2.06)	9,982	(36,634)	−35	(−128)
SSP2	9,971	(36,594)	54	(198)	−396	(−1,453)	−0.03	(−0.11)	10,348	(37,977)	−36	(−132)
SSP3	8,167	(29,973)	11	(40)	−396	(−1,453)	−3.52	(−12.92)	8,585	(31,507)	−30	(−110)
SSP4	9,218	(33,830)	74	(272)	−355	(−1,303)	−0.56	(−2.06)	9,538	(35,004)	−38	(−139)
SSP5	9,239	(33,907)	76	(279)	−355	(−1,303)	−0.43	(−1.58)	9,556	(35,071)	−38	(−139)
Total CO_2 emissions in 2015	416,000											

The total CO_2 emissions in 2015 were derived from The Environmental Protection Department of Hong Kong [215] . The emissions include those due to land use, electricity generation, town gas production, transport, industrial processes, product use, and the other end uses of fuel.

The values were converted to their nearest integers.

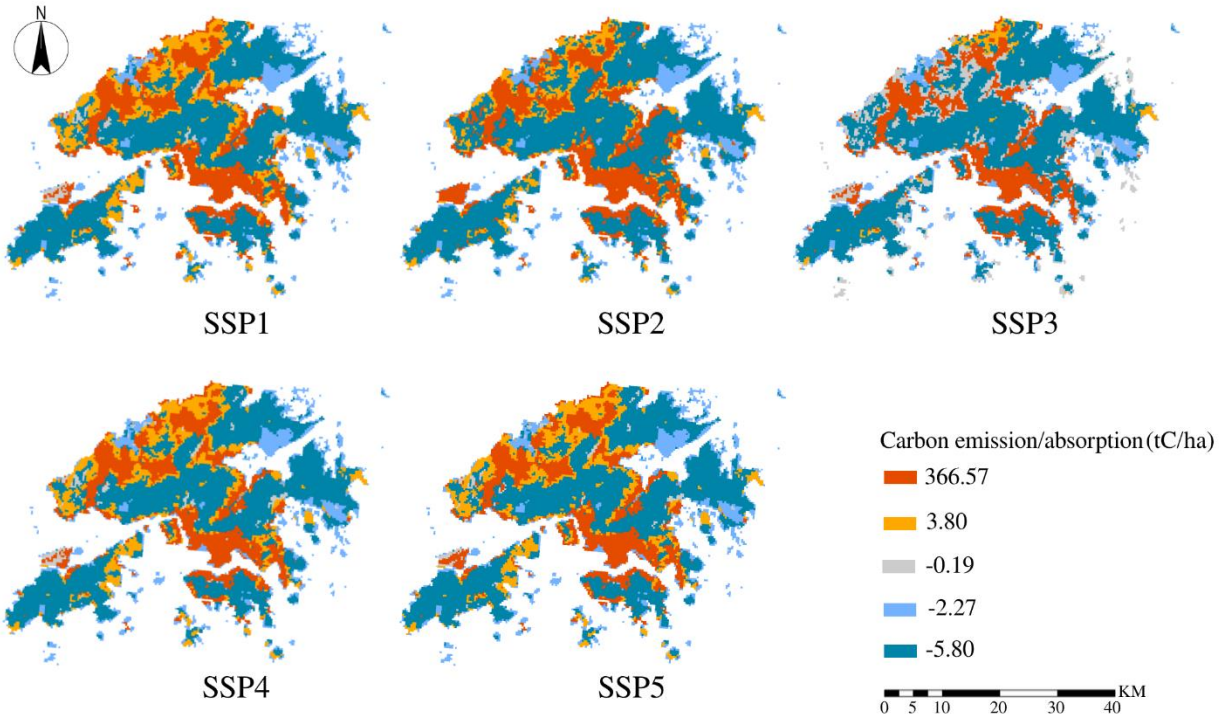

Figure 24. Spatial distributions of the carbon emissions (absorptions) in Hong Kong in 2030 under each SSP.

From ***Table 15*** and ***Figure 24***, it can be seen that urban area (366.57 tC/ha) and cropland (3.80 tC/ha) are the main contributors to the emissions. The urban area has a decisive impact on the carbon emission increase in Hong Kong. Contrarily, forest (−5.80 tC/ha), bush and grassland (−0.19 tC/ha), and water (−2.27 tC/ha) contributed to the absorption of carbon; forests in particular play a major role in absorbing carbon. The CO_2 emissions from land use in 2030 were approximately 8% of the total emissions in 2015. The highest CO_2 emission was under SSP2, which was caused by the large emissions that came from the urban area (3,797,700 $tCO_2.y^{-1}$); it was followed by the emissions under SSP1, SSP5, and SSP4. The emission from cropland in SSP5 (27,900 $tCO_2.y^{-1}$) was the largest, whereas the emission from cropland in SSP3 (4,000 $tCO_2.y^{-1}$) was the smallest. The CO_2 absorption from forests were the first and

second largest under SSP2 and SSP3 (−145,300 $tCO_2.y^{-1}$), respectively, whereas its values under SSP1, SSP4, and SSP5 were almost same.

3.5. Discussion

3.5.1. Advantages and limitations of the study

The studies by Hasan, et al. [168], Jiao, et al. [216], and Song, et al. [161] were similar to the present study with respect to the model, study area, and scenarios, respectively. Therefore, the scenarios, LULC models, and advantages and disadvantages of the methods used by the three previous studies mentioned and our study were compared (***Table S 16***) to demonstrate the differences of the four studies.

As can be seen from ***Table S 16***, the present study has two prominent advantages over the other three studies, which are listed as follows:

(1) Spatial downscaling framework: This framework can also be used for other regions in China, such as Yangtze River Delta and Beijing–Tianjin–Hebei Urban Agglomeration, or other scenarios to simulate the future land use patterns. The output map with a high resolution could help understand the implications of global environmental changes and greenhouse gas (GHG), which are crucial for studying sustainable development [217]. Among the various land-use classes, the urban and agricultural land use are the two most commonly recognized high-level classes of land use [218]. A map with an improved resolution can provide detailed and accurate land-use information for urban planning, environmental monitoring, and governmental management [219]. For instance, a 300-m resolution map can be used to observe the impact of

urbanization on the land system in terms of space and time [220], [221], thereby helping decision-makers and stakeholders to design and coordinate sustainable urban development plans [222].

(2) Elaboration of qualitative and quantitative methods of correlating LCM with localized SSPs: This is the most challenging part of scenario-based land use modeling and could make a significant impact on the projected results. However, the three previous studies did not make this elaboration. The qualitative and quantitative methods proposed in this study could be improved by considering additional factors, such as demographic, environmental, and economic factors, that would facilitate a more comprehensive and integrated simulation method for land-use change projection.

The study also had several limitations. Future infrastructure development, such as the construction of new roads, was not included in the future projections made in the study, which can affect the spatial patterns of urban expansion and associated land-use changes under the different scenarios. Besides, the yield factor and equivalence factor of the biocapacity would vary, depending on the level of technology and socioeconomic development of the SSP considered. For instance, owing to the improvements in agricultural productivity (***Table 6***), the yield factor can be relatively high in SSP1 and SSP5 and could thus lead to a large local biocapacity. However, due to data limitations, the biocapacity was calculated for each scenario using the same set of yield factors (2001) and equivalence factors (2019). In the section "Correlating land-use modeling with the local land planning policy-coupled SSPs", we referred to Liao, et al. [165] , Li and Chen [191] , and Li, et al. [176] in adjusting future land demands because reference data for all land-use classes could not be obtained from a single source. To maintain data consistency, all references were selected in accordance with SSPs narratives. The

Chinese research community can establish a unified and localized SSPs database for simulating and applying future projections. Although GHG includes CO_2, CH_4, N_2O, and fluorinated gases [223], [224], in this study, only CO_2 emissions were considered and estimated only in terms of the land-use factor. Other emission factors, including economic development, population, energy consumption, and production, also require consideration.

3.5.2. Verification and validation

As shown in ***Table 6***, from among the different socioeconomic development pathways possible in the future, urbanization will rapidly proceed under SSP1 and SSP5, whereas population growth will become relatively low with good land-use regulation and agricultural productivity improvements. Under SSP4, the urbanization level is relatively fast, and only high- and middle-income countries or upper/middle classes would be able to regulate land use and stimulate productivity. Under SSP2, land-use regulation, productivity, and population growth are all at a medium level with concentrated urbanization. However, SSP3 represents the worst-case scenario, where population growth stands in stark contrast with slow urbanization, low land-use regulation, and low productivity.

The results obtained for biocapacity (***Figure 23*** and ***Table 14***) are compatible with the SSPs narratives previously mentioned. The gaps among the biocapacities under different SSPs are mainly due to the variations in their cropland and urban areas. The urban area growth in SSP3 is lower than that in either SSP1 or SSP5, due to the differences in the human development trends caused by factors such as population and GDP growth [144], [167], [225]. In addition, due to the pressure exerted by population growth and rapid rate of urbanization, China has implemented strict cropland protection and balance policies to ensure food security [191].

Therefore, in the Greater Bay Area, the two largest cropland areas that support the sustainable development of the human society are under SSP1 and SSP5, followed by the cropland areas under SSP4 and SSP2.

However, what is good for the sustainable development of human society need not necessarily be good for the nature. The rapid development of the urban area and the implementation of cropland balance policies could be disadvantageous for low-carbon development. As presented in ***Table 15***, the carbon emissions from land use under SSP2, SSP1, and SSP5 are the highest. According to the analysis of historical land-use transitions (***Figure 19***), cropland is the main land class that can meet the requirements of urban expansion. However, in the future, the cost of urban sprawl will be indirectly transferred from cropland to other land classes, such as by the shrinking of forest, and bush and grassland, leading to a relatively low demand for forest in SSP1 (***Table 5***) due to the implementation of strict cropland protection and cultivated land requisition–compensation balance policy under SSP1(***Table 7***). The loss of vegetation would also lead to a decline in carbon absorptions and thus will not be conducive for achieving carbon neutrality before 2060 [226].

3.5.3. Policy implications

As indicated below, the implications of future sustainable development can be explored by considering the future land-use projections made by this study.

1. Biocapacity optimization: As shown in equation (8) and ***Table 9***, biocapacity is determined mainly by two factors: land area and land productivity [170]. The biocapacity would enhance if the two key drivers could be improved. Our results demonstrate that the areas of different land-use classes would vary depending on the scenario (***Figure 20*** and ***Figure 22***), and that with

limited land-use change regulation (SSP3), both the local biocapacity and cropland biocapacity would decline significantly (***Figure 23***). By contrast, the strict control of land-use conversions would mitigate the degradation of local biocapacity (SSP1 and SSP4); the local biocapacity of cropland under SSP1 is high because of improved agricultural productivity (***Table 6***). Nevertheless, the level of agricultural industrialization in the Greater Bay Area is still low, with backward agricultural socialization service systems and an imbalance in the development of different cities [227]–[229]. Therefore, according to the results of our analysis, the biocapacity in the Greater Bay Area can be significantly improved by enhancing the productivity of agriculture and the regulation of land-use conversions.

2. Mitigation of CO_2 emissions: Urban area and cropland are the main sources of emissions (***Figure 24***), whereas vegetation-covered areas and water are the main contributors to carbon absorptions. Thus, the three highest CO_2 emissions from land use occur under SSP2, SSP1, and SSP5 because the urban and cropland areas under these three scenarios are the largest of the corresponding areas under the five scenarios. Under SSP3, the emissions are low because the urban area and cropland under the scenario are small with large vegetation-covered areas. Thus, the green and blue spaces are important and effective in mitigating CO_2 emissions. However, according to ***Table 11*** and ***Table 13***, the green and blue spaces have been declining since 2000. The trend would continue into the future. To mitigate CO_2 emissions and achieve carbon neutrality before 2060, more attention would be required to the construction of blue-green infrastructure while building cities in the Greater Bay Area.

3. Further improvements: The cultivated land requisition–compensation balance policy was released in 1997 [193]. Although it has been upgraded from a quantity- and quality-oriented

policy to an ecological balance-oriented policy [230], various issues, such as inequities in crossregional transitions and imbalance of cultivated land quality, continue to appear. A large proportion of reclaimed cultivated land, which was not suitable for paddy cultivation, has been provided in mountainous areas to compensate for the loss of paddy land in the plains [231]–[233]. Moreover, when we considered this policy in our future land-use projections for the Greater Bay Area (***Table 7***), we found that it was beneficial mainly for developing urban area and protecting cropland rather than maintaining a balance among all land-use classes. For instance, the cost of urban sprawl is indirectly transferred from cropland to forest, and bush and grassland (as shown in the section "Verification and validation"). In this way, not only the biocapacity of cropland could would not be maintained but also the capacity of carbon absorption would decrease, which would be detrimental to both socio-economic and environmentally sustainable development. Therefore, the current ecological balance mechanism and regulatory regime require further improvement by considering urban area and cropland, and the balance among all land-use classes.

3.6. Conclusion

This study aimed to project future land-use patterns at a relatively high resolution to explore SSPs implications and the possible land-use changes due to urban development. Through a spatial downscaling framework that combines global SSPs narratives with local land planning policies, using a land change modeling method, the study revealed that all of the scenarios experienced a significant expansion of urban area at varying degrees of decrease in cropland and forest, thereby leading to considerable differences in the levels of local biocapacity and carbon emissions. The effects of intervention policies, such as the local land planning policy and cultivated land requisition–compensation balance policy, were examined, and our analysis revealed that they were beneficial mainly for developing urban area and protecting cropland

rather than maintaining a balance among all land-use classes. Our findings would contribute to the improvement of intervention policies related to the research area.

CHAPTER 4: Impact of Urbanization on the Food-Water-Land-Ecosystem Nexus: A Study of Shenzhen, China

4.1. Introduction

Society faces the major challenge of delivering water, energy, and food sustainably under the global trends of population growth and economic development [234]. In 2011, the German Federal Government organized the Bonn Conference to address the interconnection among water, energy, and food security [235]; thus, a nexus lens was first used on the three fields [236]. In addition, the United Nations set 17 Sustainable Development Goals (SDGs) in 2015 to facilitate global sustainability (United Nations, 2015). Thus, the nexus approaches can help enhance sustainability pathways [238]. Kebede et al. (2021) identified that the food–water–land–ecosystem (FWLE) nexus is fundamental for achieving the SDGs, such as SDG2: Zero Hunger (sustainable food production), SDG11: Sustainable Cities and Communities (sustainable urbanization), SDG 12: Responsible Consumption and Production (transformation toward the sustainable use and management of natural resources), and SDG 15: Life on Land (protection and promotion of the sustainable use of terrestrial ecosystems and reversal of land degradation and biodiversity loss).

Ecosystems play a major role in the interconnections within the nexus [240], because ecosystem services serve as the pillars that maintain biodiversity and support the availability of food, water, land, and energy in relation to the life-sustaining needs for human well-being [241]–[243]. These services can be classified into four categories, namely, provision (e.g., food production), regulation (e.g., water regulation), culture (e.g., outdoor recreation), and support (e.g., providing habitat for species and biodiversity) [244], [245]. The International Water Association and the International Union for the Conservation of Nature have collaborated to

discuss ecosystem-based solutions to the nexus problems [240]. The International Centre for Integrated Mountain Development (2012) used a nexus approach that considered ecosystem services to gain an in-depth understanding of the interlinkages among water, energy, and food in South Asia. Kebede et al. (2021) applied a regional integrated assessment platform of Europe to assess interactions with the FWLE nexus and present the implications for sustainability. Karabulut et al. (2016) conducted a spatially explicit assessment of water provision services in the Danube river basin by considering the FWLE nexus. Moreover, Kati et al. (2021) proposed a novel method for a windfarm planning strategy that offers a sustainable scenario for biodiversity–wind energy–land use nexus.

The abovementioned studies convey that the nexus cognition and method are based on wide and multiple perspectives, which can provide remarkable contributions to the field of sustainability. However, studies on the FWLE nexus remain scarce. Especially in China, nexus-related research mainly revolves around the water–energy–food nexus [236], [249], [250] or only focuses on one aspect [251]–[253]. As such, land use and ecosystem services are rarely discussed. Thus, improving the understanding of the FWLE nexus interactions and changes under potential futures is key to identifying the synergies and tradeoffs between the food, water, and land-use systems [239].

Therefore, the motivation and novelty of the study are to fill the research gap in the nexus field and, thus, contribute to the limited research in terms of the quantitative assessment of the FWLE nexus. The objectives are as follows:

1. Temporally and spatially assess the land, water, food, and habitat in the rapidly urbanized area.

2. Explore the tradeoffs between the FWLE nexus and urbanization.

Shenzhen was selected as the subject of the study as a representative megacity. Under the business-as-usual (BaU) scenario, which represents the continuation of the recent trend, we first project the land-use pattern by 2030 using a land change modeler (LCM) software. Second, the Integrated Valuation of Ecosystem Services and Tradeoffs (InVEST) was used to assess habitat quality, water yield, and water supply between 2000 and 2030. Furthermore, crop production was estimated by referring to statistical materials.

4.2. Study area

Shenzhen (22°27′–22°52′ N, 113°46′–114°37′ E) is located in the Guangdong province in South China (**Figure *25***) and situated immediately across the border from Hong Kong. This region is characterized as a mild, subtropical maritime climate with a mild winter and a hot and humid summer. Moreover, land elevation in Shenzhen declines from the southeast to the northwest, whereas the western part comprises coastal plains with a coastal length of approximately 230 km [254]. By the end of 2019, the permanent population was 13.44 million [255]. Since 1980, as China's first special economic zone, Shenzhen has developed from a small fishing village to a global first-tier city. It forms part of the Pearl River Delta megalopolis and became the first city in China without a rural institution [256]. Since 2005, its urban population has reached 100% [257], and, in 2020, its economy ranked third in China with 1.98 trillion yuan in annual gross domestic product [258]. However, with the increased urbanization, industrialization, and modernization, many environmental problems are becoming increasingly apparent, such as the reduction of food self-sufficiency [259], shrinking of cultivated land [260], increased levels of carbon dioxide emissions [261], and water pollution [262], [263]. Although Shenzhen has plenty of rain, the pressure on water use is overloaded. Thus, water scarcity in

Shenzhen has become a bottleneck for development since the 1980s [264]. Over the past decade, the general trend of water use increased, where domestic water use (35%) and urban public water use (30%) were the two major parts of the total water use, followed by urban industrial water use (approximately 25%) [265]. Shenzhen has initiated the transformation of its previous development mode to address these challenges and pursue a sustainable future for society and the ecosystem [266]. Therefore, the FWLE nexus philosophy could contribute to this sustainable transformation. Hereby, Shenzhen was selected as the case study.

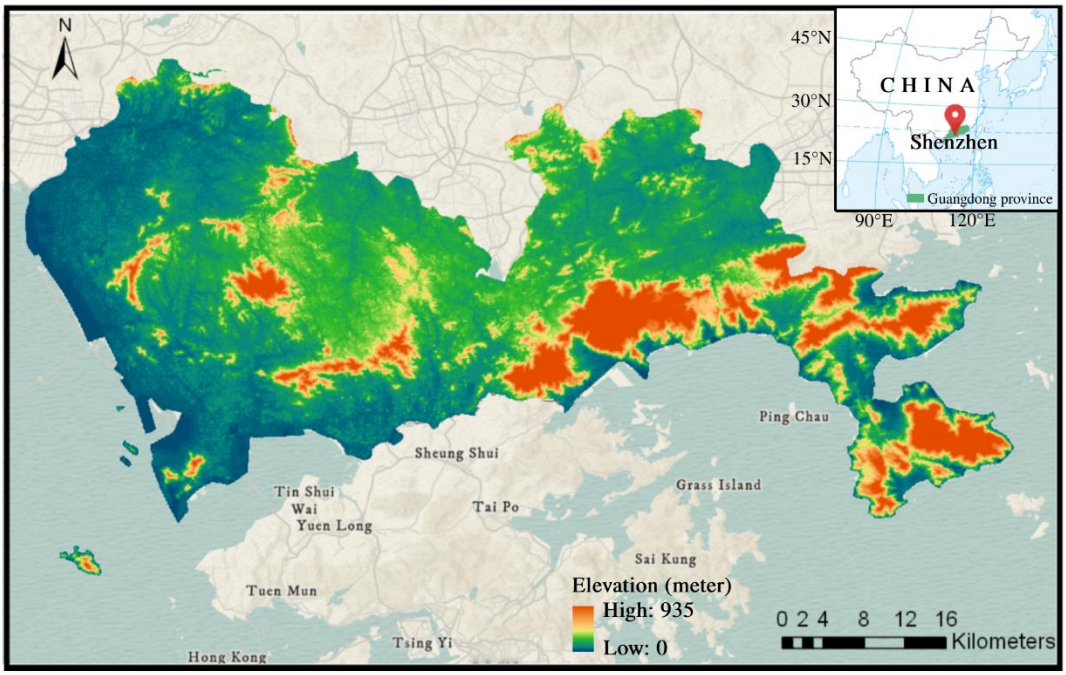

Figure 25. Location of Shenzhen, China.

4.3. Materials and Methods

Figure *26* puts forward the framework for the FWLE nexus, where land is viewed as the point that links society and the environment and not only underpins the ecosystem but also provides fundamental support to human development [267]. In turn, urbanization due to human activities can shape the land-use pattern and drive land-use changes, which lead to

further impacts on the ecosystem, such as crop production and water yield. Finally, the linkage effect will reflect on society. Among these linkages, land-use change can be considered a crucial variable in the transformation toward the sustainable development of urbanization and the ecosystem. In the present study, land was deemed as the entry point, whereas habitat quality was used as an indicator to reflect the integrity of ecosystem. In other words, an ecosystem with a high-quality habitat can better support ecosystem services [268], such as the provision of food and water. Thus, the impact of urbanization on the FWLE nexus can be explored based on land-use changes.

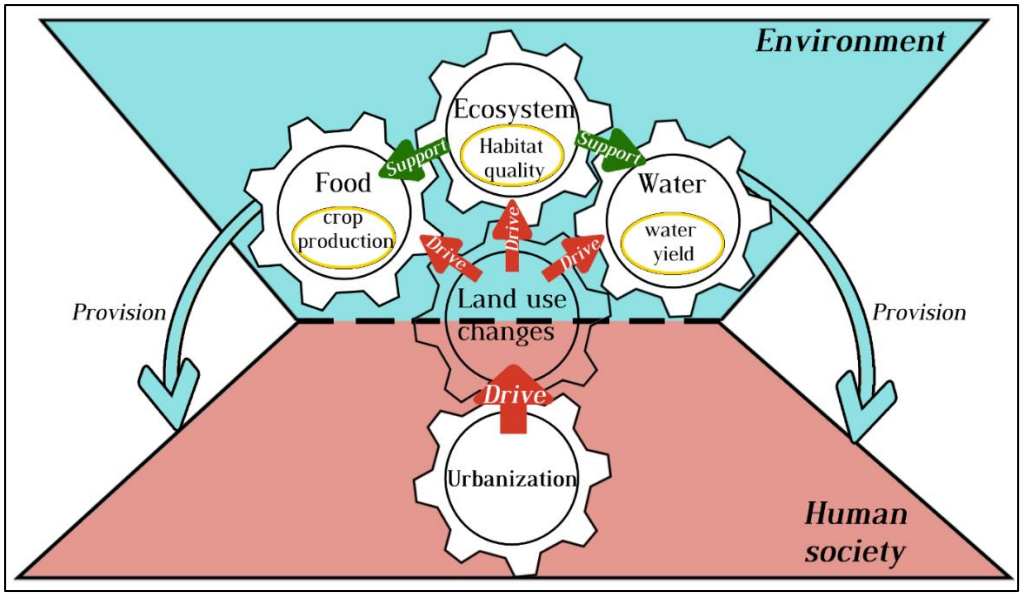

Figure 26. Framework of the FWLE nexus (yellow ellipses represent three indicators, namely, the ecosystem, food, and water)

Figure *27* presents the workflow of land-use projection under the BaU scenario for the year 2030 and the assessment of ecosystem services related to food, water, and habitat. The LCM software, which is an integrated module of TerrSet 2020 [269], was used to simulate future land-use changes. Consequently, the outcome (30-m resolution) was deemed as the BaU scenario land-use map for 2030, which represents the continuation of recent trends in Shenzhen. It could be simulated directly by generating a default transition probability matrix based on the

analyses of historical land-use change and the training of transition potential modeling. The assumptions of the BaU scenario are as follows:

- The topography, geographic landscape, and urban development pattern will not change to a large extent. For instance, the city center will not be relocated; the forest will not be intensively exploited; and the major development of transportation will continue to revolve around the city and its adjacent areas.
- The scenario will extrapolate the recent trend of land-use changes observed between two time periods, namely, 2000 and 2010, into the future [270].
- No additional intervention factors will be involved, such as the new socioeconomic change, policy intervention, urban design, and land-use planning.

Thus, the BaU scenario can be used for observing the FWLE nexus as shaped by recent urbanization, which is similar to obtaining a diagnosis (i.e., the projection of future events if the recent situation continues). Implications for sustainable transformation are then drawn.

Next, based on the InVEST model and statistical materials, historical and projected land-use maps were used to assess the ecosystem services from 2000 to 2030. Thus, the study can constitute temporal and spatial assessments and analyses with 10-year intervals of land-use changes and ecosystem services to explore the FWLE nexus against the background of recent urbanization. ***Table 16*** presents a list of the sources of data used in this study.

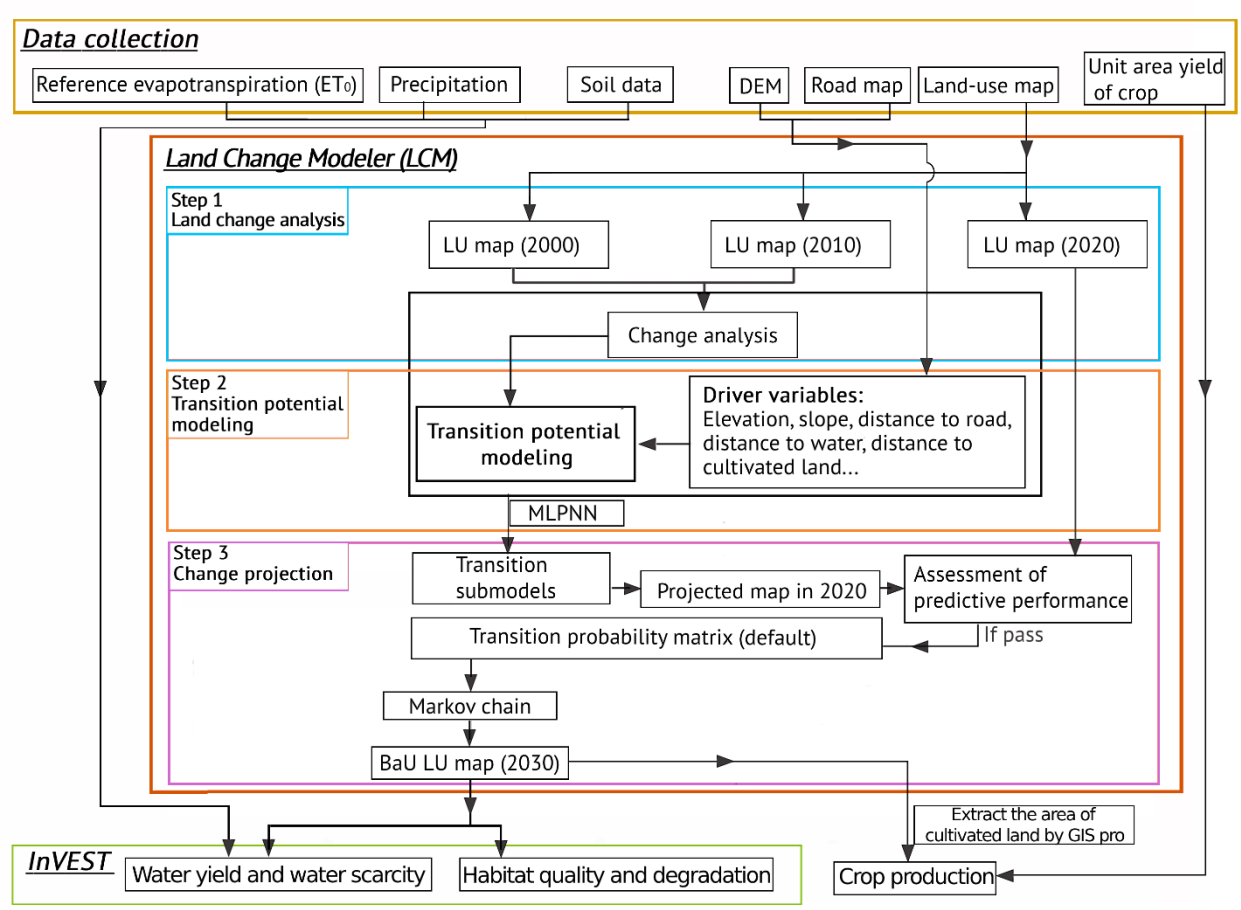

Figure 27. The overall projection framework of land-use pattern in 2030 under the BaU scenario and assessments of ecosystem services.

LU stands for land-use, whereas MLPNN stands for multilayer perceptron neural network. (The yellow, red, and green solid lines denote the data collection, LCM simulation, and the assessment by InVEST, respectively; the blue, orange, and magenta boxes denote the three subcomponents of the LCM, respectively.)

Table 16. Data source.

Data	Data description	Source
Land use/cover	Land use/cover in 2000, 2010, and 2020 at a resolution of 30 m	GLOBELAND30 (http://www.globallandcover.com/)
Digital elevation model (DEM)	For the year 2019 at a resolution of 30 m	JAXA-DEM (https://www.eorc.jaxa.jp/ALOS/en/aw3d30/)
Road map	Polyline shape file in 2013	OpenStreetMap (https://download.geofabrik.de/)

Soil data	Soil texture at a resolution of 10 km (%clay, %sand, %silt, %organic matter)	National Tibetan Plateau/Third Pole Environment Data Center, China (https://data.tpdc.ac.cn/zh-hans/disallow/11573187-fd64-47b1-81a6-0c7c224112a0/)
	Soil depth, available water capacity (1-km resolution)	Harmonized World Soil Database v 1.2 (http://www.fao.org/soils-portal/soil-survey/soil-maps-and-databases/harmonized-world-soil-database-v12/en/)
Precipitation	Mean annual precipitation for 2017 at a resolution of 500 m	Resource and Environment Science and Data Center, China (http://www.resdc.cn/DOI/doi.aspx?DOIid=39)
Reference evapotranspiration (ET_0)	Global raster climate data (30 arc-seconds) for the 1970–2000 period	Global Aridity Index and Potential Evapotranspiration Climate Database v2 (https://cgiarcsi.community/2019/01/24/global-aridity-index-and-potential-evapotranspiration-climate-database-v2/)
Unit area yield of crop	Annual crop yield per square kilometers in 2000, 2010, and 2019	Shenzhen Statistical Yearbook (http://tjj.sz.gov.cn/attachment/0/736/736628/8386382.pdf)

4.3.1. LCM

The LCM is an integrated vertical application embedded within TerrSet. It is used for the analyzing past land cover changes, modeling the potential for change, projecting the course of change into the future, and evaluating planning interventions to maintain ecological sustainability [271]. The LCM has been applied across many disciplines [182] and proven an effective and powerful model due to its Markov Chain-based neural network [168], [272]. Therefore, we selected the LCM to project the land-use patterns in Shenzhen under the BaU scenario for the year 2030. The study employed the three major subcomponents of LCM version 19.0.4 (**Figure *27***), namely, land change analysis, transition potential modeling, and change projection.

4.3.1.1. Step 1: Change analysis

This step analyzes past land-use changes to identify the transition from one land-use state to another. Two land-use maps for 2000 and 2010 (**Figure *27***, ***Table 16***) were used, whereas seven land-use classes were identified, namely, artificial surfaces, cultivated land, forest, shrubland, grassland, wetland, and water bodies. Moreover, we specified that the land transitions in areas that exceed 10 km^2 could be considered, that is, only dominant transitions, which cover approximately 82.2% of the total transitions were used for modeling.

4.3.1.2. Step 2: Transition potentials

At this stage, the transition submodel, which utilizes the same underlying driver variables, was built to simulate the potential for land transitions [273]. The study employed two primary setups of the transition submodels to compute transition potentials, namely, the transition submodel structure and simulation approach. First, Cramer's V approach was used for building the transition submodel to quantitatively measure the level of association between drivers and land-use class [274]. In essence, the higher the value of Cramer's V, the better the potential explanatory of the driver. Moreover, a Cramer's V value of more than 0.15 [189] was identified as a strongly associated variable that can be used for the structure of submodel (**Figure *27***). In this study, 13 variables (**Figure *28***) were selected to build the transition submodels. The evidence likelihood is an effective means of incorporating categorical variables into the analysis, which is highly recommended for use in building transition submodels [189]. This likelihood can be generated in the variable transformation utility panel of the LCM.

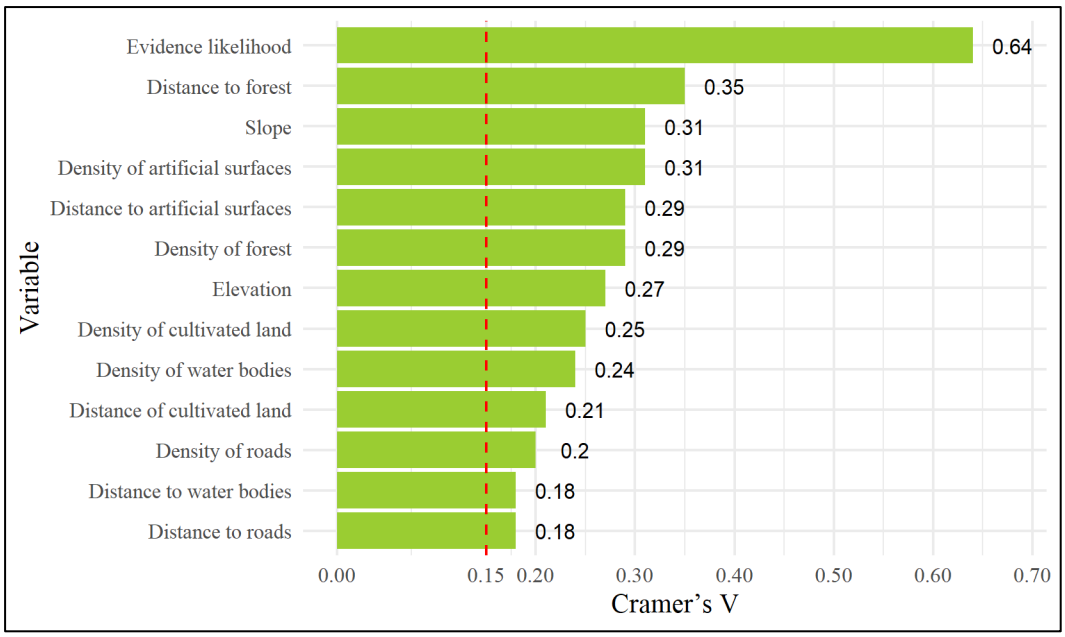

Figure 28. Variables for the transition submodel structure in the LCM.

Second, the multilayer perceptron neural network (MLPNN), which is a feed-forward artificial neural network [275], was used for the simulation approach. It requires relatively less data for training [276] and can run multiple transitions (up to nine) per submodel [189]. Moreover, it can simulate nonlinear relationships in a robust manner [277]. Therefore, MLPNN simulation was adopted to model the land-use transitions from 2000 to 2010.

4.3.1.3. Step 3: Change projection

The number of changes in land transitions can be computed through a Markov Chain after specifying the year 2030 as the end date. Consequently, the BaU scenario can be generated, where two types of results can be obtained via LCM (i.e., hard- and soft-projection maps) using the default transition probability matrix. A hard projection is a specific scenario of a landcover map with the same categories as the inputs. By contrast, the soft projection is a continuous mapping of the degree of vulnerability to change ranging from 0 to 1, which indicates the extent

to which an area possess adequate conditions to undergo changes instead of pointing out specific changes [189]. Therefore, the study employed hard projection to assess predictive performance and as the input related to land use for the InVEST model.

4.3.2. InVEST

InVEST is a suite of models that can be used to map the goods and services from nature that support human life and help explore changes in ecosystems [278]. One of the advantages of the InVEST is the relatively low requirements of data and expertise. Therefore, the tool is appropriate for assessing multiple ecosystem services influenced by land-use changes [279]–[281], such as habitat quality, water yield, and water scarcity (supply). Thus, the ecosystem services related to the FWLE nexus could be quantified and mapped via the InVEST model.

4.3.2.1. Habitat quality model

InVEST assesses habitat quality as a function of (1) the suitability of each land-use class for providing habitat for biodiversity using a relative habitat quality score from 0 to 1 (**Table S *17***), where 1 denotes the highest suitability for species, such as the forest, and (2) threats that likely impair habitat quality and the sensitivity of each land-use class to each threat [282] (***Table S 17*** and ***Table S 18***). Three factors, namely, distance, weight, and the sensitivity of land-use class to the threat are used to determine the impact of threats on habitat. In general, the degradation of habitat quality is a result of the intensity of nearby human activities and land-use changes [283]. The total threat level and a half-saturation function are used to translate a pixel cell of threat level into habitat quality [284]. Section I of Appendix C provides specific calculations.

4.3.2.2. Annual water yield model

The annual water yield model offers insight into the influence of the changes in land-use patterns on annual surface water yield by estimating the relative contributions of water from different parts of a landscape [285]. Although the model does not differentiate between surface and baseflow, it assumes that all water yield from a pixel reaches the point in question through one of these pathways. The water yield of a sub-watershed is then generated by the summation and average methods [286]. Section II of Appendix C presents specific calculations.

4.3.2.3. Water scarcity (realized supply)

Based on the calculated water yield and consumptive water use in the watersheds of interest, the realized supply option of the model (called water scarcity in the tool interface) can be used to calculate the water inflow to a reservoir [285]. Therefore, the consumptive water use for land use/cover should be identified to calculating water scarcity, that is, water incorporated into products or crops, consumed by humans or livestock, or removed from the watershed water balance [285]. This study considered two types of land-use classes, namely, cultivated land related to agricultural water use, such as water used for paddy fields, vegetable fields, forestry, and fruit irrigation, and artificial surfaces related to industrial, public, and domestic water use. Section III of Appendix C illustrates the specific calculations.

4.3.3. Crop production

Crop production was estimated based on the annual yield per square kilometer and the area of cultivated land in Shenzhen. According to the Shenzhen Statistical Yearbook 2020 [255], vegetable mainly comprises the local farm crops since 2000. As a result, the yield of vegetables was used to estimate crop production. In 2000, 2010, and 2019, the vegetable

yields were 1,892, 1,742, and 1,653 t/km^2, respectively [255]. We assumed that the vegetable yield in 2020 was equal to that in 2019 due to data constraints. Moreover, the annual yield per square kilometer in 2030 was assumed as a continuation of the trend of change between 2000 and 2020. Thus, it can be estimated on the basis of the average annual growth rate from 2000 to 2020.

4.4. Results and Analyses

4.4.1. Predictive performance of the LCM

The actual land-use map of 2020 and the projected land-use map of 2020 were used to calculate the confusion matrix for assessing predictive performance (**Table *17***) and overall accuracy. The kappa coefficients were 0.78 and 0.67, respectively, which demonstrates that the predictive performance of the model was substantial, whereas the output was acceptable. Furthermore, precision and recall metrics were calculated to reflect the predictive performance of each land-use class. Precision denotes the fraction of images that project a particular land-use class that turns out to actually have that land-use class; recall is the fraction of images with a particular land-use class that has been projected to have that land-use class [211]. To capture the priorities of the precision and recall metrics, the F-score, which is a single measure, was used and is calculated as (2 × Precision × Recall)/(Precision + Recall) [212]. The F-scores for forest (0.81) and artificial surfaces (0.86), which compose the largest proportion of land area in Shenzhen, were high. In contrast, the F-scores for wetland (0.0) and grassland (0.36) were low. Nevertheless, these two land-use classes did not significantly influence predictive accuracy due to their results are negligible. In summary, the validation demonstrated that the model possessed substantial predictive ability.

Table 17. Validation of predictive performance of the model.

		Projected land-use map of Shenzhen in 2020								
	Land-use class	Cultivated land	Forest	Grassland	Shrubland	Wetland	Water bodies	Artificial surfaces	Area (km^2)	Recall
Actual land-use map of Shenzhen in 2020	Cultivated land	47.11	7.40	0.89	0.24	0.00	1.60	13.00	70	0.67
	Forest	4.94	511.37	11.50	30.28	0.00	1.55	47.01	607	0.84
	Grassland	1.36	22.74	29.65	13.85	0.00	0.87	21.63	90	0.33
	Shrubland	0.25	31.98	12.39	88.45	0.00	0.46	8.15	142	0.62
	Wetland	0.00	0.01	0.00	0.00	0.00	0.01	0.00	0.02	0.00
	Water bodies	4.37	12.96	2.72	5.47	0.00	34.28	13.33	73	0.47
	Artificial surfaces	31.33	71.19	16.26	13.67	0.00	21.18	814.82	969	0.84
	Area (km^2)	90	658	74	152	0.00	60	918	1,952	
Precision		0.53	0.78	0.40	0.58	0.00	0.57	0.89	Overall accuracy: 0.78	
F-score		0.59	0.81	0.36	0.60	0.00	0.52	0.86	Kappa: 0.67	

Note: The decimal values of the subtotal and total areas were converted to the nearest integers.

4.4.2. Land-use changes from 2000 to 2030

Table 18. Summary of land-use classes and actual land-use changes in Shenzhen from 2000 to 2020 and the projected land-use for 2030 under the BaU scenario (in units of km^2). Brackets denote the percentage for each land-use class

Land-use class	2000		2010		2020		2030	
Cultivated land	149	(0.08)	117	(0.06)	70	(0.04)	70	(0.04)
Forest	666	(0.34)	668	(0.34)	607	(0.31)	641	(0.33)
Grassland	164	(0.08)	110	(0.06)	90	(0.05)	56	(0.03)
Shrubland	148	(0.08)	156	(0.08)	142	(0.07)	151	(0.08)
Wetland	0.47	(0.00)	0.00	(0.00)	0.02	(0.00)	0.00	(0.00)
Water bodies	158	(0.08)	92	(0.05)	73	(0.04)	41	(0.02)
Artificial surfaces	667	(0.34)	808	(0.41)	969	(0.50)	992	(0.51)
Total	1,952							

Note: The area value was rounded.

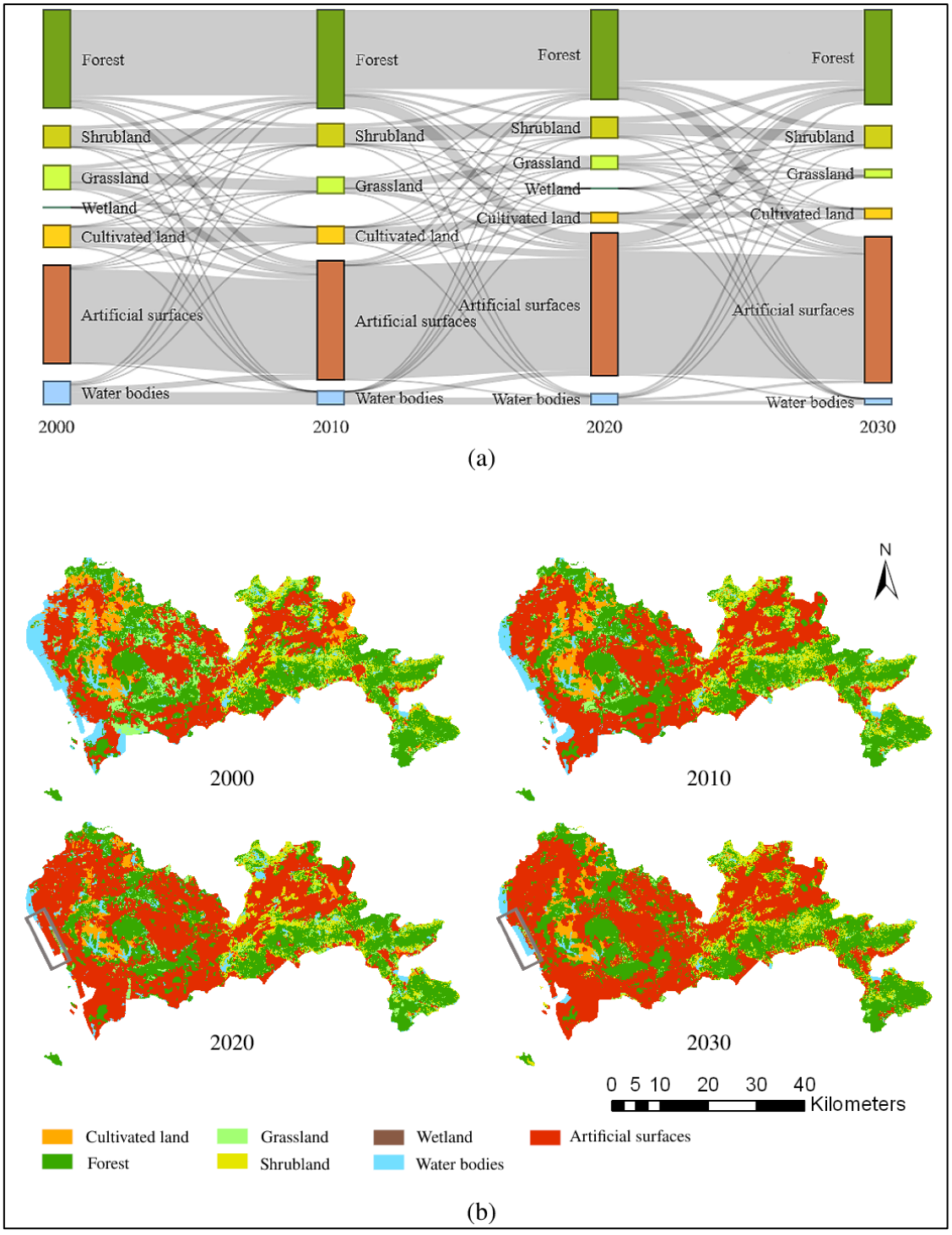

Figure 29. (a). The flow of land-use change in Shenzhen for four time periods, namely, 2000, 2010, 2020, and the 2030 BaU map. (b). The spatial distribution of land-use pattern in Shenzhen from 2000 to 2030. (area in gray box denotes the comparative part between 2020 and 2030).

In the past 20 years, the land-use pattern in Shenzhen has changed dramatically. ***Table 18*** and **Figure *29*** depict the time series of the proportion of land-use and land changes, respectively.

Table 18 demonstrates that the dominant land-use classes in Shenzhen are forest and artificial surfaces, which account for more than 60% of the total area. Moreover, only artificial surfaces displayed a continuous and significant increase from 2000 to 2030. The proportion was projected to reach 51% (992 km^2) by 2030, whereas shrubland exhibited a slight increase. Furthermore, cultivated land, grassland, and water bodies experienced significant declines, whereas the forest indicated a relatively small decrease. Over three decades, their proportions were reduced by approximately half, especially for water bodies, which decreased from 8% (158 km^2, 2000) to 2% (41 km^2, 2030). The wetland area was extremely small and exhibited a shrinking trend, which nearly indicates the point of negligence. The study observed that, between 2000 and 2010, conversions of the forest, cultivated land, and grassland were significant contributors to the development of artificial surfaces in Shenzhen (**Figure *29 (a)***). By 2020, forest and cultivated land continue to be the primary sources for the sprawl of artificial surfaces, especially for the forest. Moreover, its conversion increased by nearly twofold, which indicates that Shenzhen was urbanized rapidly at the cost of cultivated land or forest.

Figure *29 (b)* presents the spatial distribution of land-use patterns, where the development of artificial surfaces expanded rapidly throughout Shenzhen. In contrast, only the mountainous southeast region covered by forest was relatively less affected by human activities. The gray box in **Figure *29 (b)*** represents the coastal area, which was developed into built-up land through reclamation since 2020. However, the projection in LCM was based on the land-use maps for 2000 and 2010. At the time, this coastal area had not been rapidly developed, which led to the projected increase in artificial surfaces (2030) that was less than the actual increase in 2020. This result indirectly implied the dramatic occurrence of land-use transitions in Shenzhen.

4.4.3. Habitat quality and degradation assessments

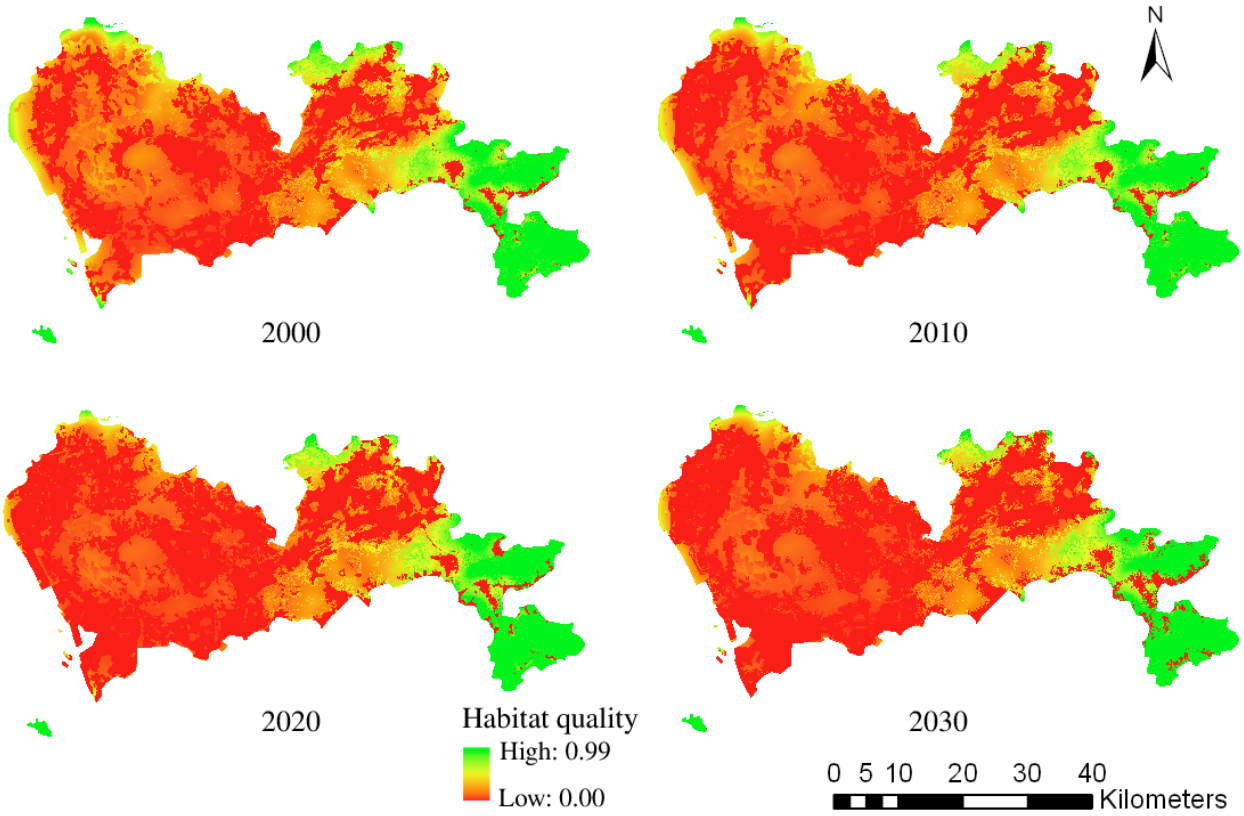

Figure 30. Spatial distribution of habitat quality in Shenzhen from 2000 to 2030.

Figure 30 depicts that the value of habitat quality ranged from 0 to 0.99, where the smaller the value, the lower the habitat quality. The habitat quality in the majority of areas was approximately 0.5, which indicates that the overall level of habitat quality in Shenzhen was comparably low. Places with high levels of habitat quality (a value of approximately 0.9) are mainly concentrated in the southeastern side, which is a mountainous area. In contrast, the expansion of artificial surfaces negatively impacted habitat quality. From 2000 to 2020, significant degradation occurred around artificial surfaces (**Figure S *1***), where many cultivated land and forest areas were converted to artificial surfaces. As a result, the highest degradation

value increased from 0.24 to 0.27. Moreover, the degradation trend is projected to continue until 2030. On the contrary, the east side of Shenzhen exhibited a relatively slight degradation due to the slow development of the built-up area. Thus, land use exerts a significant influence in shaping habitat quality and degradation rate.

4.4.4. Assessment of water yield changes and water supply

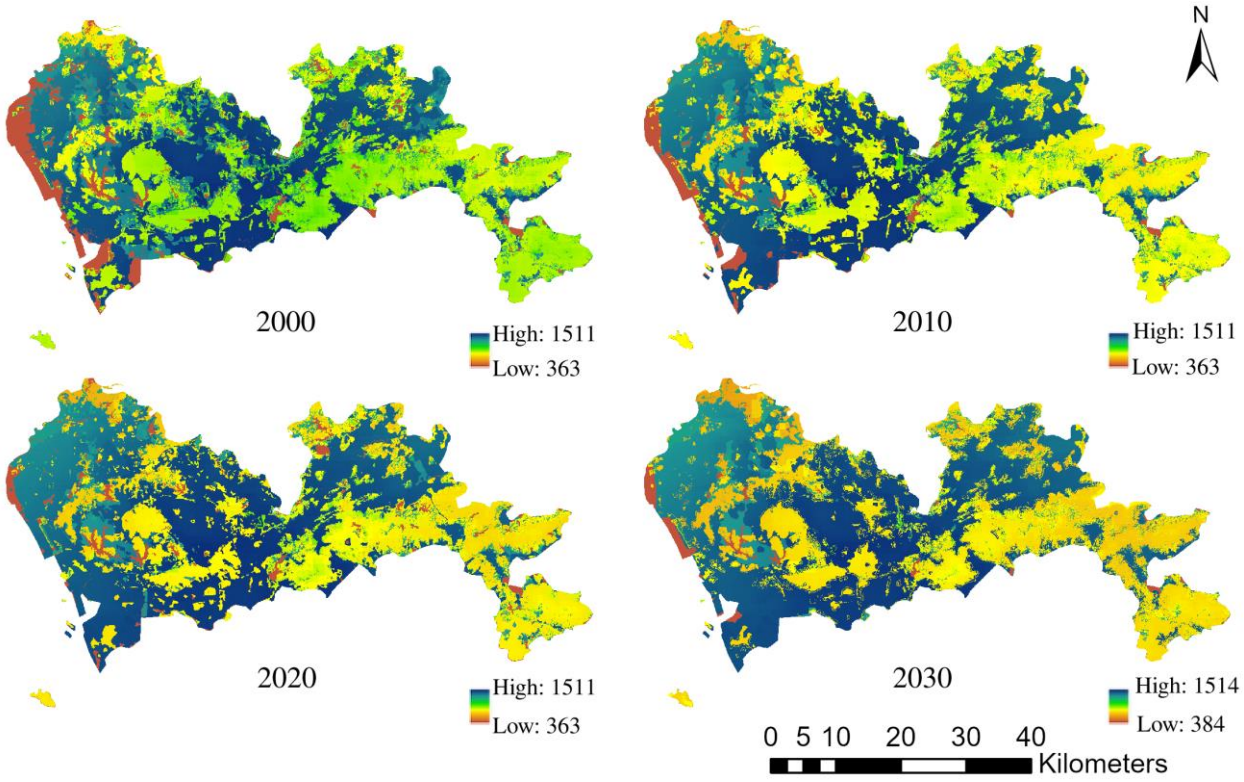

Figure 31. Spatial distribution of water yield (in mm) in Shenzhen from 2000 to 2030.

In Shenzhen, the total annual volumes of water yield, which were determined by modeling its actual annual evapotranspiration (AET) and annual precipitation (P), were 22.93×10^8, 23.61×10^8, 24.18×10^8, and 24.35×10^8 m^3 in 2000, 2010, 2020, and 2030, respectively, which indicated an increasing trend. However, in ***Figure 31***, the bluish-green color represents areas with relatively high water yield, whereas the yellowish-brown color characterizes those with relatively low water yield. Consequently, regions with the artificial surfaces (i.e., bluish-

green colored area mainly covered by forest, shrubland, and grassland) gradually changed into yellow from 2000 to 2030, which indicates that the water yield per unit area declined in forest, cultivated land, and shrubland. Conversely, the water yield in regions with artificial surfaces was higher due to the lower AET, which was determined using the evapotranspiration coefficient (Kc, **Table S *19***). In addition, the increase in the water yield from artificial surfaces was greater than the loss of water yield from other regions, which led to an increase in total water yield.

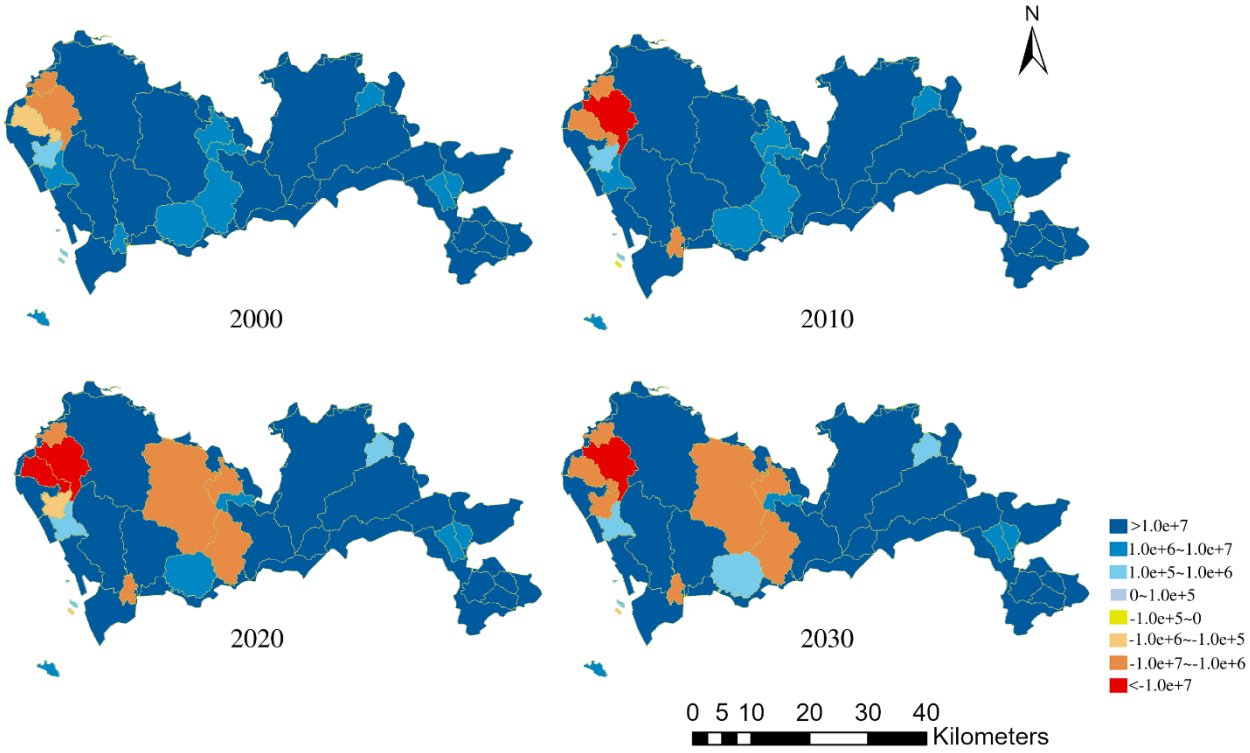

Figure 32. Total realized water supply volume (in m^3) for each sub-watershed (bright yellow lines denote the boundary of sub-watersheds).

Findings related to the water supply for each sub-watershed can be obtained using the water scarcity tool in InVEST (**Figure *32***). In 2000, water-scarce areas only existed in the northwestern side of Shenzhen, where the water supply value ranged from −7,709.3 m^3/km^2 to 104,362.3 m^3/km^2. By 2020, however, the lowest and highest water supply values decreased to −33,199.0 and 102,253.0 m^3/km^2, respectively. From 2010 to 2030, sizable

water-scarce areas were observed to be concentrated in the mid-western side, which was dominated by artificial surfaces. Conversely, the east side retained a relatively high level of water supply. In 2030, the water supply value was projected to range from −30,196.1 m^3/km^2 to 108,875.3 m^3/km^2. In summary, the water supply in Shenzhen declined gradually between 2000 and 2020 with an apparent increase in water-scarce sub-watersheds. Furthermore, against the background of urban expansion, the water supply shortage in Shenzhen was projected to continue through 2030.

4.4.5. Estimation of crop production

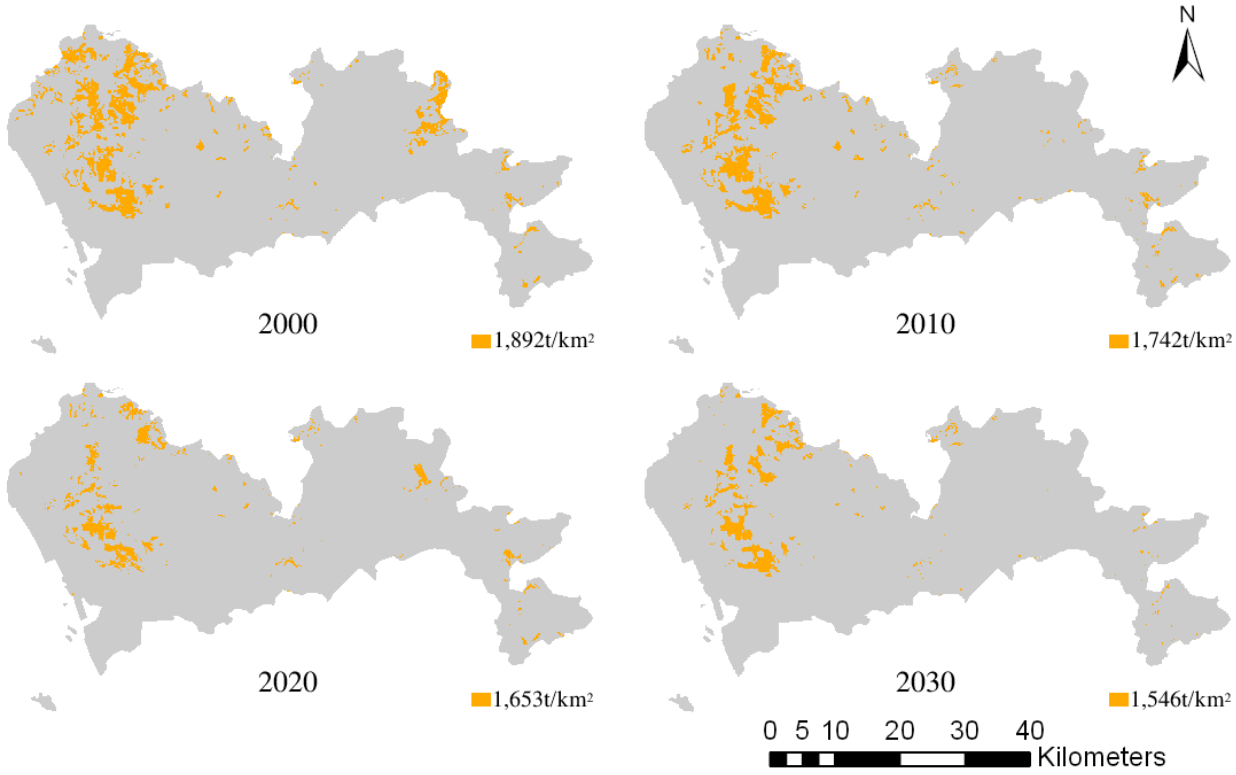

Figure 33. Spatial distribution of crop production in Shenzhen from 2000 to 2030.

The main cultivated land in Shenzhen is concentrated in the west, whereas the rest is mainly located close to the city boundary (***Figure 33***). Therefore, cultivated land experienced a significant decrease between 2000 and 2030, whereas the total crop production declined from 281,908 t (2000) to 108,220 t (2030). This result indicated that the crop production in Shenzhen sharply decreased by more than half over three decades. This consequence mainly resulted from two factors. The first is the rapid shrinking of cultivated land (***Table 18*** and **Figure *29 (a)***). From 2000 to 2030, the area of cultivated land decreased by approximately 79 km^2, where the conversion of cultivated land was one of the main sources for the expansion of artificial surfaces. The second is the decline in annual yield per unit area, where the average annual growth rate of crop production in Shenzhen between 2000 and 2020 was

−0.67% (with a net loss of 239 t/ km^2), which increased the severity of the reduction of food self-sufficiency.

4.4.6. Tradeoffs between urbanization and the FWLE nexus.

The urbanization in Shenzhen contributed significantly to the expansion of artificial surfaces, whereas water yield benefited from this change (***Figure 34***). On the contrary, the increase in artificial surfaces negatively influenced crop production, water supply, and habitat quality. Especially, crop production was the most affected by the sprawl of artificial surfaces, which exhibited growth rates of −28% (2000–2010) and −43% (2010–2020), followed by water supply and habitat quality, whereas the water yield increased only by 3% (2000–2010) and 2% (2010–2020). This finding demonstrated that urbanization could lead to an obvious increase in artificial surfaces and evidently exerted negative impacts on food production, water supply, and habitat quality. Moreover, its contribution to the increase in water yield was very limited.

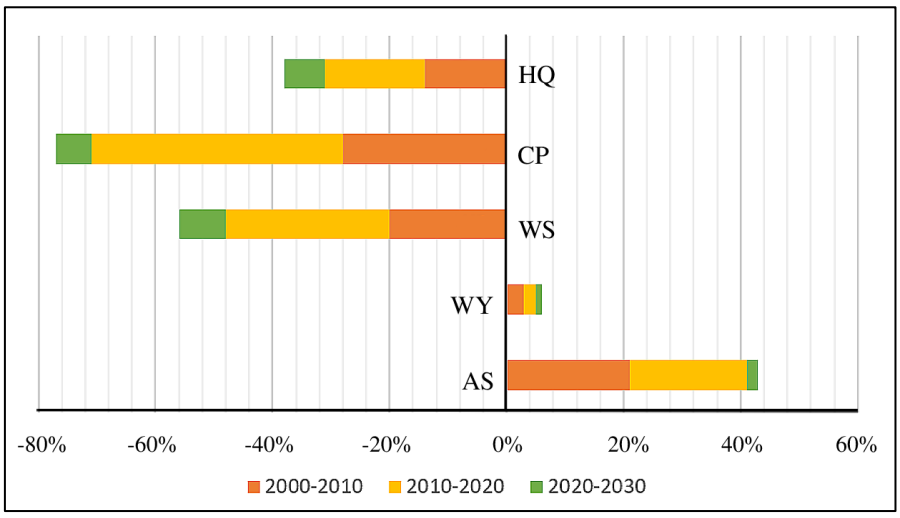

Figure 34. Growth rates of habitat quality (HQ), crop production (CP), water supply (WS), water yield (WY), and artificial surfaces (AS) in Shenzhen from 2000 to 2030. The growth rates for HQ, WS, and WY were calculated based on mean values for 2000, 2010, 2020, and 2030, whereas those

for CP and AS were calculated based on the annual crop production and areas with artificial surfaces for 2000, 2010, 2020, and 2030.

Based on the abovementioned results, the main tradeoffs between urbanization and the FWLE nexus were increases in artificial surfaces and water yield and decreases in habitat quality, crop production, and water supply. However, ***Figure 34*** indicates that the disadvantages (degradation of habitat quality and decline in food production and water supply) outweighed the advantages (increase in water yield and artificial surfaces) in terms of the FWLE nexus. Nevertheless, urbanization can still hold a powerful transformative potential to optimize the FWLE nexus and achieve the SDGs [287]. In 2016, the United Nations Conference on Housing and Sustainable Urban Development (Habitat III) adopted the New Urban Agenda [288]. This document mentions that urbanization can contribute to a better and more sustainable future given that cities are well-planned and well-managed. From this perspective, the spatially explicit assessment of the nexus can help present tradeoffs for mitigating the contradictions between urbanization and the FWLE nexus. For instance, the spatial distributions of water yield and habitat quality in 2020 can be combined to provide integrated information (***Figure 35***). In this case, the greener the color, the higher the values of water yield and habitat quality. Conversely, the redder the color, the lower the values of water yield and habitat quality. Areas with high levels of water yield and high habitat quality were mainly located on the eastern side, which should be protected from intensive land-use changes. Moreover, areas with low water yield and high habitat quality could be considered priorities for restoration or optimization. In addition, areas with low habitat quality and low water yield can be considered potential areas for urban development. This integrated spatial assessment captures and presents the characteristics of the FWLE nexus of a place and helps facilitate the identification of areas that require protection from intensive development or that

are considered potential candidates for development. In this manner, contributions to tradeoffs in the sustainable development of urbanization can be made.

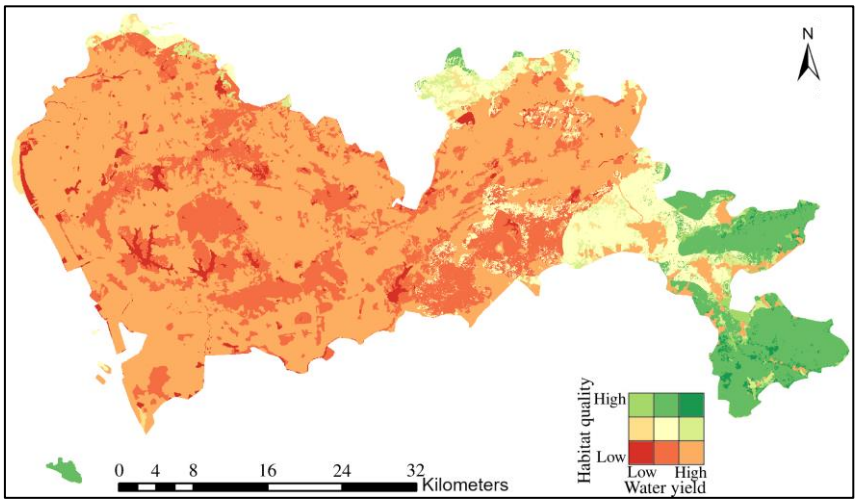

Figure 35. Bivariate mapping of habitat quality and water yield in 2020

4.5. Discussion

4.5.1. Impact of urbanization on the FWLE nexus

A habitat denotes a place that offer food, water, and reproductive and nursery grounds for the preservation of an abundant biodiversity [289]. Thus, degradation and loss of habitat for biodiversity can reduce the efficiency of nutrient cycling, soil formation, and water purification [290], [291]. However, in Shenzhen, the study demonstrated that habitat degradation has occurred and will continue in the future under the BaU scenario (***Figure 30*** and **Figure S *1***). The study identified a remarkable urban expansion in Shenzhen and the occurrence of intensive development in the coastal area (e.g., reclamation), such that the area for artificial surfaces increased to nearly 1.5 times compared with that for 2000 (***Table 18***). Large amounts of forest and cultivated land were converted to artificial surfaces (**Figure *29 (a)***). This finding is in accordance with those for other cities in China, such as the Huang-Huai-Hai Plain [292], Yangtze River Delta [293], and the Pearl River Delta [216].

The trend of increasing urbanization is likely to intensify the existing challenges for urban sustainability [294] and the security of the food–water–ecosystem nexus, because rapid urban expansion accelerates the decline of habitat quality and threatens biodiversity [295]. This scenario can lead to a significant degradation in agroecosystem services [296], [297] and negatively affect crop production, which was demonstrated by this study. In ***Figure 36***, the annual crop yield in Shenzhen sharply decreased from 2000 to 2020 with an average decline rate of approximately 36%. This decrease poses a threat to food security. Moreover, we observed that the mean box value for each habitat quality and water supply indicated downward trends, which signifies that the overall level of habitat quality and water supply gradually deteriorated with the increase in the sprawl of artificial surfaces. Alternatively, the mean value for the annual volume of water yield in Shenzhen increased between 2000 and 2030 due to the conversion of cultivated land or forest into built-up land, which was mainly covered by impervious surfaces. This change, thus, decreased the evapotranspiration and infiltration of precipitation and accelerating runoff [279]. Nevertheless, areas for other land uses in Shenzhen experienced a reduction in water yield (***Figure 31***), such as the transition from grassland to artificial surfaces and from wetland to cultivated land [298]–[300]. However, a positive nexus was noted between the development of artificial surfaces and water yield as a whole (**Figure S *2***).

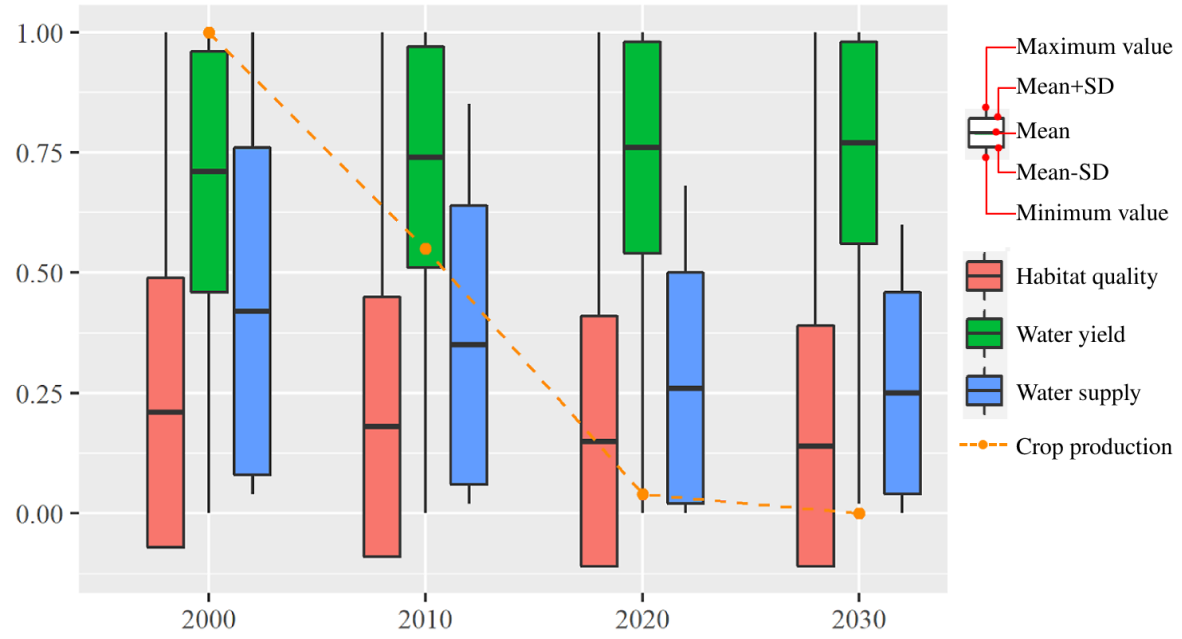

Figure 36. Normalization of habitat quality, water yield, water supply, and crop production in Shenzhen (SD represents the standard deviation)

Furthermore, spatial assessment can not only help analyze tradeoffs and synergies among land-use and ecosystem services and goods [301] but can also play an essential role in sustainable management [302]. At this point, a continuous monitoring of urbanization dynamics and forecasting of the trend and consequence of plausible land-use development are necessary to increase awareness about their positive and negative impacts. The present study provided a convenient means for projecting future land-use patterns under the current context of urbanization and its corresponding impact on FWLE nexus. Thus, we provided evidence for guiding current or future policy decisions and planning. Furthermore, the study explored the spatial associations between the spatial distribution of ecosystem services and land-use changes in Shenzhen. The results revealed that cropland, which is located in regions with low elevation (***Figure 25*** and ***Figure 33***), was rapidly converted into artificial surfaces, which resulted in area reduction by approximately 50% between 2000 and 2020. Moreover, the low habitat quality (***Figure 30***) and relatively severe degradation (**Figure S *1***) were predominantly concentrated in the western side of Shenzhen, where the intense expansion of artificial surfaces occurred. The

water supply (**Figure *32***) also exhibited high spatial heterogeneity and relatively high water supply as indicated in the mountainous region of the eastern side. At the same time, the study identified severe water-scarce sub-watersheds on the western side and coastal areas from 2010 to 2030. In contrast, the spatial characteristic of water yield considerably differed from the other services, where water yield was found to increase in the sub-watersheds, where forest and cropland were replaced by artificial surfaces (***Figure 31***).

Moreover, this study analyzed the tradeoffs between urbanization and the FWLE nexus (***Figure 34***) and reported that land-use change is a critical factor of the changes in the supply of food, water, and ecosystem services. However, we highlight that although land-use change is a key that triggers the changes in the FWLE nexus (e.g., decreases in crop production and water supply), other factors affected by urbanization, such as the growth of domestic water consumption [303], [304] and the degradation of soil fertility and quality [37], [305], may also exert a considerable influence on the FWLE nexus.

4.6. Conclusion

The FWLE nexus is crucial for the sustainable development of the environment and the well-being of humans. In the present study, land-use change was deemed as the joint point for exploring the impact of urbanization on the FWLE nexus, where Shenzhen was taken as the case study to project the future land-use pattern in 2030 under the BaU scenario of the LCM. Moreover, we estimated the influence of land-use changes on habitat quality, water yield, water supply, and crop production from 2000 to 2030 via InVEST. The result indicated that assessment of past changes is possible, and the consequence of future trends and impacts can be estimated. In this manner, the study conducted temporal and spatial analyses and assessments to explore the FWLE nexus under the trend of recent urbanization. We found

that habitat quality gradually declined from 2000 to 2030, especially for areas adjacent to artificial surfaces, where degradation and water scarcity were concentrated. Moreover, crop production also exhibited a downward trend, which sharply decreased by more than half over the three decades. Such a trend poses a threat to food self-sufficiency in Shenzhen. However, the total annual volume of water yield increased due to the expansion of artificial surfaces, whereas the sub-water yield in other land-use areas gradually declined. Finally, analysis of tradeoffs and discussion revealed the negative correlations of artificial surfaces with habitat quality, water supply, and crop production. Notably, an arguably positive correlation is noted with total water yield. In summary, the disadvantages outweighed the advantages under the BaU scenario in terms of the FWLE nexus. Thus, this study proposed an integrated spatial assessment that may contribute to the tradeoffs in the sustainable development of urbanization in the future.

CHAPTER 5: General discussion and conclusion

5.1. Conclusion of the three subtopics

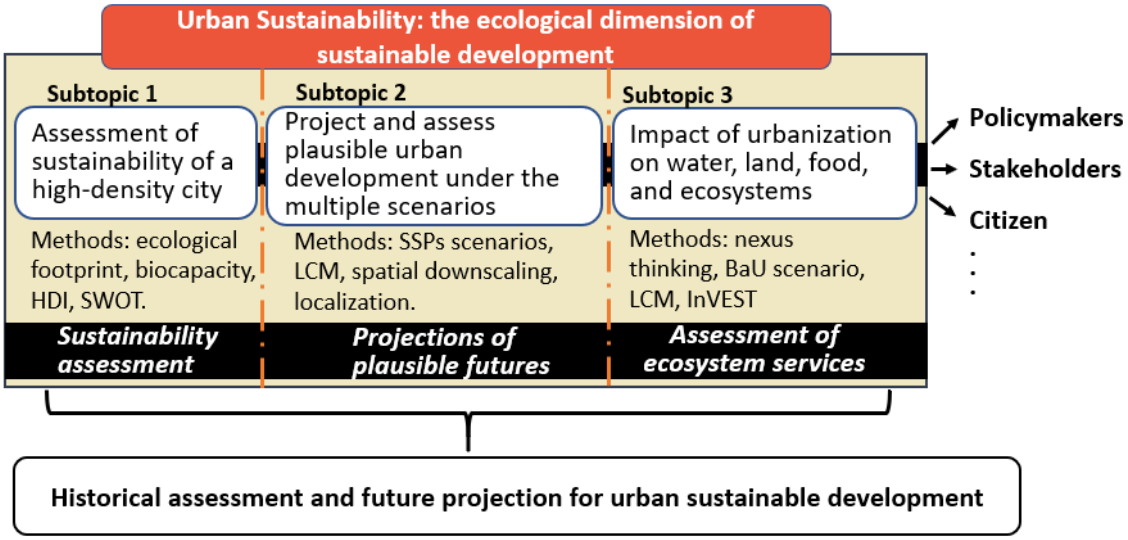

Figure 37. The summary of three subtopics.

The sustainable urban development issues are the focus of the thesis, as shown in ***Figure 37***, three subtopics were conducted for the spatio-temporal analyses and projections of the socio-ecological system. The first stage is the assessment of the sustainability of the relationship between environment and human society in the high-density urban area. As a typical megacity in Asia, Hong Kong was chosen as the study case and the time horizon was from 1995 to 2016. The ecological footprint and biocapacity were used to measure the natural resources consumed by population and the supply from ecosystem, respectively. Next, the Human Development Index (HDI) was adopted to evaluate the human well-being that related to healthy life, education and a decent standard of living. Finally, a further comparative analysis and a SWOT analysis of Singapore and Hong Kong were performed to demonstrate the high ecological footprint could be decoupled from the development of human society. The results showed that the per capita ecological footprint of Hong Kong increased evidently between 1995 and 2016, it rose from 4.842 gha to 6.223 gha, and the fossil energy

consumption accounted for the largest proportion of growth, followed by the ecological footprints of arable land and water area. The HDI also showed a slight upward trend, it increased from 0.808 to 0.9, however, the biocapacity and ecological deficit deteriorated over time. By contrast, Singapore, a city-state with an area and circumstance similar to Hong Kong's, presented the opposite situation—the HDI rose while the ecological footprint decreased from 2011 to 2015, this indicated that there is a great potential to decouple the high ecological footprint from the development of human society. Therefore, learning from the experience of Singapore, some policy suggestions were put forward in terms of energy consumption, marine environment protection and changes in the behavior of citizens and government, thus achieving "a high HDI and low footprint society" on the way to sustainability.

The second stage is the projections of plausible futures. In order to explore possible land-use patterns for helping achieve sustainable development in urban agglomeration area, a spatial downscaling framework was proposed, it couples the five SSPs narratives (they are, SSP1— Sustainability, SSP2— Middle of the road, SSP3— Reginal rivalry, SSP4— Inequality, SSP5— Fossil-fueled development) and local land planning policy using a land change modeling method to simulate the future land-use scenarios, besides, the BaU scenario was also simulated. The Guangdong–Hong Kong–Macao Greater Bay Area, China was chosen as the study case and the time horizon was from 2000 to 2030. Then, the biocapacity and carbon emissions from land-use were estimated to demonstrate the application of the projected land-use maps. The results of the future projections showed that there is a significant expansion in the urban area under all the scenarios, with varying degrees of decrease in cropland and forest among the different scenarios, and cropland was the major contributor to the expansion of

urban area, approximately 22% of cropland had been converted into urban area between 2000 and 2030. Among the SSPs, cropland and urban area were the largest in SSP1, followed by their respective areas in SSP5 and SSP4, whereas the cropland and urban area were the lowest in SSP3. In addition, the considerable differences in local biocapacity and carbon emissions were resulted from the different changes of land-use. The analysis found that the intervention policies, such as the cultivated land requisition–compensation balance policy, were beneficial mainly for developing urban area and protecting cropland. For achieving sustainable development not only urban area and cropland should be involved for consideration but should also cover the balance between all land-use classes, and based on the findings, three implications were also drawn in terms of the biocapacity optimization, mitigation of CO_2 emissions, and improvements of policy.

The third stage, an original framework of the FWLE nexus was proposed for exploring the correlations between food, water, land, and ecosystem in the context of urbanization. First, the historical land-use changes from 2000 to 2010 were analyzed by using the Land Change Modeler (LCM), then the land-use transition potential submodels were built for projecting the future land-use pattern in 2030 under the BaU scenario. Next, based on the results of land-use changes, the habitat quality, water yield, water supply, and crop production between 2000 and 2030 were assessed by using the InVEST model and statistical materials. Lastly, the temporal and spatial assessment and trade-offs between the urbanization and FWLE nexus were analyzed and discussed. Shenzhen, China was used as the study case and the time horizon was from 2000 to 2030. The results of land-use changes indicated that a significant expansion of artificial surfaces occurred in Shenzhen, with varying degrees of decrease in cultivated land, forest and grassland. Moreover, the habitat quality, water supply, and crop production were decreased obviously due to the rapid urbanization, whereas the total water

yield showed an upward trend. The analysis revealed that there was an arguably positive correlation between artificial surfaces and total water yield, and negative correlations with habitat quality, water supply, and crop production interactions. Furthermore, an integrated spatial assessment was made to capture and present characteristics between the FWLE nexus of a place and helps facilitate the identification of areas that need to be improved or protected for promoting sustainable urbanization. The study provided a convenient way to explore the correlations and trade-off between urbanization and FWLE nexus.

5.2. Achievements, limitations and future research prospect

The study first assessed urban sustainability from the perspective of supply-demand aspect, and put forward policy suggestions for decoupling high ecological footprint from the development of society. Then scenario simulation method was employed to project future land-use change in urban area thus analyzing and assessing the possible impacts on ecosystem, besides, an original framework of the food-water-land-ecosystem nexus was proposed to contribute to the limited research in terms of the quantitative assessment of the nexus.

The sustainable urban development is a comprehensive and complicated issue, it involves not only the environmental factor but also the social and economic factors. In the study, the sustainability of urban area was mainly assessed and analyzed from an environmental-ecological perspective, such as the land-use changes, ecosystem services, resource consumption and biodiversity, etc. and only a few social factors (population and policies) were considered. The results could be improved further by combining economic factors, such as gross domestic product, green economy, and environmental economics, etc.

As a popular index, ecological footprint can be calculated and compared for systems of any scale, from an urban scale to a national scale [306]. It was promoted as a policy guide and planning tool for sustainability [307]. However, the ecological footprint for consumption as it relates to the total amount of resources available does not reflect the "production footprint," or differences in intensity of resource use [308]. It has also been criticized as an oversimplification [309]. For instance, in the case of energy consumption, the ecological footprint analysis does not tell the whole story with respect to the environmental impacts of a person or entity [310]. Therefore, we need a more comprehensive and innovative method. In 2018, the Nature's Contributions to People (NCP) framework was put forward by Díaz et al. [311]. The aim is to come up with products that are more likely to be incorporated into policy and practice. NCP considers both positive and negative contributions to people's quality of life. As a more inclusive approach, NCP will improve the relevance and value of expert evidence about nature in achieving the SDGs [312].

Currently, scenarios about socioeconomic future prospects, such as the SSPs used in chapter 3, are playing a major role in making projections [313]. However, these scenarios have limitations in their applicability to biodiversity and nature research [314], [315]. To fill the gap, nature-centered scenarios, including the Nature Futures Framework (NFF), developed by the Intergovernmental Science-Policy Platform on Biodiversity and Ecosystem Services (IPBES), were proposed. The NFF describes positive relationships between people and nature, from multiple aspects, such as nature as culture, nature for society, and nature for nature [316], to capture interlinkages of social-ecological systems across biodiversity, ecosystem functions and services, and human well-being [151], [317]. In Japan, a new research project named Predicting and Assessing Natural Capital and Ecosystem Services (PANCES), which uses an integrated

social-ecological system approach, was launched to predict and assess the natural capital and ecosystem services under national-scale future scenarios [318]. A strong international cooperation is also being established. The IPBES-IPCC co-sponsored workshop, which was the first collaboration between IPBES and IPCC, was held in December 2020 to build a multidisciplinary expert group to meet both climate change- and biodiversity-related goals [319]. Therefore, the combination of socioeconomic scenarios and nature-centered scenarios will become more productive toward the sustainable development of cities in the future.

Chapter 4 analyzed the impact of urbanization on the FWLE nexus based on the BaU scenario for Shenzhen. This scenario extrapolated recent trends (from 2000 to 2010) into the future; however, other plausible scenarios can be used for further exploration. For instance, the shared socioeconomic pathway scenarios consist of five developments and quantitatively describe key drivers, such as population and economic growth [143]. In addition, the nature futures framework, which is a heuristic tool for connecting nature and people, provides a structure for consistency in the scenarios [320]. Moreover, the scenario can be localized by considering the planning documents of the government [321]. Multiple scenarios based on socio-economy and nature can be used for future research on the FWLE nexus. Besides, it also should be noted that the drives of changes in crop production, habitat quality, water supply, and water yield are multiple, such as climate change, policy intervention, changes in lifestyle and technology, etc., they can be considered into the further research.

The LCM was used to predict future land-use pattern. However, we expected misses or errors in predictions, because the simulation is based on the change analysis of a past period. Specifically, if the future development did not follow the pattern of the past, such as the gray

box in **Figure *29 (b)***, which is an area that experienced dramatic changes over a short period, then the accuracy of the prediction would be relatively low.

Moreover, the parameters used for modeling were collected from various datasets or references (***Table 16***), such as soil data, due to the limitations of data sources. Thus, inconsistency in the data may occur, which can lead to a negative impact on the accuracy of the results. In addition, the water yield model in InVEST is sensitive to modeled changes in drivers, such as land-use change or climate change [322]. According to the sixth assessment report of the Intergovernmental Panel on Climate Change [323], climate change may also exert an impact on water cycle, water balance, and agricultural and ecological droughts. However, only land-use maps that varied according to the time series were used in this study, because climate change is beyond the scope of our work. Other variables, such as precipitation and ET_0, were assumed to remain constant. Therefore, results related to water yield may be further enhanced by considering the climate data corresponding to different years. Furthermore, Shenzhen Statistical Yearbook 2020 [255] demonstrates a downward trend in the annual yield of crop per unit area from 2000 to 2019. Under the projection of the BaU scenario, the annual yield of crop per unit area in 2030 should become less than that for 2019. We estimated the annual yield of crop per unit area in 2030 based on the average annual growth rate of the last 20 years due to the limitation of data. However, more accurate results could be obtained using crop yield prediction models, such as statistical and crop simulation models, as well as artificial neural networks [324]. Alternatively, the validation of InVEST is limited due to the requirements for empirical or statistical observations [322], [325], such as observations of habitat quality and water yield. As a widely used model for spatializing ecosystem services [325], building an efficient validation method for InVEST

will contribute to the improvement of the simulation of ecosystem services, which can be considered a potential prospect for future research.

Appendix A. Supplementary materials of Chapter 2.

Table S 1. Hong Kong's per capita ecological footprint by land categories during 1995-2016. (unit: gha/cap)

Years	Arable land	Forest land	Grazing land	Water area	Fossil land	Built-up land	Ecological footprint
1995	1.088	0.075	0.430	1.661	1.578	0.010	4.842
1996	1.107	0.075	0.420	1.515	1.528	0.010	4.655
1997	1.185	0.080	0.449	1.273	1.318	0.010	4.315
1998	1.219	0.079	0.396	1.316	1.604	0.010	4.624
1999	1.403	0.080	0.331	1.144	1.930	0.010	4.898
2000	1.390	0.085	0.318	1.338	1.795	0.011	4.937
2001	1.282	0.079	0.285	1.420	1.888	0.011	4.965
2002	1.241	0.079	0.251	1.463	1.951	0.011	4.996
2003	1.240	0.080	0.227	1.399	2.007	0.012	4.965
2004	1.042	0.083	0.232	1.488	2.136	0.012	4.993
2005	1.017	0.085	0.237	1.476	2.174	0.013	5.002
2006	1.096	0.088	0.245	1.529	2.298	0.012	5.268
2007	1.230	0.091	0.240	1.466	2.422	0.012	5.461
2008	1.591	0.090	0.227	1.347	2.268	0.012	5.535
2009	1.679	0.087	0.246	1.385	2.532	0.012	5.941
2010	1.846	0.092	0.260	1.529	2.612	0.012	6.351
2011	1.985	0.096	0.290	1.552	2.522	0.012	6.457
2012	1.611	0.093	0.333	1.545	2.402	0.012	5.996
2013	1.757	0.086	0.346	1.665	2.439	0.012	6.305
2014	1.976	0.083	0.368	1.646	2.377	0.012	6.462
2015	1.636	0.086	0.345	1.576	2.481	0.012	6.136
2016	1.758	0.089	0.378	1.468	2.518	0.012	6.223

Table S 2. Hong Kong's ecological footprint of energy during 1995-2016. (unit: gha/cap)

Years	Kerosene	Gasoline	Diesel oil	Coal	Fuel oil	LPG	Natural gas	Gas	Electricity
1995	0.262	0.027	0.291	0.552	0.117	0.014	0.002	0.038	0.241
1996	0.277	0.026	0.259	0.390	0.124	0.017	0.121	0.037	0.242
1997	0.230	0.017	0.150	0.329	0.069	0.017	0.189	0.039	0.244
1998	0.232	0.015	0.337	0.405	0.088	0.014	0.176	0.039	0.26 1
1999	0.269	0.025	0.627	0.361	0.111	0.012	0.192	0.039	0.257
2000	0.292	0.025	0.447	0.339	0.148	0.034	0.159	0.041	0.271
2001	0.303	0.027	0.393	0.445	0.164	0.035	0.164	0.042	0.276
2002	0.309	0.024	0.383	0.479	0.202	0.035	0.160	0.041	0.279
2003	0.284	0.023	0.398	0.585	0.218	0.024	0.111	0.042	0.281
2004	0.348	0.022	0.373	0.557	0.299	0.031	0.144	0.040	0.283
2005	0.386	0.023	0.280	0.592	0.337	0.033	0.152	0.042	0.287
2006	0.392	0.021	0.283	0.620	0.398	0.037	0.169	0.042	0.292
2007	0.439	0.023	0.263	0.660	0.473	0.034	0.155	0.041	0.294
2008	0.418	0.022	0.196	0.606	0.438	0.038	0.175	0.042	0.292
2009	0.402	0.024	0.407	0.656	0.458	0.037	0.169	0.041	0.296
2010	0.450	0.024	0.351	0.538	0.628	0.038	0.205	0.041	0.296
2011	0.480	0.025	0.286	0.653	0.498	0.039	0.163	0.041	0.296
2012	0.452	0.026	0.240	0.643	0.469	0.038	0.150	0.042	0.299
2013	0.476	0.026	0.228	0.672	0.481	0.036	0.141	0.042	0.295
2014	0.466	0.023	0.216	0.710	0.402	0.038	0.135	0.042	0.302
2015	0.490	0.032	0.316	0.571	0.483	0.036	0.170	0.041	0.299
2016	0.521	0.031	0.353	0.567	0.456	0.034	0.174	0.041	0.298

Table S 3. Hong Kong's per capita biocapacity by land categories during 1995-2016. **(unit: gha/cap)**

Years	Arable land	Forest land	Grazing land	Water land	Built-up land	Biocapacity
1995	0.0042	0.0043	0.0192	0.0007	0.0101	0.0385
1996	0.0039	0.0041	0.0183	0.0007	0.0099	0.0369
1997	0.0038	0.0041	0.0182	0.0007	0.0099	0.0367
1998	0.0037	0.0041	0.0180	0.0007	0.0100	0.0364
1999	0.0036	0.0040	0.0178	0.0007	0.0100	0.0362
2000	0.0034	0.0066	0.0103	0.0007	0.0112	0.0322
2001	0.0033	0.0066	0.0102	0.0007	0.0113	0.0320
2002	0.0032	0.0065	0.0101	0.0007	0.0114	0.0319
2003	0.0034	0.0077	0.0074	0.0007	0.0116	0.0307
2004	0.0034	0.0071	0.0080	0.0007	0.0123	0.0315
2005	0.0035	0.0071	0.0082	0.0007	0.0125	0.0321
2006	0.0032	0.0070	0.0086	0.0007	0.0122	0.0318
2007	0.0031	0.0071	0.0082	0.0007	0.0121	0.0313
2008	0.0032	0.0070	0.0082	0.0007	0.0120	0.0311
2009	0.0031	0.0069	0.0083	0.0007	0.0121	0.0312
2010	0.0031	0.0081	0.0056	0.0007	0.0121	0.0297
2011	0.0031	0.0078	0.0060	0.0007	0.0121	0.0298
2012	0.0031	0.0076	0.0062	0.0007	0.0120	0.0296
2013	0.0031	0.0075	0.0062	0.0007	0.0119	0.0295
2014	0.0030	0.0076	0.0058	0.0007	0.0119	0.0291
2015	0.0030	0.0075	0.0060	0.0007	0.0119	0.0290
2016	0.0030	0.0075	0.0058	0.0007	0.0122	0.0292

Table S 4. Singapore's per capita ecological footprint by land categories from 1995 to 2016.

(unit: gha/cap)

(Reference source: Global Footprint Network [99])

Years	Arable land	Forest land	Grazing land	Water area	Fossil land	Built-up land	Ecological footprint
1995	0.441	0.698	0.244	0.189	4.940	0.006	6.518
1996	0.441	0.665	0.209	0.182	5.115	0.007	6.618
1997	0.410	0.557	0.221	0.186	5.859	0.008	7.241
1998	0.280	0.470	0.195	0.144	4.787	0.009	5.885
1999	0.491	0.497	0.230	0.161	5.189	0.010	6.578
2000	0.475	0.479	0.235	0.159	6.952	0.010	8.311
2001	0.518	0.366	0.209	0.161	6.145	0.011	7.411
2002	0.460	0.340	0.258	0.186	5.349	0.013	6.604
2003	0.472	0.443	0.180	0.243	4.509	0.022	5.869
2004	0.455	0.557	0.238	0.226	5.592	0.025	7.093
2005	0.445	0.444	0.229	0.248	5.273	0.026	6.665
2006	0.439	0.565	0.214	0.260	5.708	0.029	7.215
2007	0.458	0.569	0.224	0.258	5.366	0.025	6.900
2008	0.507	0.489	0.199	0.250	6.148	0.029	7.623
2009	0.509	0.366	0.212	0.250	5.633	0.030	7.000
2010	0.563	0.433	0.215	0.247	5.258	0.032	6.748
2011	0.609	0.735	0.252	0.247	5.779	0.034	7.655
2012	0.668	0.759	0.236	0.220	5.667	0.035	7.585
2013	0.584	0.543	0.242	0.220	5.008	0.040	6.638
2014	0.591	0.350	0.264	0.238	4.476	0.042	5.961
2015	0.610	0.330	0.281	0.218	4.657	0.043	6.140
2016	0.578	0.260	0.250	0.221	4.528	0.042	5.879

Table S 5. Singapore's per capita biocapacity by land categories from 1995 to 2016. **(unit: gha/cap)**
(Reference source: Global Footprint Network [99])

Years	Built-up land	Arable land	Water area	Forest land	Grazing land	Biocapacity
1995	0.006	0.000	0.021	0.004	0.000	0.031
1996	0.007	0.000	0.020	0.004	0.000	0.031
1997	0.008	0.000	0.020	0.004	0.000	0.032
1998	0.009	0.000	0.019	0.004	0.000	0.033
1999	0.010	0.001	0.019	0.004	0.000	0.033
2000	0.010	0.001	0.019	0.003	0.000	0.033
2001	0.011	0.001	0.018	0.003	0.000	0.034
2002	0.013	0.001	0.018	0.003	0.000	0.034
2003	0.022	0.001	0.017	0.003	0.000	0.043
2004	0.025	0.001	0.017	0.003	0.000	0.045
2005	0.026	0.001	0.016	0.003	0.000	0.046
2006	0.029	0.001	0.016	0.003	0.000	0.049
2007	0.025	0.001	0.015	0.003	0.000	0.044
2008	0.029	0.001	0.015	0.003	0.000	0.047
2009	0.030	0.001	0.015	0.003	0.000	0.048
2010	0.032	0.001	0.014	0.003	0.000	0.050
2011	0.034	0.001	0.014	0.003	0.000	0.051
2012	0.035	0.001	0.014	0.003	0.000	0.052
2013	0.040	0.001	0.013	0.002	0.000	0.057
2014	0.042	0.001	0.013	0.002	0.000	0.059
2015	0.043	0.001	0.013	0.002	0.000	0.060
2016	0.042	0.001	0.013	0.002	0.000	0.059

Appendix B. Supplementary materials of Chapter 3.

I. The population projection maps of Hong Kong and Macao under SSPs.

Due to the population projection maps of SSPs which created by Chen, et al. [186] do not involve Hong Kong and Macao, we calculated the population projection maps for these two areas in a simplified method. Compared with 2020, the spatial distribution pattern of population in 2030 will essentially stay the same [177], therefore, by using R software and according to each grid cell's proportion of Hong Kong and Macao in 2020 [maps derived from Worldpop [190]] to distribute their total population data of 2030 (IIASA [187]) to generate the population maps in 2030.

The specific four steps and codes used in R as shown below:

```
library(raster)

library(sp)
```

#1. Import the 2020 population raster maps and 2030 total population data of MACAO and Hong Kong (HK)

```
MacaoPop2020=raster("mac2020pop100m.tif")

HKPop2020=raster("hk2020pop100m.tif")


Macao2030_ssp1=669000

Macao2030_ssp2=678000

Macao2030_ssp3=649000
```

Macao2030_ssp4=666000

Macao2030_ssp5=704000

HK2030_ssp1=8183000

HK2030_ssp2=8253000

HK2030_ssp3=7857000

HK2030_ssp4=8117000

HK2030_ssp5=8633000

#2. Calculate each grid cell's proportion in 2020

Proportion_Macao=MacaoPop2020/cellStats(MacaoPop2020,sum)

Proportion_HK=HKPop2020/cellStats(HKPop2020,sum)

#3. According to the proportion calculated above to distribute the total population data in 2030

 # 3.1 For Macao

Macao2030_distribution1=Macao2030_ssp1*Proportion_Macao

Macao2030_distribution2=Macao2030_ssp2*Proportion_Macao

Macao2030_distribution3=Macao2030_ssp3*Proportion_Macao

Macao2030_distribution4=Macao2030_ssp4*Proportion_Macao

Macao2030_distribution5=Macao2030_ssp5*Proportion_Macao

3.2 For Hong Kong

HK2030_distribution1=HK2030_ssp1*Proportion_HK

HK2030_distribution2=HK2030_ssp2*Proportion_HK

HK2030_distribution3=HK2030_ssp3*Proportion_HK

HK2030_distribution4=HK2030_ssp4*Proportion_HK

HK2030_distribution5=HK2030_ssp5*Proportion_HK

4. Export the population maps in 2030

writeRaster (HK2030_distribution1, "HK2030_SSP1Pop100m.tif")

II. The conversion cost matrix

Table S 6. Conversion cost matrix of SSP1.

	Cropland	Bush and grassland	Forest	Water	Urban area	Barren land
Cropland	0.000	0.150	1.350	1.200	0.150	0.600
Bush and grassland	0.250	0.000	0.400	0.400	0.300	0.100
Forest	0.525	0.450	0.000	1.485	1.485	1.200
Water	1.350	1.350	1.350	0.000	1.485	0.750

Urban area	1.000	1.000	1.000	1.000	0.000	1.000
Barren land	0.900	0.500	0.495	0.800	0.150	0.000

Table S 7. Conversion cost matrix of SSP3.

	Cropland	Bush and grassland	Forest	Water	Urban area	Barren land
Cropland	0.000	0.050	0.450	0.400	0.025	0.200
Bush and grassland	0.750	0.000	1.200	0.400	0.150	0.100
Forest	0.175	0.150	0.000	0.495	0.495	0.400
Water	0.450	0.450	0.450	0.000	0.495	0.250
Urban area	1.000	1.000	1.000	1.000	0.000	1.000
Barren land	0.900	0.500	0.990	0.800	0.450	0.000

Table S 8. Conversion cost matrix of SSP4.

	Cropland	Bush and grassland	Forest	Water	Urban area	Barren land
Cropland	0.000	0.100	0.900	0.800	0.050	0.400
Bush and grassland	0.750	0.000	1.200	0.400	0.450	0.100
Forest	0.525	0.300	0.000	0.990	0.990	0.800
Water	0.900	0.900	0.900	0.000	0.990	0.500
Urban area	1.000	1.000	1.000	1.000	0.000	1.000
Barren land	0.900	0.500	0.990	0.800	0.150	0.000

Table S 9. Conversion cost matrix of SSP5.

	Cropland	Bush and grassland	Forest	Water	Urban area	Barren land
Cropland	0.000	0.100	0.900	0.800	0.050	0.400
Bush and grassland	0.250	0.000	0.800	0.400	0.300	0.100
Forest	0.350	0.300	0.000	0.990	0.990	0.800
Water	0.900	0.900	0.900	0.000	0.990	0.500
Urban area	1.000	1.000	1.000	1.000	0.000	1.000
Barren land	0.900	0.500	0.990	0.800	0.150	0.000

III. The land transition probability matrices of the Greater Bay Area under SSPs

Table S 10. Land transition probability matrix of SSP1.

	Cropland	Bush and grassland	Forest	Water	Urban area	Barren land
Cropland	0.8316	0.0000	0.0000	0.0000	0.1684	0.0000
Bush and grassland	0.0000	1.0000	0.0000	0.0000	0.0000	0.0000
Forest	0.1402	0.0048	0.8550	0.0000	0.0000	0.0000
Water	0.0000	0.0000	0.0000	0.9469	0.0394	0.0137
Urban area	0.0000	0.0000	0.0000	0.0000	1.0000	0.0000
Barren land	0.0000	0.0000	0.0000	0.0000	1.0000	0.0000

Table S 11. Land transition probability matrix of SSP2.

	Cropland	Bush and grassland	Forest	Water	Urban area	Barren land
Cropland	0.8823	0.0000	0.0000	0.0000	0.1177	0.0000

Bush and grassland	0.0000	0.5918	0.0000	0.0000	0.4082	0.0000
Forest	0.0000	0.0873	0.9127	0.0000	0.0000	0.0000
Water	0.0000	0.0000	0.0000	0.9469	0.0123	0.0408
Urban area	0.0000	0.0000	0.0000	0.0000	1.0000	0.0000
Barren land	0.0000	0.0000	0.0000	0.0000	1.0000	0.0000

Table S 12. Land transition probability matrix of SSP3.

	Cropland	Bush and grassland	Forest	Water	Urban area	Barren land
Cropland	0.8234	0.0423	0.0000	0.0000	0.1343	0.0000
Bush and grassland	0.0000	1.0000	0.0000	0.0000	0.0000	0.0000
Forest	0.0000	0.0707	0.9293	0.0000	0.0000	0.0000
Water	0.0000	0.0263	0.0000	0.9469	0.0000	0.0268
Urban area	0.0000	0.0000	0.0000	0.0000	1.0000	0.0000
Barren land	0.0000	0.0000	0.0000	0.0000	0.0000	1.0000

Table S 13. Land transition probability matrix of SSP4.

	Cropland	Bush and grassland	Forest	Water	Urban area	Barren land
Cropland	0.8290	0.0000	0.0000	0.0000	0.1710	0.0000
Bush and grassland	0.0000	1.0000	0.0000	0.0000	0.0000	0.0000
Forest	0.1304	0.0054	0.8642	0.0000	0.0000	0.0000
Water	0.0134	0.0000	0.0000	0.9469	0.0000	0.0397

Urban area	0.0000	0.0000	0.0000	0.0000	1.0000	0.0000
Barren land	0.0000	0.0000	0.0000	0.0000	1.0000	0.0000

Table S 14. Land transition probability matrix of SSP5.

	Cropland	Bush and grassland	Forest	Water	Urban area	Barren land
Cropland	0.8412	0.0000	0.0000	0.0000	0.1588	0.0000
Bush and grassland	0.0000	0.8872	0.0000	0.0000	0.1128	0.0000
Forest	0.1292	0.0000	0.8708	0.0000	0.0000	0.0000
Water	0.0068	0.0000	0.0000	0.9469	0.0000	0.0462
Urban area	0.0000	0.0000	0.0000	0.0000	1.0000	0.0000
Barren land	0.0000	0.0000	0.0000	0.0000	1.0000	0.0000

IV. Sub-model and skill measure

Table S 15. Submodel and their skill breakdown by transition and persistence.

Submodel	Accuracy	Class	Skill measure
Cropland submodel	99.01%	Transition: bush and grassland to cropland	0.977
		Transition: forest to cropland	1.000
		Transition: water to cropland	0.976
		Persistence: bush and grassland	1.000
		Persistence: forest	1.000
		Persistence: water	0.977

Urban development submodel	91.86%	Transition: cropland to urban area	0.790
		Transition: bush and grassland to urban area	0.911
		Transition: forest to urban area	0.765
		Transition: water to urban area	0.961
		Persistence: cropland	1.000
		Persistence: bush and grassland	0.885
		Persistence: forest	0.994
		Persistence: water	0.950
Bush and grassland submodel	81.25%	Transition: cropland to bush and grassland	0.811
		Transition: forest to bush and grassland	0.773
		Transition: water to bush and grassland	0.631
		Persistence: cropland	0.716
		Persistence: forest	1.000
		Persistence: water	0.726
Forest submodel	94.31%	Transition: cropland to forest	1.000
		Transition: bush and grassland to forest	0.967
		Transition: water to forest	0.852
		Persistence: cropland	0.981
		Persistence: bush and grassland	0.913
		Persistence: water	0.878
Water submodel	100%	Transition: forest to water	1.000
		Persistence: forest	1.000

V. Discussion: Advantages and limitations of the study

Table S 16. The comparison of the present study and previous researches in terms of future land-use projection.

	The present study	Hasan et al. [168]	Jiao et al. [216]	Song et al. [161]
Study area	The Greater Bay Area (56,000 km^2)	Guangdong, Hong Kong, and Macao regions (196,342 km^2)	The Pearl River Delta, China (54,000 km^2)	The Hohhot-Baotou-Ordos-Yulin urban agglomeration, China (174,600 km^2)
Scenario	Localized SSPs	BaU	Three scenarios set by authors [a]	Localized SSPs
LULC model	LCM	LCM	The System Dynamics (SD) model; Grey Prediction (GM) model; Markov model	The Land Use Scenario Dynamics-urban (LUSD-urban) model
Advantages	(1) Proposed a spatial downscaling framework (2) The qualitative and quantitative methods of correlating LCM with the localized SSPs were elaborated (3) Constraints and incentives were involved	Simulated with high resolution (30m)	(1) Multiple factors were involved: social, economic, land policy, and constraints factors (2) Multiple models were used for simulation and comparison	(1) Multiple factors were used to localize the SSPs: the latest census data, population policy, migration, and economic factor (2) The localized SSPs were demonstrated to be more reliable than original SSPs in terms of sub-national simulation.
Disadvantages	(1) Only land policies were used to localize the SSPs, the demographic, economic factors, and etc. were not included (2) Future infrastructure development was not considered	(1) Only six variables were used to build the submodel structure and the evidence likelihood was not included (2) Scenarios, constraints and incentives, economic, demographic, and policy factors were not involved in simulation (3) Future infrastructure development was not considered	(1) The design and narratives of these three scenarios were undefined and ambiguous (2) The quantitative method of different variable values which have decisive impacts on projected results was not elaborated	(1) The narrative of each localized SSP was ambiguous and the quantitative method of factor values under different SSP was not elaborated (2) Only urban area was simulated (3) The future urban land demand was projected by a multiple linear regression model (4) A simplified "adaptive Monte Carlo" method was used to calibrate and verify the LUSD-urban model

[a] The three scenarios are: (1) environmental conservation development scenario; (2) rapid economic development scenario; (3) coordinated development of the environment and economy scenario.

Appendix C. Supplementary materials of Chapter 4.

I. The InVEST habitat quality model

equations (1) and (2). By combining information on land use and threats to biodiversity, the model can generate maps that reflect the status of and change in habitat for biodiversity, providing useful information in making an initial assessment of conservation [285].

$$D_{xj} = \sum_{r=1}^{R} \sum_{y=1}^{Y_r} (W_r / \sum_{r=1}^{R} W_r) r_y i_{rxy} \beta_x S_{jr} \quad (1)$$

$$Q_{xj} = H_j \times \left[1 - \left(\frac{D_{xj}^z}{D_{xj}^z + k^z}\right)\right] \quad (2)$$

where D_{xj} is the total threat level in grid cell x with land-use class j, R is the number of ecological threat factors, and Y_r is the set of grid cells on an r raster map. In addition, y is all grid cells, W_r is the threat weight that relates destructiveness of a degradation source to all habitats, r_y is raster map r, i_{rxy} is the distance function of habitat quality and ecological threat factor, β_x is the level of accessibility in grid cell x, where 1 denotes complete accessibility, and S_{jr} is the sensitivity of land-use class j (habitat type) to the ecological threat factor r. Finally, Q_{xj} is the ecological habitat quality value of land-use class j, H_j is a habitat quality score that ranges from 0 to 1, k is the half-saturation constant defaulted at 0.05 [285], and Z is a constant.

Table S 17. Habitat quality score and sensitivity of each land-use class to each threat.

Land-use class	Habitat quality score	Sensitivity of each land-use class to threats				Reference
		Cultivated land	Artificial surfaces	Roads	Railways	
Cultivated land	0.60	0.00	0.65	0.70	0.80	Jiao et al. (2021)
Forest	1.00	0.70	0.85	1.00	1.00	
Grassland	0.70	0.50	0.65	0.90	0.90	

Shrubland	0.80	0.40	0.50	0.60	0.80	Gong et al. (2019)
Wetland	0.85	0.60	0.90	0.60	0.50	Zhu et al. (2020)
Water bodies	0.85	0.35	0.70	0.60	0.70	Jiao et al. (2021)
Artificial surfaces	0.00	0.00	0.00	0.00	0.00	

Table S 18. Maximum distance (in units of km), weight, and decay function of the threats affecting habitat quality

Threat factor	Maximum distance	Weight	Decay
Cultivated land	3.0	0.6	linear
Artificial surfaces	5.0	1.0	exponential
Roads	2.5	0.8	linear
Railways	3.0	0.8	linear

The data in this Table were referred to the work by Jiao et al. (2021)

II. The InVEST annual water yield model

The annual water yield *Y(x)* per pixel on the landscape *x* is calculated according to:

$$Y(x) = \left(1 - \frac{AET(x)}{P(x)}\right) \times P(x) \quad (3)$$

where *AET(x)* is the actual annual evapotranspiration for pixel *x* and *P(x)* is the annual precipitation on pixel *x*, and there are two methods to determine the *AET(x)* depending on the different land-use classes:

(1) For artificial surfaces, wetland, and open water land-use class, *AET(x)* is directly computed as follows:

$$AWC(x) = Min(K_c(lx) \times ET_0(x), P(x))$$

(4)

where $ET_0(x)$ is reference evapotranspiration, and $K_c(lx)$ is the evaporation factor for each land-use class.

(2) For vegetated land-use class, based on an expression of the Budyko curve proposed by Fu (1981) and Zhang et al. (2004), the evapotranspiration portion of the water balance, $AET(x)/P(x)$, is calculated as follows:

$$\frac{AET(x)}{P(x)} = 1 + \frac{PET(x)}{P(x)} - \left[1 + \left(\frac{PET(x)}{P(x)}\right)^{\omega}\right]^{1/\omega}$$

(5)

where $PET(x)$ is the potential evapotranspiration and $\omega(x)$ is a non-physical parameter. Potential evapotranspiration $PET(x)$ is defined as:

$$PET(x) = K_c(l_x) \times ET_0(x)$$

(6)

where $ET_0(x)$ is the reference evapotranspiration from pixel x and $K_c(lx)$ is the plant (vegetation) evapotranspiration coefficient associated with the land-use lx on pixel x.

$\omega(x)$ is defined [330] as:

$$\omega(x) = Z\frac{AWC(x)}{P(x)} + 1.25$$

(7)

where $AWC(x)$ is the volumetric (mm) plant available water content and it is estimated as the product of the plant available water capacity (PAWC) and the minimum of root restricting layer depth and vegetation rooting depth:

$$AWC(x) = Min(Rest.layer.depth, root.depth) \times PAWC$$

(8)

In summary, based on the information above, the InVEST requires nine input data for calculating the water yield, namely, precipitation, ET_0, root restricting layer depth, vegetation

rooting depth, PAWC, land-use maps, (sub)watersheds, K_c, and Z parameter. ***Table S 19*** exhibits the biophysical data on land-use classes, root depth, and K_c. Moreover, the ET_0, root restricting layer depth (refers to soil depth), and precipitation data used in this study were listed in ***Table 16***. Based on the DEM, the sub-watershed vector file could be generated using the DelineateIt model [285], a supporting tool in InVEST. The derivation of the PAWC and Z parameter is shown below:

PAWC

A method that based on the chemical and physical properties of soil to estimate PAWC in China [331] was adopted in this study, the equation (9) as shown below:

$$\begin{aligned} PAWC = {} & 54.509 - 0.132 \times sand\% - 0.003 \times (sand\%)^2 - 0.055 \times silt\% \\ & - 0.006 \times (silt\%)^2 - 0.738 \times clay\% + 0.007 \times (clay\%)^2 \\ & - 2.688 \times OM\% + 0.501 \times (OM\%)^2 \end{aligned} \quad (9)$$

where *sand %*, *silt%*, *clay%*, and *OM%* are the proportion of sand, silt, clay, and organic matter in the soil. The unit of PAWC is $10^{-2}cm^3.cm^{-3}$. Furthermore, the value of PAWC is converted to a fraction from zero to one to meet the model's input requirement.

Z parameter

Z is an empirical constant that represents the local precipitation pattern and hydrogeological characteristics calculated by equation (10) [285]:

$$Z = \frac{(\omega - 1.25) \times P}{AWC} \quad (10)$$

where *P* (mm) and *AWC* (mm) should be average values of Precipitation and Available Water Capacity, respectively, in the study area.

In Shenzhen, the P-value is 1935.8 mm [332]. According to the Harmonized World Soil Database v 1.2 [333], the value of AWC is 150 mm. The estimated value of ω is 1.76 and 3.37 for the high and low water yielding regions in China, respectively [334], since Shenzhen is an area with abundant rainfall [332]. Therefore, 1.76 was used to calculate the Z parameter and the result was 6.58.

Table S 19. Biophysical table used for the InVEST water yield model. *(Kc is the evapotranspiration coefficient)*

lucode	LULC_desc	LULC_veg	root_depth(mm)	Kc
1	Cultivated land	1	350	0.65
2	Forest	1	3000	1.00
3	Grassland	1	500	0.65
4	Shrubland	1	2150	0.90
5	Wetland	0	1	1.00
6	Water bodies	0	1	1.00
7	Artificial surfaces	0	1	0.30

Note: LULC_desc denotes the descriptive name of land-use/land cover class; with respect to LULC_veg, a value of 1 is used for vegetated land-use except wetland, and 0 for all other land uses, including wetlands, urban, and water bodies. The root depths of forest and shrubland were derived from the work by Schenk and Jackson (2002), and the root depths of cultivated land and grassland were referred to the work by Bao et al. (2016); Kc of wetland was referred to the Appendix 1: Data Sources of Annual Water Yield [285], Kc of shrubland was derived from the work by Zhao et al. (2019), the rest of Kc values were derived from the work by Li et al. (2021).

III. Water scarcity (realized supply)

The estimated average consumptive water use for the two land-use classes of each year is listed in ***Table S 20*** since the main focus of this study is to explore the interactions of FWLE nexus based on the land-use changes. Therefore, the mean value was used for calculating the water supply from 2000 to 2030 to avoid the influence of water consumption changes.

$$V_{in} = Y - u$$

(11)

where V_{in} is the realized supply (volume inflow to a reservoir), u is the total volume of water consumed in the watershed, and Y is the total water yield from the watershed.

Table S 20. The estimated average consumptive water use (in units of cubic meters per year per pixel, in this study, the area of one pixel is 900 m^2) for cultivated land and artificial surfaces [a]

Year	Cultivated land	Artificial surfaces
2000	1,252.03	1,375.93
2010	484.00	2,043.89
2020	870.82	1,852.22
Mean value	868.95	1,757.35

Note: [a] Data was referred to the *Water Resources Bulletin* [265]. Due to the limitation of data, we assumed that the value for 2020 was equal to that of 2019.

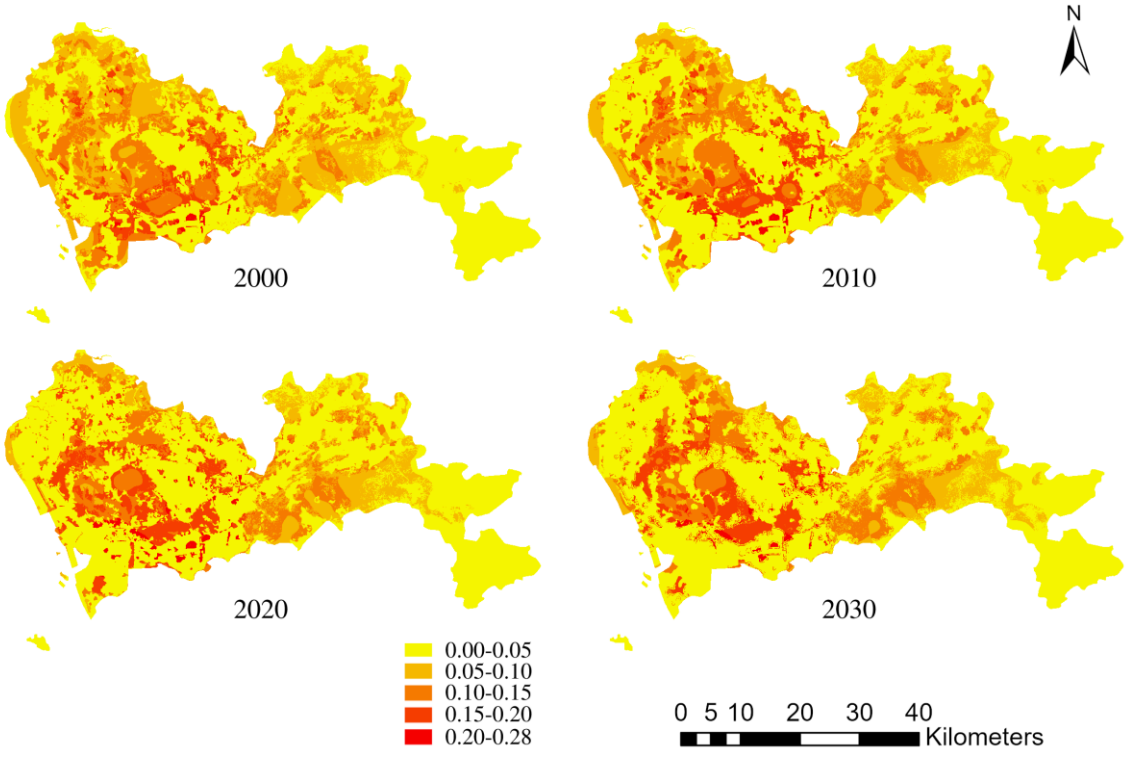

Figure S 1. Spatial distribution of degradation in Shenzhen from 2000 to 2030

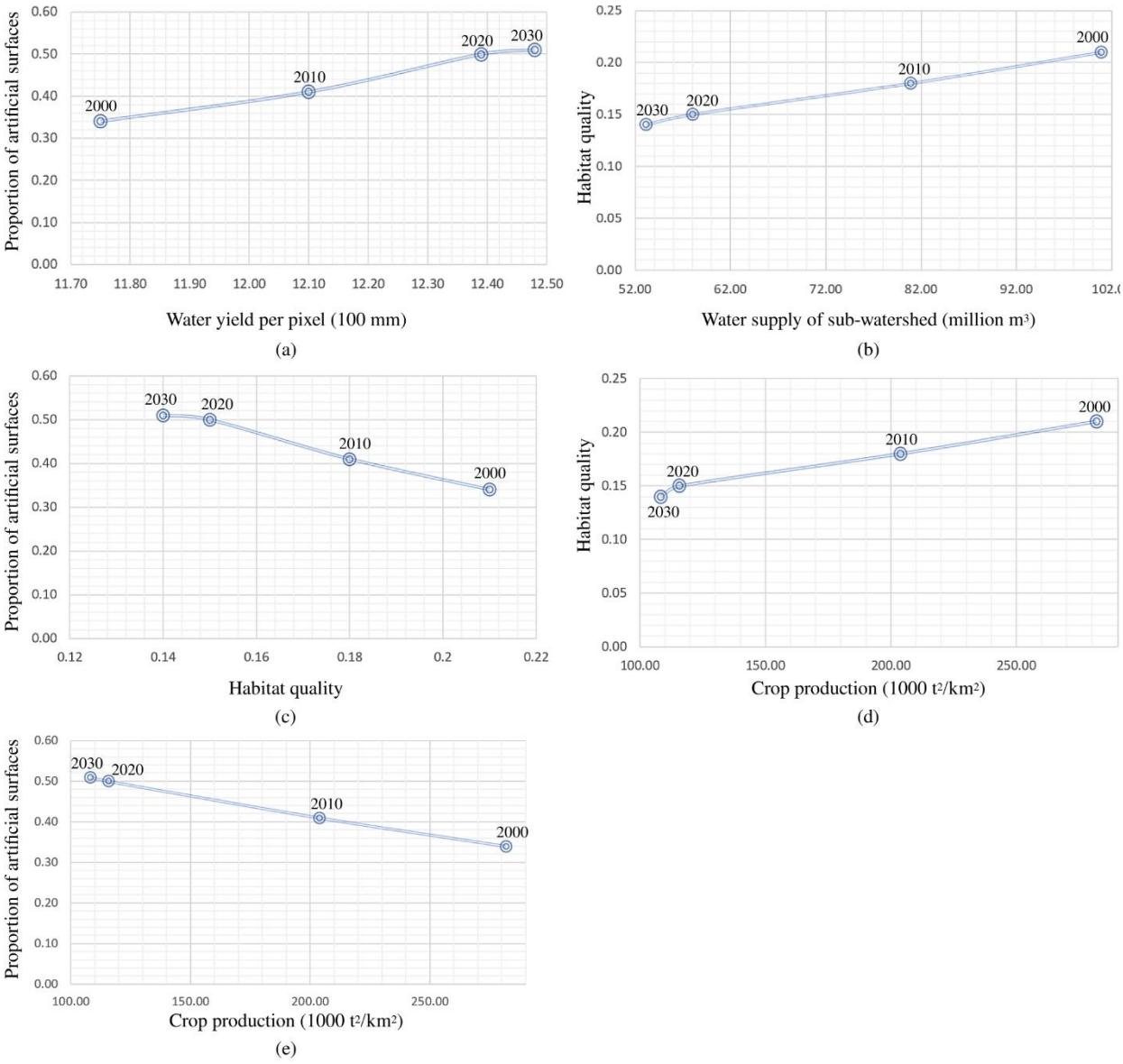

Figure S 2. The nexus between water yield, water supply, habitat quality, crop production, and artificial surfaces in Shenzhen. *(All five subfigures were plotted based on the mean value)*

References

[1] Bill Hopwood, Mary Mellor, and Geoff O'Brien, "Sustainable development: mapping different approaches," *Sustain. Dev.*, vol. 13, pp. 38–52, 2005, doi: https://doi.org/10.1002/sd.244.

[2] M. Zika and K.-H. Erb, "The global loss of net primary production resulting from human-induced soil degradation in drylands," *Ecol. Econ.*, vol. 69, no. 2, pp. 310–318, Dec. 2009, doi: 10.1016/j.ecolecon.2009.06.014.

[3] D. J. Rapport, R. Costanza, and A. J. McMichael, "Assessing ecosystem health," *Trends Ecol. Evol.*, vol. 13, no. 10, pp. 397–402, Oct. 1998, doi: 10.1016/S0169-5347(98)01449-9.

[4] M. Azam, "Does environmental degradation shackle economic growth? A panel data investigation on 11 Asian countries," *Renew. Sustain. Energy Rev.*, vol. 65, pp. 175–182, Nov. 2016, doi: 10.1016/j.rser.2016.06.087.

[5] M. W. Rosegrant and S. A. Cline, "Global Food Security: Challenges and Policies," *Science*, vol. 302, no. 5652, pp. 1917–1919, Dec. 2003, doi: 10.1126/science.1092958.

[6] J. F. Sundström *et al.*, "Future threats to agricultural food production posed by environmental degradation, climate change, and animal and plant diseases – a risk analysis in three economic and climate settings," *Food Secur.*, vol. 6, no. 2, pp. 201–215, Apr. 2014, doi: 10.1007/s12571-014-0331-y.

[7] OECD, *OECD Environmental Outlook*. Paris, France: OECD, 2001. [Online]. Available: https://www.oecd.org/environment/indicators-modelling-outlooks/oecd-environmental-outlook-1999155x.htm

[8] P. J. Gregory, J. S. I. Ingram, and M. Brklacich, "Climate change and food security," *Philos. Trans. R. Soc. B Biol. Sci.*, vol. 360, no. 1463, pp. 2139–2148, Nov. 2005, doi: 10.1098/rstb.2005.1745.

[9] C. Sneddon, R. B. Howarth, and R. B. Norgaard, "Sustainable development in a post-Brundtland world," *Ecol. Econ.*, vol. 57, no. 2, pp. 253–268, May 2006, doi: 10.1016/j.ecolecon.2005.04.013.

[10] Independent Group of Scientists appointed by the Secretary-General, "Global Sustainable Development Report 2019: The Future is Now – Science for Achieving Sustainable Development," United Nations, New York, 2019.

[11] Jennifer A. Elliott, *An introduction to sustainable development*, Fourth edition. Abingdon, Oxon OX14 4RN: Routledge, 2013. [Online]. Available: http://www.ru.ac.bd/wp-content/uploads/sites/25/2019/03/408_01_Jennifer-An-Introduction-to-Sustainable-Development-2012.pdf

[12] Jan Bebbington and Jeffrey Unerman, "Achieving the United Nations Sustainable Development Goals: An enabling role for accounting research," *Account. Audit. Account. J.*, vol. 31, no. 1, pp. 2–24, 2018, doi: https://doi.org/10.1108/AAAJ-05-2017-2929.

[13] Subhas K. Sikdar, "Sustainable development and sustainability metrics," *AIChE J.*, vol. 49, no. 8, pp. 1928–1932, 2003, doi: https://doi.org/10.1002/aic.690490802.

[14] B. Purvis, Y. Mao, and D. Robinson, "Three pillars of sustainability: in search of conceptual origins," *Sustain. Sci.*, vol. 14, no. 3, pp. 681–695, May 2019, doi: 10.1007/s11625-018-0627-5.

[15] GLOPP, "The Three Dimensions of Sustainable Development," 2012. http://www.glopp.ch/A2/en/html/resear_area_present_1_3.html (accessed May 17, 2021).

[16] B. Giddings, B. Hopwood, and G. O'Brien, "Environment, economy and society: fitting them together into sustainable development," *Sustain. Dev.*, vol. 10, no. 4, pp. 187–196, 2002, doi: https://doi.org/10.1002/sd.199.

[17] W. H. Organization, *World Health Statistics 2016: Monitoring Health for the SDGs Sustainable Development Goals*. World Health Organization, 2016.

[18] C. Folke, R. Biggs, A. V. Norström, B. Reyers, and J. Rockström, "Social-ecological resilience and biosphere-based sustainability science," *Ecol. Soc.*, vol. 21, no. 3, 2016, Accessed: May 20, 2021. [Online]. Available: https://www.jstor.org/stable/26269981

[19] United Nations, "Historic New Sustainable Development Agenda Unanimously Adopted by 193 UN Members," 2015. https://www.un.org/sustainabledevelopment/blog/2015/09/historic-new-

sustainable-development-agenda-unanimously-adopted-by-193-un-members/ (accessed May 20, 2021).
[20] C. S. Pedersen, “The UN Sustainable Development Goals (SDGs) are a Great Gift to Business!,” *Procedia CIRP*, vol. 69, pp. 21–24, Jan. 2018, doi: 10.1016/j.procir.2018.01.003.
[21] the Population Division of the UN Department of Economic and Social Affairs, “2014 revision of the World Urbanization Prospects,” New York, USA, Report, 2014. Accessed: May 17, 2021. [Online]. Available: 2014-revision-world-urbanization-prospects.html
[22] United Nations, “Goal 11: Make cities inclusive, safe, resilient and sustainable,” 2019. https://www.un.org/sustainabledevelopment/cities/ (accessed May 17, 2021).
[23] WHO and UN-Habitat, “Global report on urban health: Equitable healthier cities for sustainable development,” World Health Organization, 2016. Accessed: May 17, 2021. [Online]. Available: http://www.who.int/gender-equity-rights/knowledge/global-report-on-urban-health/en/
[24] United Nations Development Programme, “Cities are engines for achieving the Sustainable Development Goals,” 2018. https://www.undp.org/press-releases/cities-are-engines-achieving-sustainable-development-goals (accessed May 17, 2021).
[25] Mistra Urban Futures, “Implementing the New Urban Agenda and The Sustainable Development Goals: Comparative Urban Perspectives,” 2020. https://www.mistraurbanfutures.org/en/project/implementing-new-urban-agenda-and-sustainable-development-goals-comparative-urban (accessed May 18, 2021).
[26] D. Loorbach and H. Shiroyama, “The Challenge of Sustainable Urban Development and Transforming Cities,” in *Governance of Urban Sustainability Transitions: European and Asian Experiences*, D. Loorbach, J. M. Wittmayer, H. Shiroyama, J. Fujino, and S. Mizuguchi, Eds. Tokyo: Springer Japan, 2016, pp. 3–12. doi: 10.1007/978-4-431-55426-4_1.
[27] United Nations-ESCAP, “Urbanization trends in Asia and the Pacific,” 2013. https://www.unescap.org/sites/default/files/SPPS-Factsheet-urbanization-v5.pdf
[28] UN-Habitat, “Sustainable Urbanization in Asia,” 2012. https://unhabitat.org/sustainable-urbanization-in-asia (accessed May 18, 2021).
[29] United Nations, “The New Urban Agenda - Habitat III,” 2017. https://habitat3.org/the-new-urban-agenda/ (accessed May 18, 2021).
[30] Department of Economic and Social Affairs, United Nations, “Sustainable cities and human settlements,” 2020. https://sdgs.un.org/topics/sustainable-cities-and-human-settlements (accessed May 18, 2021).
[31] Sustainable Development Solutions Network, “Why the World Needs an Urban Sustainable Development Goal,” 2013. http://resources.unsdsn.org/why-the-world-needs-an-urban-sustainable-development-goal (accessed May 18, 2021).
[32] Y. Chen, “Sustainable development: The course and insight of China’s 40 years of reform and opening up,” *Frontiers*, no. 20, pp. 58–64, 2018.
[33] J. Wang and L. Long, “A Preliminary Study on the Rational Utilization of Land Resources in the Poverty-Stricken Mountainous Areas in the Upper Reaches of the Yangtze River: A Case Study of Xueshan Township,” *Asian Agric. Res.*, vol. 12, no. 2, pp. 17–27, 2020, doi: 10.22004/ag.econ.304069.
[34] National Development and Reform Commission, China, “Develop the circular economy and build a resource-conserving and environment-friendly society,” 2005. https://www.ndrc.gov.cn/fggz/hjyzy/fzxhjj/200511/t20051108_1203206.html?code=&state=123
[35] Sustainable Development Strategy Study Group Chinese Academy of Sciences, “China Sustainable Development Report 2012—China’s Sustainable Development in the Shifting Global Context,” 2012. [Online]. Available: http://www.casisd.cn/zkcg/ndbg/201610/t20161017_4680908.html

[36] Chinese government, “China’s National Plan on Implementation of the 2030 Agenda for Sustainable Development,” 2016. https://www.fmprc.gov.cn/web/zyxw/W020161012709956373709.pdf
[37] J. Chen, “Rapid urbanization in China: A real challenge to soil protection and food security,” *CATENA*, vol. 69, no. 1, pp. 1–15, Jan. 2007, doi: 10.1016/j.catena.2006.04.019.
[38] B. Yu, “Ecological effects of new-type urbanization in China,” *Renew. Sustain. Energy Rev.*, vol. 135, p. 110239, Jan. 2021, doi: 10.1016/j.rser.2020.110239.
[39] X. Guan, H. Wei, S. Lu, Q. Dai, and H. Su, “Assessment on the urbanization strategy in China: Achievements, challenges and reflections,” *Habitat Int.*, vol. 71, pp. 97–109, Jan. 2018, doi: 10.1016/j.habitatint.2017.11.009.
[40] S. Wang, G. Hua, and C. Li, “Urbanization, Air Quality, and the Panel Threshold Effect in China Based on Kernel Density Estimation,” *Emerg. Mark. Finance Trade*, vol. 55, no. 15, pp. 3575–3590, Dec. 2019, doi: 10.1080/1540496X.2019.1665016.
[41] Matteo Purer, “Urbanisation with Chinese characteristics: Will the National New Type Urbanisation Plan of 2014 – 2020 benefit the rural and migrating population or is China repeating the same faults of the past?,” Extended dissertation, University of London, London, UK, 2019. [Online]. Available: https://www.china-files.com/wp-content/uploads/2020/03/DISSERTATION-MATTEO-PURER.pdf
[42] Y. Zhang, Y. Liu, Y. Zhang, Y. Liu, G. Zhang, and Y. Chen, “On the spatial relationship between ecosystem services and urbanization: A case study in Wuhan, China,” *Sci. Total Environ.*, vol. 637–638, pp. 780–790, Oct. 2018, doi: 10.1016/j.scitotenv.2018.04.396.
[43] H. Long, Y. Liu, X. Hou, T. Li, and Y. Li, “Effects of land use transitions due to rapid urbanization on ecosystem services: Implications for urban planning in the new developing area of China,” *Habitat Int.*, vol. 44, pp. 536–544, Oct. 2014, doi: 10.1016/j.habitatint.2014.10.011.
[44] D. Shi *et al.*, “Effects of disturbed landforms on the soil water retention function during urbanization process in the Three Gorges Reservoir Region, China,” *CATENA*, vol. 144, pp. 84–93, Sep. 2016, doi: 10.1016/j.catena.2016.04.010.
[45] K. Luo *et al.*, “Impacts of rapid urbanization on the water quality and macroinvertebrate communities of streams: A case study in Liangjiang New Area, China,” *Sci. Total Environ.*, vol. 621, pp. 1601–1614, Apr. 2018, doi: 10.1016/j.scitotenv.2017.10.068.
[46] D. Zhou, D. Li, G. Sun, L. Zhang, Y. Liu, and L. Hao, “Contrasting effects of urbanization and agriculture on surface temperature in eastern China,” *JGR Atmospheres*, vol. 121, no. 16, pp. 9597–9606, 2016, doi: https://doi.org/10.1002/2016JD025359.
[47] S. Wang, S. Gao, S. Li, and K. Feng, “Strategizing the relation between urbanization and air pollution: Empirical evidence from global countries,” *J. Clean. Prod.*, vol. 243, p. 118615, Jan. 2020, doi: 10.1016/j.jclepro.2019.118615.
[48] The Economist, “Building the dream. Special report—China.,” 2014. [Online]. Available: https://www.economist.com/sites/default/files/20140419_china.pdf
[49] S. L. R. Wood *et al.*, “Distilling the role of ecosystem services in the Sustainable Development Goals,” *Ecosyst. Serv.*, vol. 29, pp. 70–82, Feb. 2018, doi: 10.1016/j.ecoser.2017.10.010.
[50] F. DeClerck *et al.*, “Agricultural ecosystems and their services: the vanguard of sustainability?,” *Curr. Opin. Environ. Sustain.*, vol. 23, pp. 92–99, Dec. 2016, doi: 10.1016/j.cosust.2016.11.016.
[51] C. Allen, R. Nejdawi, J. El-Baba, K. Hamati, G. Metternicht, and T. Wiedmann, “Indicator-based assessments of progress towards the sustainable development goals (SDGs): a case study from the Arab region,” *Sustain. Sci.*, vol. 12, no. 6, pp. 975–989, 2017.
[52] M. Kissinger and D. Gottlieb, “Place oriented ecological footprint analysis—The case of Israel’s grain supply,” *Ecol. Econ.*, vol. 69, no. 8, pp. 1639–1645, 2010.
[53] G. Li, Q. Wang, X. Gu, J. Liu, Y. Ding, and G. Liang, “Application of the componential method for ecological footprint calculation of a Chinese university campus,” *Ecol. Indic.*, vol. 8, no. 1, pp. 75–78, 2008.
[54] A. Galli *et al.*, “Questioning the Ecological Footprint,” *Ecol. Indic.*, vol. 69, pp. 224–232, 2016.

[55] M. Wackernagel and W. E. Rees, *Our ecological footprint: Reducing human impact on the Earth.* Gabriola Island: New Society Publishers, 1996.
[56] Central Committee of the Communist Party of China, "Outline Development Plan for the Guangdong-Hong Kong-Macao Greater Bay Area.," 2019. https://www.bayarea.gov.hk/filemanager/en/share/pdf/Outline_Development_Plan.pdf (accessed May 19, 2021).
[57] "Hong Kong 2030+: Towards a Planning Vision and Strategy Transcending 2030." http://www.hk2030plus.hk/index.htm (accessed Jun. 17, 2019).
[58] "The sustainable cities index 2018-Hong Kong." https://www.arcadis.com/media/D/D/4/%7BDD49CD66-FDE6-406F-9557-20023D4DAC6D%7DSustainable%20Cities%20Index%202018%20Hong%20Kong%20-%20Chinese.pdf (accessed Jun. 17, 2019).
[59] "Four opportunities to make Hong Kong Asia's most sustainable city." https://www.wwf.org.hk/en/news/?15961/Feature-story-Four-Opportunities-to-Make-Hong-Kong-Asias-Most-Sustainable-City (accessed Jun. 06, 2019).
[60] "How Can Renewable Energy Thrive in Hong Kong?" https://www.wwf.org.hk/en/whatwedo/climate_and_energy/climateupdates.cfm?18080/Feature-Story-How-Can-Renewable-Energy-Thrive-in-Hong-Kong. (accessed Apr. 11, 2020).
[61] "Hong Kong in the global context." https://www.hk2030plus.hk/document/Hong%20Kong%20in%20the%20Global%20Context_Eng.pdf (accessed Jun. 07, 2019).
[62] "Chinese ecological footprint report." https://www.footprintnetwork.org/content/images/uploads/China_Report_zh.pdf (accessed Jul. 15, 2019).
[63] D. Liu, Z. Feng, and Y. Yang, "Ecological balance between supply and demand in China using ecological footprint method," *J. Nat. Resour.*, vol. 27, no. 4, pp. 614–624, 2012.
[64] Y. X. Chai, L. Guo, and N. Zhu, "Research progress of ecological footprint in China," *China Sci. Technol. Inf.*, vol. 12, pp. 20–21, 2005.
[65] D. Zheng, X. Liu, Y. Wang, and L. Lv, "Spatiotemporal evolution and driving forces of natural capital utilization in China based on three-dimensional ecological footprint," *Prog. Geogr.*, vol. 37, pp. 1328–1339, 2018.
[66] X. Zhang and H. Zeng, "Dynamic of three dimensional ecological footprint in the Pearl River Delta and its driving factors," *Acta Sci. Circumstantiae*, vol. 37, no. 2, pp. 771–778, 2017.
[67] Z. Xu, Z. Zhang, G. Cheng, and D. Chen, "Ecological footprint calculation and development capacity analysis of China in 1999," *J. Appl. Ecol.*, vol. 14, no. 2, pp. 280–285, 2003.
[68] Y. Qi, G. Xie, L. Ge, C. Zhang, and S. Li, "Estimation of China's carbon footprint based on apparent consumption," *Resour. Sci.*, vol. 32, no. 11, pp. 2053–2058, 2010.
[69] W. Steffen *et al.*, "Planetary boundaries: Guiding human development on a changing planet," *Science*, vol. 347, no. 6223, p. 1259855, 2015.
[70] "Human development indices and indicators: 2018 statistical update." http://hdr.undp.org/en/content/human-development-indices-indicators-2018-statistical-update (accessed Sep. 24, 2019).
[71] L. Huang, J. Wu, and L. Yan, "Defining and measuring urban sustainability: a review of indicators," *Landsc. Ecol.*, vol. 30, no. 7, pp. 1175–1193, 2015.
[72] "China national human development report 2016." http://www.cn.undp.org/content/china/zh/home/library/human_development/china-human-development-report-2016.html (accessed Aug. 21, 2019).
[73] "Standard Map services." http://bzdt.ch.mnr.gov.cn/download.html?superclassName=%25E4%25B8%2596%25E7%2595%258C%25E5%259C%25B0%25E5%259B%25BE%25EF%25BC%2588%25E8%258B%25B1%25EF%25BC%2589 (accessed May 09, 2020).

[74] "Hong Kong Annual Digest of Statistics." http://www.censtatd.gov.hk/hkstat/sub/sp20.jsp?productCode=B1010003 (accessed Jun. 20, 2019).
[75] "Hong Kong Energy Statistics 2017 annual report." https://www.statistics.gov.hk/pub/B11000022017AN17B0100.pdf (accessed Jun. 20, 2019).
[76] "The Agriculture, the Fisheries and Conservation Department Report of Hong Kong." https://sc.afcd.gov.hk/gb/www.afcd.gov.hk/tc_chi/publications/publications_dep/publications_dep.html (accessed Jun. 20, 2019).
[77] "Food and Agriculture Organization of the United Nations." http://www.fao.org/home/en/ (accessed Jun. 18, 2019).
[78] "Yearbook of Statistics Singapore." https://www.singstat.gov.sg/publications/reference/yearbook-of-statistics-singapore (accessed Jun. 11, 2019).
[79] M. Wackernagel *et al.*, "Tracking the ecological overshoot of the human economy," *Proc. Natl. Acad. Sci.*, vol. 99, no. 14, pp. 9266–9271, 2002.
[80] K. Warren-Rhodes and A. Koenig, "Ecosystem appropriation by Hong Kong and its implications for sustainable development," *Ecol. Econ.*, vol. 39, no. 3, pp. 347–359, 2001.
[81] M. Liu and W. Li, "Calculation of equivalence factor used in ecological footprint for China and its provinces based on net primary production," *J. Ecol. Rural Environ.*, vol. 26, no. 5, pp. 401–406, 2010.
[82] M. Liu, W. Li, and G. Xie, "Estimation of China ecological footprint production coefficient based on net primary productivity," *Chin. J. Ecol.*, vol. 29, no. 3, pp. 592–597, 2010.
[83] M. Borucke *et al.*, "Accounting for demand and supply of the biosphere's regenerative capacity:The National Footprint Accounts' underlying methodology and framework.," *Ecol. Indic.*, vol. 24, pp. 518–553, 2013.
[84] "Briefing note for countries on the 2018 Statistical Update: Hong Kong, China (SAR)." http://hdr.undp.org/sites/all/themes/hdr_theme/country-notes/HKG.pdf (accessed Jul. 18, 2019).
[85] "Calculating the ecological footprint and biocapacity." http://awsassets.wwfhk.panda.org/downloads/hong_kong_ecological_footprint_report_2013_appendix.pdf (accessed May 12, 2020).
[86] M. Wackernagel, S. White, and D. Moran, "Using Ecological Footprint accounts: from analysis to applications," *Int. J. Environ. Sustain. Dev.*, vol. 3, no. 3–4, pp. 293–315, 2004.
[87] "Agriculture, Fisheries and Conservation Department, Food and Health Bureau." https://www.afcd.gov.hk/english/index.html (accessed Apr. 12, 2020).
[88] W. W. Cheung and Y. Sadovy, "Retrospective evaluation of data-limited fisheries: a case from Hong Kong," *Rev. Fish Biol. Fish.*, vol. 14, no. 2, pp. 181–206, 2004.
[89] "Human development data." http://hdr.undp.org/en/data# (accessed Sep. 25, 2019).
[90] "Census and Statistics Department of Hong Kong." https://www.censtatd.gov.hk/hkstat/sub/sp20.jsp?productCode=B1010003. (accessed May 09, 2020).
[91] "Updated income classifications." https://blogs.worldbank.org/opendata/updated-income-classifications (accessed Sep. 25, 2019).
[92] Z. Naveh, *Transdisciplinary challenges in landscape ecology and restoration ecology-an anthology*, vol. 6. Dordrecht, Netherland: Springer, 2007.
[93] W. Fung, K. Lam, W. Hung, S. Pang, and Y. Lee, "Impact of urban temperature on energy consumption of Hong Kong," *Energy*, vol. 31, no. 14, pp. 2623–2637, 2006.
[94] C. V. Barber and V. R. Pratt, "Poison and profits: cyanide fishing in the Indo-Pacific," *Environ. Sci. Policy Sustain. Dev.*, vol. 40, no. 8, pp. 4–9, 1998.
[95] WWF, "Transform Hong Kong into Asia's most sustainable city," 2016. http://awsassets.wwfhk.panda.org/downloads/wwfhk_advocacy_chi.pdf

[96] "Marine health report of Hong Kong." http://awsassets.wwfhk.panda.org/downloads/WWF_Marine_Health_Check_Report_tc.pdf (accessed Aug. 17, 2019).
[97] L. B. Krause, "Hong Kong and Singapore: Twins or kissing cousins?," *Econ. Dev. Cult. Change*, vol. 36, no. S3, pp. S45–S66, 1988.
[98] "Sustainable Singapore Blueprint." https://www.mewr.gov.sg/docs/default-source/module/ssb-publications/41f1d882-73f6-4a4a-964b-6c67091a0fe2.pdf (accessed Aug. 20, 2019).
[99] "Global Footprint Network." https://www.footprintnetwork.org/licenses/public-data-package-free/ (accessed May 09, 2020).
[100] "Singapore positioned to lead regional footprint reduction." https://www.wwf.sg/?203930/Singapore-pos (accessed Sep. 23, 2019).
[101] "World Wide Fund for Nature Singapore Annual Report 2012." https://www.wwf.sg/wwf_singapore/ (accessed Aug. 26, 2019).
[102] "World Wide Fund for Nature Singapore Annual Report 2011." https://www.wwf.sg/wwf_singapore/ (accessed Sep. 26, 2019).
[103] "Overview of Gas Market." https://www.ema.gov.sg/Gas_Market_Overview.aspx (accessed Apr. 20, 2020).
[104] "World Wide Fund for Nature Singapore Annual Report 2016." https://www.wwf.sg/wwf_singapore/ (accessed Sep. 26, 2019).
[105] "World Wide Fund for Nature Singapore Annual Report 2017." https://www.wwf.sg/wwf_singapore/ (accessed Sep. 26, 2019).
[106] "Sustainable transport." https://www.mot.gov.sg/about-mot/land-transport/sustainable-transport (accessed Apr. 19, 2020).
[107] T. D. Toan and D. Van Dong, "Integrated Transport Planning for Sustainable Urban Development–Singapore'Approach and Lessons for Vietnam," in *CIGOS 2019, Innovation for Sustainable Infrastructure*, Berlin/Heidelberg, Germany: Springer, 2020, pp. 947–952.
[108] "EMA-Annual report 2011-2012." https://www.ema.gov.sg/cmsmedia/EMA_Annual_Report_2012.pdf (accessed Sep. 28, 2019).
[109] "World Wide Fund for Nature Singapore Annual Report 2015." https://www.wwf.sg/wwf_singapore/ (accessed Aug. 28, 2019).
[110] Y. Zhou, T. Chen, and H. Zhang, "The spatial evaluation and scale trend of Singapore's reclamation area.," *Urban Plan. Int.*, vol. 31, no. 03, pp. 71–77, 2016.
[111] L. M. Chou, T. C. Toh, and C. S. L. Ng, "Effectiveness of reef restoration in Singapore's rapidly urbanizing coastal environment," *Int. J. Environ. Sci. Dev.*, vol. 8, no. 8, pp. 576–580, 2017.
[112] Z. Yi, G. Liu, W. Lang, A. Shrestha, and I. Martek, "Strategic approaches to sustainable urban renewal in developing countries: A case study of Shenzhen, China," *Sustainability*, vol. 9, no. 8, p. 1460, 2017.
[113] "Hong Kong has most sustainable transport system globally." https://hongkongbusiness.hk/transport-logistics/news/hong-kong-has-most-sustainable-transport-system-globally (accessed Apr. 19, 2020).
[114] "Clean energy." https://www.edb.gov.sg/zh/industries/industries/clean-energy.html (accessed Jul. 20, 2019).
[115] "Life behavior- the fallacy idea of protecting environment in Hong Kong." https://www.greenpeace.org/hongkong/issues/health/update/1348/%e5%be%9e%e7%94%9f%e6%b4%bb%e8%a1%8c%e7%82%ba%e8%aa%aa%e8%b5%b7-%e9%a6%99%e6%b8%af%e5%b0%8d%e5%be%85%e7%92%b0%e4%bf%9d%e7%9a%84%e8%ac%ac%e8%aa%a4%e6%80%9d%e6%83%b3/ (accessed Aug. 14, 2019).
[116] "Hong Kong has a monumental waste problem." https://www.bbc.com/future/article/20170427-hong-kong-has-a-monumental-waste-problem (accessed May 12, 2020).

[117] "Towards a sustainable and resilient Singapore." https://sustainabledevelopment.un.org/content/documents/19439Singapores_Voluntary_National_Review_Report_v2.pdf (accessed Jul. 17, 2019).
[118] "Water resources management and urban planning." https://www.edb.gov.sg/content/edb/zh/resources/downloads/articles/sustainable-water.html (accessed Jul. 28, 2019).
[119] J. Pope, D. Annandale, and A. Morrison-Saunders, "Conceptualising sustainability assessment," *Environ. Impact Assess. Rev.*, vol. 24, no. 6, pp. 595–616, 2004.
[120] L. Brown, *Ecopsychology and the environmental revolution*. Berkeley, California: Counterpoint Press, 1995.
[121] Z. HU, J. GE, and A. HAN, "A Comparative Study of Chinese Metropolis Ecological Footprint: The Case of Beijing, Shanghai, Tianjin and Chongqing," *Mod. Urban Res.*, no. 2, p. 13, 2017.
[122] "Overview of Hong Kong's electricity supply." https://www.ls-energy.hk/en/energy-demand-supply.html (accessed Aug. 30, 2019).
[123] D. N. Mah, J. M. van der Vleuten, P. Hills, and J. Tao, "Consumer perceptions of smart grid development: Results of a Hong Kong survey and policy implications," *Energy Policy*, vol. 49, pp. 204–216, 2012.
[124] G. R. Russ, A. C. Alcala, A. P. Maypa, H. P. Calumpong, and A. T. White, "Marine reserve benefits local fisheries," *Ecol. Appl.*, vol. 14, no. 2, pp. 597–606, 2004.
[125] "Raising the ocean." https://plasticschange.hk/wp-content/uploads/2018/12/CoastalWatchReport_CHI-compressed.pdf (accessed Sep. 30, 2019).
[126] "Report of the source and destination of marine litter in Hong Kong." https://www.epd.gov.hk/epd/clean_shorelines/sites/default/files/common2015/MarineRefuseStudyReport_CHI_Final.pdf (accessed Sep. 30, 2019).
[127] N. Myers, R. A. Mittermeier, C. G. Mittermeier, G. A. Da Fonseca, and J. Kent, "Biodiversity hotspots for conservation priorities," *Nature*, vol. 403, no. 6772, p. 853, 2000.
[128] "The Marine Ecological Hotspot Map." https://apps.wwf.org.hk/hotspot-map/others-en.html (accessed Aug. 27, 2019).
[129] W. Liu, W. Chen, and C. Peng, "Assessing the effectiveness of green infrastructures on urban flooding reduction: A community scale study," *Ecol. Model.*, vol. 291, pp. 6–14, 2014.
[130] R. Silva *et al.*, "Coastal risk mitigation by green infrastructure in Latin America," *Proc. Inst. Civ. Eng. Marit. Eng.*, vol. 170, no. 2, pp. 39–54, 2017.
[131] J. Maes *et al.*, "More green infrastructure is required to maintain ecosystem services under current trends in land-use change in Europe," *Landsc. Ecol.*, vol. 30, no. 3, pp. 517–534, 2015.
[132] "After the Binge, the Hangover, insights into the Minds of Clothing Consumers." https://storage.googleapis.com/planet4-international-stateless/2017/05/2da03645-after-the-binge-the-hangover.pdf (accessed Aug. 01, 2019).
[133] "Environmentally friendly Mid-Autumn festival." https://www.greenpower.org.hk/html5/chi/fe_121.shtml (accessed Aug. 01, 2019).
[134] "Transform Hong Kong Into Asia's Most Sustainable City." http://awsassets.wwfhk.panda.org/downloads/wwfhk_advocacy_chi.pdf (accessed Aug. 11, 2019).
[135] K. Kok, S. Pedde, M. Gramberger, P. A. Harrison, and I. P. Holman, "New European socio-economic scenarios for climate change research: operationalising concepts to extend the shared socio-economic pathways," *Reg. Environ. Change*, vol. 19, no. 3, pp. 643–654, 2019.
[136] IPBES, "Methodological assessment report on scenarios and models of biodiversity and ecosystem services—summary for policymakers," 2016. https://ipbes.net/sites/default/files/downloads/pdf/spm_deliverable_3c_scenarios_20161124.pdf (accessed Aug. 30, 2020).

[137] C. Allen, G. Metternicht, and T. Wiedmann, “An iterative framework for national scenario modelling for the Sustainable Development Goals (SDGs),” *Sustain. Dev.*, vol. 25, no. 5, pp. 372–385, 2017.
[138] N. Nakicenovic, R. J. Lempert, and A. C. Janetos, “A framework for the development of new socio-economic scenarios for climate change research: introductory essay,” *Clim. Change*, vol. 122, no. 3, pp. 351–361, 2014.
[139] R. C. Estoque *et al.*, “The future of Southeast Asia’s forests,” *Nat. Commun.*, vol. 10, no. 1, pp. 1–12, 2019.
[140] B. J. Van Ruijven *et al.*, “Enhancing the relevance of Shared Socioeconomic Pathways for climate change impacts, adaptation and vulnerability research,” *Clim. Change*, vol. 122, no. 3, pp. 481–494, 2014.
[141] B. Jones and B. C. O’Neill, “Spatially explicit global population scenarios consistent with the Shared Socioeconomic Pathways,” *Environ. Res. Lett.*, vol. 11, no. 8, p. 084003, 2016.
[142] B. C. O’Neill *et al.*, “The roads ahead: Narratives for shared socioeconomic pathways describing world futures in the 21st century,” *Glob. Environ. Change*, vol. 42, pp. 169–180, 2017.
[143] K. Riahi *et al.*, “The shared socioeconomic pathways and their energy, land use, and greenhouse gas emissions implications: an overview,” *Glob. Environ. Change*, vol. 42, pp. 153–168, 2017.
[144] “Explainer: How ‘Shared Socioeconomic Pathways’ explore future climate change.” https://www.carbonbrief.org/explainer-how-shared-socioeconomic-pathways-explore-future-climate-change (accessed Aug. 19, 2020).
[145] M. Kindu, T. Schneider, M. Döllerer, D. Teketay, and T. Knoke, “Scenario modelling of land use/land cover changes in Munessa-Shashemene landscape of the Ethiopian highlands,” *Sci. Total Environ.*, vol. 622, pp. 534–546, 2018.
[146] G. B. Ruben, K. Zhang, Z. Dong, and J. Xia, “Analysis and Projection of Land-Use/Land-Cover Dynamics through Scenario-Based Simulations Using the CA-Markov Model: A Case Study in Guanting Reservoir Basin, China,” *Sustainability*, vol. 12, no. 9, p. 3747, 2020.
[147] C. Wang, Y. Wang, R. Wang, and P. Zheng, “Modeling and evaluating land-use/land-cover change for urban planning and sustainability: a case study of Dongying city, China,” *J. Clean. Prod.*, vol. 172, pp. 1529–1534, 2018.
[148] M. Acheampong, Q. Yu, L. D. Enomah, J. Anchang, and M. Eduful, “Land use/cover change in Ghana’s oil city: Assessing the impact of neoliberal economic policies and implications for sustainable development goal number one–A remote sensing and GIS approach,” *Land Use Policy*, vol. 73, pp. 373–384, 2018.
[149] S. Díaz *et al.*, “Summary for policymakers of the global assessment report on biodiversity and ecosystem services of the Intergovernmental Science-Policy Platform on Biodiversity and Ecosystem Services,” 2020.
[150] Y. Lu, P. Wu, X. Ma, and X. Li, “Detection and prediction of land use/land cover change using spatiotemporal data fusion and the Cellular Automata–Markov model,” *Environ. Monit. Assess.*, vol. 191, no. 2, p. 68, 2019.
[151] IPBES, “Scenarios and models: new scenarios and supporting assessments,” 2016. https://ipbes.net/scenarios-models (accessed Aug. 30, 2020).
[152] A. Popp *et al.*, “Land-use futures in the shared socio-economic pathways,” *Glob. Environ. Change*, vol. 42, pp. 331–345, 2017.
[153] A. Palazzo *et al.*, “Linking regional stakeholder scenarios and shared socioeconomic pathways: Quantified West African food and climate futures in a global context,” *Glob. Environ. Change*, vol. 45, pp. 227–242, 2017.
[154] R. O. Valdivia *et al.*, “Representative agricultural pathways and scenarios for regional integrated assessment of climate change impacts, vulnerability, and adaptation,” *Handb. Clim. Change Agroecosystems*, vol. 3, pp. 101–156, 2015.

[155] B. C. O'Neill *et al.*, "Achievements and needs for the climate change scenario framework," *Nat. Clim. Change*, pp. 1–11, 2020.
[156] M. Chen *et al.*, "Global land use for 2015–2100 at 0.05° resolution under diverse socioeconomic and climate scenarios," *Sci. Data*, vol. 7, no. 1, pp. 1–11, 2020.
[157] L. Gomes, F. Bianchi, I. Cardoso, R. Schulte, B. Arts, and E. Fernandes Filho, "Land use and land cover scenarios: An interdisciplinary approach integrating local conditions and the global shared socioeconomic pathways," *Land Use Policy*, vol. 97, p. 104723, 2020.
[158] R. J. Hewitt *et al.*, "Impacts and trade-offs of future land use and land cover change in Scotland: spatial simulation modelling of shared socioeconomic pathways at regional scales (SSPs)," 2020.
[159] E. Yirsaw, W. Wu, X. Shi, H. Temesgen, and B. Bekele, "Land use/land cover change modeling and the prediction of subsequent changes in ecosystem service values in a coastal area of China, the Su-Xi-Chang Region," *Sustainability*, vol. 9, no. 7, p. 1204, 2017.
[160] L. Chu, T. Sun, T. Wang, Z. Li, and C. Cai, "Evolution and Prediction of Landscape Pattern and Habitat Quality Based on CA-Markov and InVEST Model in Hubei Section of Three Gorges Reservoir Area (TGRA)," *Sustainability*, vol. 10, no. 11, p. 3854, 2018.
[161] S. Song, Z. Liu, C. He, and W. Lu, "Evaluating the effects of urban expansion on natural habitat quality by coupling localized shared socioeconomic pathways and the land use scenario dynamics-urban model," *Ecol. Indic.*, vol. 112, p. 106071, 2020.
[162] W. Lin, Y. Sun, S. Nijhuis, and Z. Wang, "Scenario-based flood risk assessment for urbanizing deltas using future land-use simulation (FLUS): Guangzhou Metropolitan Area as a case study," *Sci. Total Environ.*, p. 139899, 2020.
[163] N. Dong, L. You, W. Cai, G. Li, and H. Lin, "Land use projections in China under global socioeconomic and emission scenarios: Utilizing a scenario-based land-use change assessment framework," *Glob. Environ. Change*, vol. 50, pp. 164–177, 2018.
[164] X. Liu *et al.*, "A future land use simulation model (FLUS) for simulating multiple land use scenarios by coupling human and natural effects," *Landsc. Urban Plan.*, vol. 168, pp. 94–116, 2017.
[165] W. Liao *et al.*, "Projections of land use changes under the plant functional type classification in different SSP-RCP scenarios in China," *Sci. Bull.*, 2020.
[166] Y. Chen, X. Li, X. Liu, Y. Zhang, and M. Huang, "Tele-connecting China's future urban growth to impacts on ecosystem services under the shared socioeconomic pathways," *Sci. Total Environ.*, vol. 652, pp. 765–779, 2019.
[167] C. He, J. Li, X. Zhang, Z. Liu, and D. Zhang, "Will rapid urban expansion in the drylands of northern China continue: A scenario analysis based on the Land Use Scenario Dynamics-urban model and the Shared Socioeconomic Pathways," *J. Clean. Prod.*, vol. 165, pp. 57–69, 2017.
[168] S. Hasan, W. Shi, X. Zhu, S. Abbas, and H. U. A. Khan, "Future Simulation of Land Use Changes in Rapidly Urbanizing South China Based on Land Change Modeler and Remote Sensing Data," *Sustainability*, vol. 12, no. 11, Art. no. 11, Jan. 2020, doi: 10.3390/su12114350.
[169] J. Li and J. Wang, "Identification，classification，and mapping of coastal ecosystem services of the Guangdong，Hong Kong，and Macao Great Bay Area," *Acta Ecol. Sin.*, vol. 9, no. 17, pp. 6393–6403, 2019.
[170] WWF, "Guangdong-Hong Kong-Macao Greater Bay Area Ecological Footprint Report," 2019. http://www.wwf-opf.org.cn/upload/news/609b9697e4abe961e224e401852e41f2.pdf (accessed Oct. 13, 2020).
[171] Greater Bay Area, "Overview," 2018. https://www.bayarea.gov.hk/en/about/overview.html (accessed Aug. 03, 2020).
[172] WWF, "Hong Kong ecological footprint report 2013," 2013. https://www.footprintnetwork.org/content/images/article_uploads/hong_kong_ecological_footprint_report_2013.pdf (accessed Dec. 09, 2020).

[173] N. Asia, “Hong Kong wants a massive new island, but where will it get the sand?,” 2020. https://asia.nikkei.com/Opinion/Hong-Kong-wants-a-massive-new-island-but-where-will-it-get-the-sand (accessed Dec. 09, 2020).
[174] DSEC, “Statistical website of the Guangdong-Hong Kong-Macao Greater Bay Area,” 2020. https://www.dsec.gov.mo/BayArea/en-US/#home (accessed Dec. 08, 2020).
[175] Clark labs, “Land change modeler in Terrset,” 2020. https://clarklabs.org/terrset/land-change-modeler/ (accessed Dec. 30, 2020).
[176] X. Li *et al.*, “A cellular automata downscaling based 1 km global land use datasets (2010–2100),” *Sci. Bull.*, vol. 61, no. 21, pp. 1651–1661, 2016.
[177] L. Wang, Y. Yang, Z. Feng, and Z. You, “Prediction of China’s population in 2020 and 2030 on county scale,” *Geogr. Res.*, vol. 33, no. 2, 2014.
[178] B. Rimal, L. Zhang, H. Keshtkar, B. N. Haack, S. Rijal, and P. Zhang, “Land use/land cover dynamics and modeling of urban land expansion by the integration of cellular automata and markov chain,” *ISPRS Int. J. Geo-Inf.*, vol. 7, no. 4, p. 154, 2018.
[179] J. Mas, M. Paegelow, and M. C. Olmedo, “LUCC modeling approaches to calibration,” in *Geomatic Approaches for Modeling Land Change Scenarios*, Springer, 2018, pp. 11–25.
[180] G. Vázquez-Quintero, R. Solís-Moreno, M. Pompa-García, F. Villarreal-Guerrero, C. Pinedo-Alvarez, and A. Pinedo-Alvarez, “Detection and projection of forest changes by using the Markov Chain Model and cellular automata,” *Sustainability*, vol. 8, no. 3, p. 236, 2016.
[181] M. C. Olmedo and J. Mas, “Markov Chain,” in *Geomatic Approaches for Modeling Land Change Scenarios*, Springer, 2018, pp. 441–445.
[182] J. R. Eastman and J. Toledano, “A Short Presentation of the Land Change Modeler (LCM),” in *Geomatic Approaches for Modeling Land Change Scenarios*, M. T. Camacho Olmedo, M. Paegelow, J.-F. Mas, and F. Escobar, Eds. Cham: Springer International Publishing, 2018, pp. 499–505. doi: 10.1007/978-3-319-60801-3_36.
[183] T. M. Kikuko Shoyama Shizuka Hashimoto, Kei Kabaya, Akiko Oono, Osamu Saito., “Development of land-use scenarios using vegetation inventories in Japan,” *Sustain. Sci.*, vol. 14, pp. 39–52, 2019, doi: 10.1007/s11625-018-0617-7.
[184] T. S. Aung, T. B. Fischer, and J. Buchanan, “Land use and land cover changes along the China-Myanmar Oil and Gas pipelines–Monitoring infrastructure development in remote conflict-prone regions,” *PloS One*, vol. 15, no. 8, p. e0237806, 2020.
[185] K. S. Kumar, P. U. Bhaskar, and K. Padmakumari, “Application of Land Change Modeler For Prediction of Future Land Use Land Cover: A Case Study of Vijayawada City,” *Int. J. Adv. Technol. Eng. Sci.*, vol. 3, no. 1, pp. 773–783, 2015.
[186] Y. Chen, X. Li, K. Huang, M. Luo, and M. Gao, “High-Resolution Gridded Population Projections for China Under the Shared Socioeconomic Pathways,” *Earths Future*, vol. 8, no. 6, p. e2020EF001491, 2020.
[187] IIASA, “SSP database version 2.0,” 2018. https://tntcat.iiasa.ac.at/SspDb/dsd?Action=htmlpage&page=welcome (accessed Sep. 03, 2020).
[188] S. Hashimoto *et al.*, “Scenario analysis of land-use and ecosystem services of social-ecological landscapes: implications of alternative development pathways under declining population in the Noto Peninsula, Japan,” *Sustain. Sci.*, vol. 14, no. 1, pp. 53–75, 2019.
[189] J. R. Eastman, *TerrSet manual*. Worcester: Clark University, 2015.
[190] Worldpop, “Population counts-individual countries 2000-2020 UN adjusted (100m resoultion),” 2020. https://www.worldpop.org/geodata/listing?id=69 (accessed Aug. 28, 2020).
[191] X. Li and Y. Chen, “Projecting the future impacts of China’s cropland balance policy on ecosystem services under the shared socioeconomic pathways,” *J. Clean. Prod.*, vol. 250, p. 119489, 2020.
[192] People’s government of Guangdong province, “The Ministry of Natural Resources issued nine guidelines to support the Greater Bay Area and Shenzhen in exploring the reform of natural

resources, and Guangdong province in exploring the built-up land trading mechanism on the provincial scale.," 2020. http://www.gd.gov.cn/gdywdt/gdyw/content/post_3058085.html (accessed Oct. 13, 2020).
[193] The National People's Congress of the PRC, "Land Administration Law of the PRC," 2019. http://www.npc.gov.cn/npc/c30834/201909/d1e6c1a1eec345eba23796c6e8473347.shtml (accessed Oct. 13, 2020).
[194] Department of Natural Resources of Guangdong Province, "Land planning of Guangdong Province (2016-2030)," 2017. Accessed: Nov. 23, 2020. [Online]. Available: http://nr.gd.gov.cn/attachment/0/188/188208/506474.pdf
[195] Department of Natural Resources of Guangdong Province, "Land Planning of Guangdong Province (2016-2035)," 2018. Accessed: Nov. 23, 2020. [Online]. Available: http://nr.gd.gov.cn/attachment/0/187/187183/586580.pdf
[196] People's government of Guangdong province, "Issuance of the work plan for the compilation of land planning of Guangdong Province (2020-2035)," 2019. http://www.gd.gov.cn/zwgk/zcjd/snzcsd/content/post_2530532.html (accessed Dec. 30, 2020).
[197] R. DasGupta, S. Hashimoto, T. Okuro, and M. Basu, "Scenario-based land change modelling in the Indian Sundarban delta: an exploratory analysis of plausible alternative regional futures," *Sustain. Sci.*, vol. 14, no. 1, pp. 221–240, 2019.
[198] D. D. Moran, M. Wackernagel, J. A. Kitzes, S. H. Goldfinger, and A. Boutaud, "Measuring sustainable development—Nation by nation," *Ecol. Econ.*, vol. 64, no. 3, pp. 470–474, 2008.
[199] M. Borucke *et al.*, "Accounting for demand and supply of the biosphere's regenerative capacity: The National Footprint Accounts' underlying methodology and framework," *Ecol. Indic.*, vol. 24, pp. 518–533, 2013.
[200] Global footprint network, "Glossary," 2020. https://www.footprintnetwork.org/resources/glossary/ (accessed Jan. 01, 2021).
[201] Global footprint network, "Working guidebook to the national footprint and biocapacity accounts," 2019. https://www.footprintnetwork.org/content/uploads/2019/05/National_Footprint_Accounts_Guidebook_2019.pdf (accessed Aug. 28, 2020).
[202] J. P. Caspersen, S. W. Pacala, J. C. Jenkins, G. C. Hurtt, P. R. Moorcroft, and R. A. Birdsey, "Contributions of land-use history to carbon accumulation in US forests," *Science*, vol. 290, no. 5494, pp. 1148–1151, 2000.
[203] R. A. Houghton *et al.*, "Carbon emissions from land use and land-cover change," *Biogeosciences*, no. 12, pp. 5125–5142, 2012.
[204] R. Zhang, K. Matsushima, and K. Kobayashi, "Can land use planning help mitigate transport-related carbon emissions? A case of Changzhou," *Land Use Policy*, vol. 74, pp. 32–40, 2018.
[205] B. Yang, X. Chen, Z. Wang, W. Li, C. Zhang, and X. Yao, "Analyzing land use structure efficiency with carbon emissions: A case study in the Middle Reaches of the Yangtze River, China," *J. Clean. Prod.*, vol. 274, p. 123076, 2020.
[206] W. Cao and X. Yuan, "Region-county characteristic of spatial-temporal evolution and influencing factor on land use-related CO2 emissions in Chongqing of China, 1997–2015," *J. Clean. Prod.*, vol. 231, pp. 619–632, 2019.
[207] G. Yang, W. Zhu, Y. Wen, and Y. Lin, "Spatial differentiation in the intensify and efficiency of carbon emission from land use in Guangdong province in past two decades," *Ecol. Environ. Sci.*, vol. 28, no. 2, pp. 332–340, 2019.
[208] H. Shi, X. Mu, Y. Zhang, and M. Lv, "Effects of different land use patterns on carbon emission in Guangyuan city of Sichuan province," *Bull. Soil Water Conserv.*, vol. 32, no. 3, pp. 101–106, 2012.
[209] M. Mohammady, H. Moradi, H. Zeinivand, and A. Temme, "A comparison of supervised, unsupervised and synthetic land use classification methods in the north of Iran," *Int. J. Environ. Sci. Technol.*, vol. 12, no. 5, pp. 1515–1526, 2015.

[210] S. Saxena, “Precision vs recall,” 2018. https://medium.com/@shrutisaxena0617/precision-vs-recall-386cf9f89488 (accessed Dec. 28, 2020).
[211] D. Leung and S. Newsam, “Exploring Geotagged images for land-use classification,” *Proc. ACM Multimed. 2012 Workshop Geotagging Its Appl. Multimed.*, pp. 3–8, 2012, doi: https://doi.org/10.1145/2390790.2390794.
[212] J. Brownlee, “How to Calculate Precision, Recall, and F-Measure for Imbalanced Classification,” *Machine Learning Mastery*, Jan. 02, 2020. https://machinelearningmastery.com/precision-recall-and-f-measure-for-imbalanced-classification/ (accessed May 05, 2021).
[213] X. Shi, T. Matsui, T. Machimura, X. Gan, and A. Hu, “Toward Sustainable Development: Decoupling the High Ecological Footprint from Human Society Development: A Case Study of Hong Kong,” *Sustainability*, vol. 12, no. 10, p. 4177, 2020.
[214] Global footprint network, “Open data platform,” 2020. https://data.footprintnetwork.org/?_ga=2.62753900.1324893541.1611108161-1081994963.1587799037#/ (accessed Jan. 20, 2021).
[215] The Environmental Protection Department of Hong Kong, “Hong Kong greenhouse gas inventory for 2015 released,” 2017. https://www.info.gov.hk/gia/general/201707/10/P2017071000628.htm?fontSize=1 (accessed Jan. 01, 2021).
[216] M. Jiao, M. Hu, and B. Xia, “Spatiotemporal dynamic simulation of land-use and landscape-pattern in the Pearl River Delta, China,” *Sustain. Cities Soc.*, vol. 49, p. 101581, Aug. 2019, doi: 10.1016/j.scs.2019.101581.
[217] W. D. Solecki and C. Oliveri, “Downscaling climate change scenarios in an urban land use change model,” *J. Environ. Manage.*, vol. 72, no. 1–2, pp. 105–115, 2004.
[218] Y. Zhu, X. Deng, and S. Newsam, “Fine-grained land use classification at the city scale using ground-level images,” *IEEE Trans. Multimed.*, vol. 21, no. 7, pp. 1825–1838, 2019.
[219] J. Rawat and M. Kumar, “Monitoring land use/cover change using remote sensing and GIS techniques: A case study of Hawalbagh block, district Almora, Uttarakhand, India,” *Egypt. J. Remote Sens. Space Sci.*, vol. 18, no. 1, pp. 77–84, 2015.
[220] X. Liu *et al.*, “High-spatiotemporal-resolution mapping of global urban change from 1985 to 2015,” *Nat. Sustain.*, pp. 1–7, 2020.
[221] J. van Vliet, “Direct and indirect loss of natural area from urban expansion,” *Nat. Sustain.*, vol. 2, no. 8, pp. 755–763, 2019.
[222] F. Chapa, S. Hariharan, and J. Hack, “A new approach to high-resolution urban land use classification using open access software and true color satellite images,” *Sustainability*, vol. 11, no. 19, p. 5266, 2019.
[223] H. Ritchie and M. Roser, “CO_2 and greenhouse gas emissions,” 2017. https://ourworldindata.org/greenhouse-gas-emissions (accessed Jan. 19, 2021).
[224] United States Environmental Protection Agency, “Overview of greenhouse gases,” 2018. https://www.epa.gov/ghgemissions/overview-greenhouse-gases (accessed Jan. 19, 2021).
[225] X. Li, Y. Zhou, J. Eom, S. Yu, and G. R. Asrar, “Projecting global urban area growth through 2100 based on historical time series data and future Shared Socioeconomic Pathways,” *Earths Future*, vol. 7, no. 4, pp. 351–362, 2019.
[226] S. Mallapaty, “How China could be carbon neutral by mid-century,” *Nature*, vol. 586, no. 7830, pp. 482–483, 2020.
[227] J. Wan and Y. Han, “Inter-regional comparison of edible agricultural product supply capability and agricultural industrial chain function in the Greater Bay Area,” *J. South China Univ. Technol. Soc. Sci. Ed.*, vol. 21, no. 6, pp. 9–20, 2019, doi: 10.19366/j.cnki.1009-055X.2019.06.002.

[228] ScienceNet.cn, “How to develop the eco-agricultural pathway in the Greater Bay Area,” 2019. http://news.sciencenet.cn/sbhtmlnews/2019/7/348220.shtm?id=348220 (accessed Oct. 13, 2020).
[229] X. Gu, “Agricultural cooperation and development in Guangdong-Hong Kong-Macao Great Bay Area: status quo, problems and countermeasures,” *J. Polit. Sci. Law*, no. 4, pp. 5–7, 2019.
[230] L. Han, P. Meng, R. Jiang, B. Xu, B. Zhang, and M. Chen, “Logical root, pattern exploration and management innovation of balancing cultivated land occupation and reclamation in the new era,” *China Land Sci.*, vol. 32, no. 6, pp. 90–96, 2018.
[231] W. Chen, X. Ye, J. Li, X. Fan, Q. Liu, and W. Dong, “Analyzing requisition–Compensation balance of farmland policy in China through telecoupling: A case study in the middle reaches of Yangtze River Urban Agglomerations,” *Land Use Policy*, vol. 83, pp. 134–146, 2019.
[232] H. Tang, L. Sang, and W. Yun, “China’s cultivated land balance policy implementation dilemma and direction of scientific and technological innovation,” *Bull. Chin. Acad. Sci.*, vol. 35, no. 5, pp. 637–644, 2020, doi: 10.16418/j.issn.1000-3045.20200313002.
[233] B. Gu, X. Zhang, X. Bai, B. Fu, and D. Chen, “Four steps to food security for swelling cities,” 2019.
[234] Future Earth, “Water-Energy-Food Nexus: We are the Nexus!,” 2018. https://futureearth.org/2018/07/30/water-energy-food-nexus-we-are-the-nexus/ (accessed Mar. 26, 2021).
[235] The Nexus Resource Platform, “Messages from the Bonn 2011 Conference: The water, energy and food security nexus solutions for a green economy,” Bonn, Germany, 2011. [Online]. Available: https://uploads.water-energy-food.org/resources/Messages-from-the-Bonn2011-Conference.pdf
[236] Q. Wang, S. Li, G. He, R. Li, and X. Wang, “Evaluating sustainability of water-energy-food (WEF) nexus using an improved matter-element extension model: A case study of China,” *J. Clean. Prod.*, vol. 202, pp. 1097–1106, Nov. 2018, doi: 10.1016/j.jclepro.2018.08.213.
[237] United Nations, “The 17 goals-sustainable development,” 2015. https://sdgs.un.org/goals (accessed Jul. 28, 2021).
[238] J. Liu *et al.*, “Nexus approaches to global sustainable development,” *Nat. Sustain.*, vol. 1, no. 9, Art. no. 9, Sep. 2018, doi: 10.1038/s41893-018-0135-8.
[239] A. S. Kebede, R. J. Nicholls, D. Clarke, C. Savin, and P. A. Harrison, “Integrated assessment of the food-water-land-ecosystems nexus in Europe: Implications for sustainability,” *Sci. Total Environ.*, vol. 768, p. 144461, May 2021, doi: 10.1016/j.scitotenv.2020.144461.
[240] UNECE, “Methodology for assessing the water-food-energy-ecosystems nexus in transboundary basins and experiences from its application: synthesis,” 2018. https://unece.org/environment-policy/publications/methodology-assessing-water-food-energy-ecosystems-nexus (accessed Mar. 26, 2021).
[241] A. K. Fiedler, D. A. Landis, and S. D. Wratten, “Maximizing ecosystem services from conservation biological control: The role of habitat management,” *Biol. Control*, vol. 45, no. 2, pp. 254–271, May 2008, doi: 10.1016/j.biocontrol.2007.12.009.
[242] A. A. Karabulut, E. Crenna, S. Sala, and A. Udias, “A proposal for integration of the ecosystem-water-food-land-energy (EWFLE) nexus concept into life cycle assessment: A synthesis matrix system for food security,” *J. Clean. Prod.*, vol. 172, pp. 3874–3889, Jan. 2018, doi: 10.1016/j.jclepro.2017.05.092.
[243] M.-H. Yuan and S.-L. Lo, “Ecosystem services and sustainable development: Perspectives from the food-energy-water Nexus,” *Ecosyst. Serv.*, vol. 46, p. 101217, Dec. 2020, doi: 10.1016/j.ecoser.2020.101217.
[244] MEA, “Ecosystems and human well-being: synthesis. Millennium Ecosystem Assessment.,” Washington, DC., 2005. [Online]. Available: https://www.millenniumassessment.org/documents/document.356.aspx.pdf

[245] L. Rahimi, B. Malekmohammadi, and A. R. Yavari, “Assessing and Modeling the Impacts of Wetland Land Cover Changes on Water Provision and Habitat Quality Ecosystem Services,” *Nat. Resour. Res.*, vol. 29, no. 6, pp. 3701–3718, Dec. 2020, doi: 10.1007/s11053-020-09667-7.
[246] The International Centre for Integrated Mountain Development, “Contribution of Himalayan Ecosystems to Water, Energy, and Food Security in South Asia: A nexus approach,” 2012. https://lib.icimod.org/record/1898 (accessed Mar. 27, 2021).
[247] A. Karabulut *et al.*, “Mapping water provisioning services to support the ecosystem–water–food–energy nexus in the Danube river basin,” *Ecosyst. Serv.*, vol. 17, pp. 278–292, Feb. 2016, doi: 10.1016/j.ecoser.2015.08.002.
[248] V. Kati, C. Kassara, Z. Vrontisi, and A. Moustakas, “The biodiversity-wind energy-land use nexus in a global biodiversity hotspot,” *Sci. Total Environ.*, vol. 768, p. 144471, May 2021, doi: 10.1016/j.scitotenv.2020.144471.
[249] H.-M. Deng, C. Wang, W.-J. Cai, Y. Liu, and L.-X. Zhang, “Managing the water-energy-food nexus in China by adjusting critical final demands and supply chains: An input-output analysis,” *Sci. Total Environ.*, vol. 720, p. 137635, Jun. 2020, doi: 10.1016/j.scitotenv.2020.137635.
[250] D. Han, D. Yu, and Q. Cao, “Assessment on the features of coupling interaction of the food-energy-water nexus in China,” *J. Clean. Prod.*, vol. 249, p. 119379, Mar. 2020, doi: 10.1016/j.jclepro.2019.119379.
[251] C. Liu, Z. Zhang, S. Liu, Q. Liu, B. Feng, and J. Tanzer, “Evaluating Agricultural Sustainability Based on the Water–Energy–Food Nexus in the Chenmengquan Irrigation District of China,” *Sustainability*, vol. 11, no. 19, Art. no. 19, Jan. 2019, doi: 10.3390/su11195350.
[252] S. Lu, X. Zhang, H. Peng, M. Skitmore, X. Bai, and Z. Zheng, “The energy-food-water nexus: Water footprint of Henan-Hubei-Hunan in China,” *Renew. Sustain. Energy Rev.*, vol. 135, p. 110417, Jan. 2021, doi: 10.1016/j.rser.2020.110417.
[253] H. Xu *et al.*, “Future increases in irrigation water requirement challenge the water-food nexus in the northeast farming region of China,” *Agric. Water Manag.*, vol. 213, pp. 594–604, Mar. 2019, doi: 10.1016/j.agwat.2018.10.045.
[254] C. Xu, W. Jiang, Q. Huang, and Y. Wang, “Ecosystem services response to rural-urban transitions in coastal and island cities: A comparison between Shenzhen and Hong Kong, China,” *J. Clean. Prod.*, vol. 260, p. 121033, Jul. 2020, doi: 10.1016/j.jclepro.2020.121033.
[255] Shenzhen Statistics Bureau, *Shenzhen Statistical Yearbook 2020*. Beijing, China: China Statistics Press, 2020. [Online]. Available: http://tjj.sz.gov.cn/attachment/0/736/736628/8386382.pdf
[256] W. Hong, R. Jiang, C. Yang, F. Zhang, M. Su, and Q. Liao, “Establishing an ecological vulnerability assessment indicator system for spatial recognition and management of ecologically vulnerable areas in highly urbanized regions: A case study of Shenzhen, China,” *Ecol. Indic.*, vol. 69, pp. 540–547, Oct. 2016, doi: 10.1016/j.ecolind.2016.05.028.
[257] Guangdong Statistics Bureau, *Guangdong Statistical Yearbook 2020*. Beijing, China: China Statistics Press, 2020. [Online]. Available: http://stats.gd.gov.cn/gdtjnj/content/post_3098041.html
[258] B. Zhu, “Top 10 Chinese cities by GDP in the first three quarters of 2020,” 2020. http://t.m.china.org.cn/convert/c_tevD0SXx.html (accessed Jul. 28, 2021).
[259] J. Huang, Z. Liang, S. Wu, and S. Li, “Grain Self-Sufficiency Capacity in China’s Metropolitan Areas under Rapid Urbanization: Trends and Regional Differences from 1990 to 2015,” *Sustainability*, vol. 11, no. 9, Art. no. 9, Jan. 2019, doi: 10.3390/su11092468.
[260] T. Li, F. Bai, P. Han, and Y. Zhang, “Non-Point Source Pollutant Load Variation in Rapid Urbanization Areas by Remote Sensing, Gis and the L-THIA Model: A Case in Bao’an District, Shenzhen, China,” *Environ. Manage.*, vol. 58, no. 5, pp. 873–888, Nov. 2016, doi: 10.1007/s00267-016-0743-x.

[261] W. Zhang, B. Huang, and D. Luo, “Effects of land use and transportation on carbon sources and carbon sinks: A case study in Shenzhen, China,” *Landsc. Urban Plan.*, vol. 122, pp. 175–185, Feb. 2014, doi: 10.1016/j.landurbplan.2013.09.014.
[262] S. Liu *et al.*, “Trace elements in shellfish from Shenzhen, China: Implication of coastal water pollution and human exposure,” *Environ. Pollut.*, vol. 263, p. 114582, Aug. 2020, doi: 10.1016/j.envpol.2020.114582.
[263] Y. Wang, C. Xian, Y. Jiang, X. Pan, and Z. Ouyang, “Anthropogenic reactive nitrogen releases and gray water footprints in urban water pollution evaluation: the case of Shenzhen City, China,” *Environ. Dev. Sustain.*, vol. 22, no. 7, pp. 6343–6361, Oct. 2020, doi: 10.1007/s10668-019-00482-6.
[264] T. Li, S. Yang, and M. Tan, “Simulation and optimization of water supply and demand balance in Shenzhen: A system dynamics approach,” *J. Clean. Prod.*, vol. 207, pp. 882–893, Jan. 2019, doi: 10.1016/j.jclepro.2018.10.052.
[265] Water Resources Bureau of Shenzhen Municipality, “Shenzhen Water Resources Bulletin,” *Shenzhen Water Resources Bulletin*, 2010,2004 2019. http://swj.sz.gov.cn/sjfb/szygb/index.html (accessed Apr. 12, 2021).
[266] Tokyo Metropolitan Government, “Case 6: Shenzhen International Low Carbon City (ILCC),” 2017. https://www.kankyo.metro.tokyo.lg.jp/en/int/c40/c40_pse_r.files/UEII_Chapter3.6_Shenzhen.pdf
[267] P. M. Haygarth and K. Ritz, “The future of soils and land use in the UK: Soil systems for the provision of land-based ecosystem services,” *Land Use Policy*, vol. 26, pp. S187–S197, Dec. 2009, doi: 10.1016/j.landusepol.2009.09.016.
[268] S. Carpentier, E. Filotas, I. T. Handa, and C. Messier, “Trade-offs between timber production, carbon stocking and habitat quality when managing woodlots for multiple ecosystem services,” *Environ. Conserv.*, vol. 44, no. 1, pp. 14–23, Mar. 2017, doi: 10.1017/S0376892916000357.
[269] Clark Labs, “TerrSet Geospatial Monitoring and Modeling Software,” *Clark Labs*, 2020. https://clarklabs.org/terrset/ (accessed Mar. 31, 2021).
[270] J. Bolliger *et al.*, “Effects of Land-Use Change on Carbon Stocks in Switzerland,” *Ecosystems*, vol. 11, no. 6, pp. 895–907, Sep. 2008, doi: 10.1007/s10021-008-9168-6.
[271] J. R. Eastman, *Terrset 2020 tutorial*. Worcester: Clark University, 2020.
[272] K. S. Kumar, P. U. Bhaskar, and K. Padmakumari, “Application of land change modeler for prediction of future land use land cover: a case study of Vijayawada city,” *Int J Adv Technol Eng Sci*, vol. 3, pp. 773–783, 2015.
[273] J. R. Eastman, *Terrset 2020 manual*. Worcester: Clark University, 2020.
[274] A. Kazemzadeh, S. Zanganeh, L. Salvati, and N. Neysani Samani, “A spatial zoning approach to calibrate and validate urban growth models,” *Int. J. Geogr. Inf. Sci.*, vol. 31, pp. 1–20, Oct. 2016, doi: 10.1080/13658816.2016.1236927.
[275] V. N. Mishra and P. K. Rai, “A remote sensing aided multi-layer perceptron-Markov chain analysis for land use and land cover change prediction in Patna district (Bihar), India,” *Arab. J. Geosci.*, vol. 9, no. 4, p. 249, Apr. 2016, doi: 10.1007/s12517-015-2138-3.
[276] G. Singh and M. Sachan, “Multi-layer perceptron (MLP) neural network technique for offline handwritten Gurmukhi character recognition,” in *2014 IEEE International Conference on Computational Intelligence and Computing Research*, Dec. 2014, pp. 1–5. doi: 10.1109/ICCIC.2014.7238334.
[277] K. Shoyama, T. Matsui, S. Hashimoto, K. Kabaya, A. Oono, and O. Saito, “Development of land-use scenarios using vegetation inventories in Japan,” *Sustain. Sci.*, vol. 14, no. 1, pp. 39–52, Jan. 2019, doi: 10.1007/s11625-018-0617-7.
[278] Stanford University, “InVEST software platform,” *Natural Capital Project*, Apr. 01, 2019. https://naturalcapitalproject.stanford.edu/software/invest (accessed Mar. 31, 2021).

[279] J. Gao, F. Li, H. Gao, C. Zhou, and X. Zhang, “The impact of land-use change on water-related ecosystem services: a study of the Guishui River Basin, Beijing, China,” *J. Clean. Prod.*, vol. 163, pp. S148–S155, Oct. 2017, doi: 10.1016/j.jclepro.2016.01.049.
[280] M. Li *et al.*, “Evaluation of water conservation function of Danjiang River Basin in Qinling Mountains, China based on InVEST model,” *J. Environ. Manage.*, vol. 286, p. 112212, May 2021, doi: 10.1016/j.jenvman.2021.112212.
[281] K. L. Vigerstol and J. E. Aukema, “A comparison of tools for modeling freshwater ecosystem services,” *J. Environ. Manage.*, vol. 92, no. 10, pp. 2403–2409, Oct. 2011, doi: 10.1016/j.jenvman.2011.06.040.
[282] M. Terrado, S. Sabater, B. Chaplin-Kramer, L. Mandle, G. Ziv, and V. Acuña, “Model development for the assessment of terrestrial and aquatic habitat quality in conservation planning,” *Sci. Total Environ.*, vol. 540, pp. 63–70, Jan. 2016, doi: 10.1016/j.scitotenv.2015.03.064.
[283] Y. Liang, L. Liu, and J. Huang, “Simulating Land-Use Change and Its Effect on Biodiversity,” in *Integrated Modelling of Ecosystem Services and Land-Use Change: Case Studies of Northwestern Region of China*, Y. Liang, L. Liu, and J. Huang, Eds. Singapore: Springer, 2020, pp. 135–151. doi: 10.1007/978-981-13-9125-5_8.
[284] J. Gong, Y. Xie, E. Cao, Q. Huang, and H. Li, “Integration of InVEST-habitat quality model with landscape pattern indexes to assess mountain plant biodiversity change: A case study of Bailongjiang watershed in Gansu Province,” *J. Geogr. Sci.*, vol. 29, no. 7, pp. 1193–1210, Jul. 2019, doi: 10.1007/s11442-019-1653-7.
[285] R. Sharp *et al.*, *InVEST 3.9.0.post45+ug.g162427b User’s Guide*. The Natural Capital Project, Stanford University, University of Minnesota, The Nature Conservancy, and World Wildlife Fund, 2020. Accessed: Mar. 11, 2021. [Online]. Available: https://storage.googleapis.com/releases.naturalcapitalproject.org/invest-userguide/latest/index.html#final-ecosystem-services
[286] X. Yang, R. Chen, M. E. Meadows, G. Ji, and J. Xu, “Modelling water yield with the InVEST model in a data scarce region of northwest China,” *Water Supply*, vol. 20, no. 3, pp. 1035–1045, Feb. 2020, doi: 10.2166/ws.2020.026.
[287] E. S. Brondizio, J. Settele, S. Díaz, and H. T. Ngo, “IPBES (2019): Global assessment report on biodiversity and ecosystem services of the Intergovernmental Science-Policy Platform on Biodiversity and Ecosystem Services,” Bonn, Germany, 2019.
[288] UN, “The New Urban Agenda,” *The New Urban Agenda*, 2017. https://habitat3.org/the-new-urban-agenda/ (accessed Apr. 01, 2021).
[289] C. J. Vörösmarty *et al.*, “Ecosystem-based water security and the Sustainable Development Goals (SDGs),” *Ecohydrol. Hydrobiol.*, vol. 18, no. 4, pp. 317–333, Dec. 2018, doi: 10.1016/j.ecohyd.2018.07.004.
[290] B. J. Cardinale *et al.*, “Biodiversity loss and its impact on humanity,” *Nature*, vol. 486, no. 7401, Art. no. 7401, Jun. 2012, doi: 10.1038/nature11148.
[291] A. Dobson *et al.*, “Habitat Loss, Trophic Collapse, and the Decline of Ecosystem Services,” *Ecology*, vol. 87, no. 8, pp. 1915–1924, 2006, doi: https://doi.org/10.1890/0012-9658(2006)87[1915:HLTCAT]2.0.CO;2.
[292] W. Shi, F. Tao, and J. Liu, “Changes in quantity and quality of cropland and the implications for grain production in the Huang-Huai-Hai Plain of China,” *Food Secur.*, vol. 5, no. 1, pp. 69–82, Feb. 2013, doi: 10.1007/s12571-012-0225-9.
[293] G. Liu, L. Zhang, Q. Zhang, and Z. Musyimi, “The response of grain production to changes in quantity and quality of cropland in Yangtze River Delta, China,” *J. Sci. Food Agric.*, vol. 95, no. 3, pp. 480–489, 2015, doi: https://doi.org/10.1002/jsfa.6745.
[294] J. Babí Almenar *et al.*, “Nexus between nature-based solutions, ecosystem services and urban challenges,” *Land Use Policy*, vol. 100, p. 104898, Jan. 2021, doi: 10.1016/j.landusepol.2020.104898.

[295] L. Bai, C. Xiu, X. Feng, and D. Liu, “Influence of urbanization on regional habitat quality:a case study of Changchun City,” *Habitat Int.*, vol. 93, p. 102042, Nov. 2019, doi: 10.1016/j.habitatint.2019.102042.
[296] W. Cao *et al.*, “Island urbanization and its ecological consequences: A case study in the Zhoushan Island, East China,” *Ecol. Indic.*, vol. 76, pp. 1–14, May 2017, doi: 10.1016/j.ecolind.2017.01.001.
[297] Y.-C. Lee, J. Ahern, and C.-T. Yeh, “Ecosystem services in peri-urban landscapes: The effects of agricultural landscape change on ecosystem services in Taiwan’s western coastal plain,” *Landsc. Urban Plan.*, vol. 139, pp. 137–148, Jul. 2015, doi: 10.1016/j.landurbplan.2015.02.023.
[298] A. Awotwi, F. Yeboah, and M. Kumi, “Assessing the impact of land cover changes on water balance components of White Volta Basin in West Africa,” *Water Environ. J.*, vol. 29, no. 2, pp. 259–267, 2015, doi: https://doi.org/10.1111/wej.12100.
[299] K. Bieger, G. Hörmann, and N. Fohrer, “The impact of land use change in the Xiangxi Catchment (China) on water balance and sediment transport,” *Reg. Environ. Change*, vol. 15, no. 3, pp. 485–498, Mar. 2015, doi: 10.1007/s10113-013-0429-3.
[300] C. Li *et al.*, “Impacts of Urbanization on Watershed Water Balances Across the Conterminous United States,” *Water Resour. Res.*, vol. 56, no. 7, p. e2019WR026574, 2020, doi: https://doi.org/10.1029/2019WR026574.
[301] H. Baral, R. J. Keenan, J. C. Fox, N. E. Stork, and S. Kasel, “Spatial assessment of ecosystem goods and services in complex production landscapes: A case study from south-eastern Australia,” *Ecol. Complex.*, vol. 13, pp. 35–45, Mar. 2013, doi: 10.1016/j.ecocom.2012.11.001.
[302] L. Boithias, V. Acuña, L. Vergoñós, G. Ziv, R. Marcé, and S. Sabater, “Assessment of the water supply:demand ratios in a Mediterranean basin under different global change scenarios and mitigation alternatives,” *Sci. Total Environ.*, vol. 470–471, pp. 567–577, Feb. 2014, doi: 10.1016/j.scitotenv.2013.10.003.
[303] V. Srinivasan, K. C. Seto, R. Emerson, and S. M. Gorelick, “The impact of urbanization on water vulnerability: A coupled human–environment system approach for Chennai, India,” *Glob. Environ. Change*, vol. 23, no. 1, pp. 229–239, Feb. 2013, doi: 10.1016/j.gloenvcha.2012.10.002.
[304] P. Wu and M. Tan, “Challenges for sustainable urbanization: a case study of water shortage and water environment changes in Shandong, China,” *Procedia Environ. Sci.*, vol. 13, pp. 919–927, Jan. 2012, doi: 10.1016/j.proenv.2012.01.085.
[305] S. Wang, K. Adhikari, Q. Zhuang, H. Gu, and X. Jin, “Impacts of urbanization on soil organic carbon stocks in the northeast coastal agricultural areas of China,” *Sci. Total Environ.*, vol. 721, p. 137814, Jun. 2020, doi: 10.1016/j.scitotenv.2020.137814.
[306] M. E. Dias De Oliveira, B. E. Vaughan, and E. J. Rykiel, “Ethanol as fuel: energy, carbon dioxide balances, and ecological footprint,” *BioScience*, vol. 55, no. 7, pp. 593–602, 2005.
[307] M. Wackernagel and J. Silverstein, “Big things first: focusing on the scale imperative with the ecological footprint,” *Ecol. Econ.*, vol. 32, no. 3, pp. 391–394, 2000.
[308] I. Moffatt, “Ecological footprints and sustainable development,” *Ecol. Econ.*, vol. 32, no. 3, pp. 359–362, 2000.
[309] M. Lenzen and S. A. Murray, “A modified ecological footprint method and its application to Australia,” *Ecol. Econ.*, vol. 37, no. 2, pp. 229–255, 2001.
[310] M. Scotti, C. Bondavalli, and A. Bodini, “Ecological footprint as a tool for local sustainability: the municipality of Piacenza (Italy) as a case study,” *Environ. Impact Assess. Rev.*, vol. 29, no. 1, pp. 39–50, 2009.
[311] S. Díaz *et al.*, “Assessing nature’s contributions to people,” *Science*, vol. 359, no. 6373, pp. 270–272, 2018.
[312] “Nature’s Contributions to People (NCP) - Article by IPBES Experts in Science.” https://www.ipbes.net/news/natures-contributions-people-ncp-article-ipbes-experts-science (accessed Sep. 28, 2019).

[313] A. E. Nilsson *et al.*, “Towards extended shared socioeconomic pathways: a combined participatory bottom-up and top-down methodology with results from the Barents region,” *Glob. Environ. Change*, vol. 45, pp. 124–132, 2017.
[314] L. M. Pereira *et al.*, “Developing multiscale and integrative nature–people scenarios using the Nature Futures Framework,” *People Nat.*, 2020.
[315] I. M. Rosa *et al.*, “Multiscale scenarios for nature futures,” *Nat. Ecol. Evol.*, vol. 1, no. 10, pp. 1416–1419, 2017.
[316] C. J. Lundquist *et al.*, “A pluralistic Nature Futures Framework”.
[317] I. Rosa, C. J. Lundquist, S. Ferrier, R. Alkemade, P. F. Castro, and C. A. Joly, “Increasing capacity to produce scenarios and models for biodiversity and ecosystem services,” *Biota Neotropica*, vol. 20, 2020.
[318] C. K. Osamu Saito Shizuka Hashimoto, Takanori Matsui, Kikuko Shoyama, Kei Kabaya, Tomoko Uetake, Hisatomo Taki, Yoichi Ishikawa, Kyohei Matsushita, Fumihiro Yamane, Juri Hori, Toshinori Ariga, Kazuhiko Takeuchi., “Co-design of national-scale future scenarios in Japan to predict and assess natural capital and ecosystem services,” *Sustain. Sci.*, vol. 14, pp. 5–21, 2019, doi: 10.1007/s11625-018-0587-9.
[319] IPBES, “IPBES-IPCC co-sponsored workshop: spotlighting the interactions of the science of biodiversity and climate change,” 2020. https://ipbes.net/ipbes-ipcc-cosponsored-workshop-media-release (accessed Jan. 04, 2021).
[320] L. M. Pereira *et al.*, “Developing multiscale and integrative nature–people scenarios using the Nature Futures Framework,” *People Nat.*, vol. 2, no. 4, pp. 1172–1195, 2020, doi: 10.1002/pan3.10146.
[321] X. Shi, T. Matsui, C. Haga, T. Machimura, S. Hashimoto, and O. Saito, “A scenario- and spatial-downscaling-based land-use modeling framework to improve the projections of plausible futures: a case study of the Guangdong–Hong Kong–Macao Greater Bay Area, China,” *Sustain. Sci.*, Jul. 2021, doi: 10.1007/s11625-021-01011-z.
[322] J. W. Redhead *et al.*, “Empirical validation of the InVEST water yield ecosystem service model at a national scale,” *Sci. Total Environ.*, vol. 569–570, pp. 1418–1426, Nov. 2016, doi: 10.1016/j.scitotenv.2016.06.227.
[323] IPCC, “Climate Change 2021: The Physical Science Basis. Summary for Policymakers,” Cambridge University Press, 2021. [Online]. Available: https://www.ipcc.ch/report/ar6/wg1/downloads/report/IPCC_AR6_WGI_SPM.pdf
[324] S. S. Dahikar and S. V. Rode, “Agricultural crop yield prediction using artificial neural network approach,” *Int. J. Innov. Res. Electr. Electron. Instrum. Control Eng.*, vol. 2, no. 1, pp. 683–686, 2014.
[325] V. Ochoa and N. Urbina-Cardona, “Tools for spatially modeling ecosystem services: Publication trends, conceptual reflections and future challenges,” *Ecosyst. Serv.*, vol. 26, pp. 155–169, Aug. 2017, doi: 10.1016/j.ecoser.2017.06.011.
[326] M. Jiao, Y. Wang, M. Hu, and B. Xia, “Spatial deconstruction and differentiation analysis of early warning for ecological security in the Pearl River Delta, China,” *Sustain. Cities Soc.*, vol. 64, p. 102557, Jan. 2021, doi: 10.1016/j.scs.2020.102557.
[327] C. Zhu *et al.*, “Impacts of urbanization and landscape pattern on habitat quality using OLS and GWR models in Hangzhou, China,” *Ecol. Indic.*, vol. 117, p. 106654, Oct. 2020, doi: 10.1016/j.ecolind.2020.106654.
[328] B. pu Fu, “On the Calculation of the Evaporation from Land Surface,” *Sci. Atmospherica Sin.*, vol. 5, pp. 23–31, 1981.
[329] L. Zhang, K. Hickel, W. R. Dawes, F. H. S. Chiew, A. W. Western, and P. R. Briggs, “A rational function approach for estimating mean annual evapotranspiration,” *Water Resour. Res.*, vol. 40, no. 2, 2004, doi: https://doi.org/10.1029/2003WR002710.

[330] R. J. Donohue, M. L. Roderick, and T. R. McVicar, “Roots, storms and soil pores: Incorporating key ecohydrological processes into Budyko’s hydrological model,” *J. Hydrol.*, vol. 436–437, pp. 35–50, May 2012, doi: 10.1016/j.jhydrol.2012.02.033.
[331] W. Zhou, G. Liu, J. Pan, and X. Feng, “Distribution of available soil water capacity in China,” *J. Geogr. Sci.*, vol. 15, no. 1, pp. 3–12, Jan. 2005, doi: 10.1007/BF02873101.
[332] Meteorological Bureau of Shenzhen Municipality, “The climate profile of Shenzhen and its characteristics of four seasons,” 2021. http://weather.sz.gov.cn/qixiangfuwu/qihoufuwu/qihouguanceyupinggu/qihougaikuang/ (accessed Mar. 31, 2021).
[333] FAO, “FAO SOILS PORTAL: Harmonized world soil database v1.2,” 2021. http://www.fao.org/soils-portal/soil-survey/soil-maps-and-databases/harmonized-world-soil-database-v12/en/ (accessed Mar. 31, 2021).
[334] L. Liang and Q. Liu, “Streamflow sensitivity analysis to climate change for a large water-limited basin,” *Hydrol. Process.*, vol. 28, no. 4, pp. 1767–1774, 2014, doi: https://doi.org/10.1002/hyp.9720.
[335] H. J. Schenk and R. B. Jackson, “Rooting depths, lateral root spreads and below-ground/above-ground allometries of plants in water-limited ecosystems,” *J. Ecol.*, vol. 90, no. 3, pp. 480–494, 2002, doi: https://doi.org/10.1046/j.1365-2745.2002.00682.x.
[336] Y. Bao *et al.*, “Spatial and temporal changes of water conservation of Loess Plateau in northern Shaanxi province by InVEST model,” *Geogr. Res.*, vol. 35, no. 4, pp. 664–676, 2016, doi: https://doi.org/10.11821/dlyj201604006.
[337] Y. Zhao *et al.*, “Identification of drivers for water yield in the upstream of Shiyang River based on InVEST model,” *Chin. J. Ecol.*, vol. 38, no. 12, pp. 3789–3799, 2019, doi: https://doi.org/10.13292/j.1000-4890.201912.017.